DISCOVERY OF A NOVEL PATHWAY TO SYNTHESIZE TRIACYLGLYCEROL IN PLANTS BY CHARACTERIZING THE ACCUMULATION OF SURFACE WAXES ON BAYBERRY (*MYRICA PENSYLVANICA*) FRUITS

By

Jeffrey Patrick Simpson

A DISSERTATION

Submitted to
Michigan State University
in partial fulfillment of the requirements
for the degree of

Plant Biology -Doctor of Philosophy

2015

ABSTRACT

DISCOVERY OF A NOVEL PATHWAY TO SYNTHESIZE TRIACYLGLYCEROL IN PLANTS BY CHARACTERIZING THE ACCUMULATION OF SURFACE WAXES ON BAYBERRY (*MYRICA PENSYLVANICA*) FRUITS

By

Jeffrey Patrick Simpson

The surfaces of Bayberry (*Myrica pensylvanica)* fruits are covered with an extremely thick and unusual layer of crystalline wax. The surface wax accumulates to over 30% of the total fruit mass, the highest reported accumulation of surface lipids in nature. In addition, the composition of Bayberry wax is strikingly different from other plant surface waxes, consisting almost entirely of saturated triacylglycerol (TAG) and diacylglycerol (DAG), with palmitate and myristate as the dominant acyl chains. To gain insight into the unique properties of Bayberry surface wax production and secretion I have characterized the chemical and morphological development of the wax layer, the expression of gene transcripts in the wax secreting tissue and monitored wax biosynthesis through [^{14}C]-acetate and [^{14}C]-glycerol radiolabeling. Together these data provide evidence that Bayberry synthesizes TAG via a pathway not previously described in plants. Characterization of the accumulation of the wax layer identified monoacylglycerol (MAG) with its acyl-chain on the *sn*-2 position of glycerol (*sn*-2-MAG). *sn*-2 MAG was previously shown to be an early intermediate in the biosynthesis of the surface lipid polyesters cutin and suberin, and its accumulation in Bayberry wax suggested that Bayberry wax may be synthesized similarly. Indeed, in contrast to oilseed studies, radiolabeling identified *sn*-2 MAG as an initial labeled glycerolipid and the kinetics of [^{14}C]-MAG labeling indicated a

precursor-product relationship to DAG and TAG. Regiospecificity of the [^{14}C]-acyl chains in DAG and TAG and their distribution between the wax and internal lipids strongly indicated that they were synthesized by transacylase activities with at least some reactions occurring extracellularly. RNA-seq of the wax producing tissue supported and extended the biochemical data. The most abundantly expressed transcripts during Bayberry wax accumulation were associated with surface lipid production, such as *sn*-2 glycerol-3-phosphate acyltransferases, GDSL lipases, ABC transporters, and LTPs. Transcripts encoding enzymes involved in seed TAG synthesis were 10-100 fold less abundant. The RNA seq data strongly support the hypothesis that a pathway related to cutin biosynthesis is responsible for the massive accumulation of extracellular TAG and DAG in Bayberry. This combination of a unique surface wax composition and massive secretion of lipids to the surface may help better understand how plants produce surface lipids, secrete them to the surface, and also to engineer alternative pathways to produce glycerolipids in non-seed tissue.

ACKNOWLEDGEMENTS

I would like to express gratitude to my advisor Dr. John Ohlrogge. It has been an honour to work in his lab and I greatly appreciate his guidance, encouragement and enthusiasm towards my research. During my toughest times, such as interpreting confusing data and writing this dissertation, he provided me with the time and support I needed. The most important skills I learned from John are his positive approach to discussions, how to effectively communicate data, and how to choose the most impactful and important research priorities.

Everybody I worked with contributed to creating a very friendly and encouraging environment throughout my degree. I consider myself fortunate to have been the only graduate student in a lab full of post-docs as this provided a fantastic environment for learning, scientific discussion, and extra motivation to perform and communicate my research at high levels.

I would also like to thank my advisory committee, Dr. Christoph Benning, Dr. Frank Telewski and Dr. Curtis Wilkerson for providing me with guidance when needed.

I would finally like to thank all my family and friends for their encouragement though my many years of schooling. Especially my wife Marisa, for constantly providing me with much needed support, particularly during difficult periods.

TABLE OF CONTENTS

LIST OF TABLES

LIST OF FIGURES

KEY TO SYMBOLS AND ABBREVIATIONS

ACP	acyl carrier protein
ABC	ATP binding cassette
CPT	cholinephosphotransferase
CoA	coenzyme A
DAG	diacylglycerol
DAGT	diacylglycerol acyltransferase
DCR	defective in cuticular ridges
DHP	dihydroxypalmitate
DW	dry weight
ER	endoplasmic reticulum
FAD	fatty acid desaturase
FAS	fatty acid synthase
FAT A, FAT B	fatty acid thioesterase A or B
FFA	free fatty acids
FAME	fatty acid methyl ester
FW	fresh weight
G3P	glycerol-3-phosphate
GC-FID	gas chromatography- flame ionization detector
GC-MS	gas chromatography- mass spectrometer
GPAT	glycerol-3-phosphate acyltransferase

KCS	ketoacyl-ACP synthase
LPA	lysophosphatidic acid
LPAAT	lysophosphatidic acid acyltransferase
LPC	lysophosphatidylcholine
LPCAT	lysophosphatidylcholine acyltransferase
LTP	lipid transport protein
MAG	monoacylglycerol
MGAT	monoacylglycerol acyltransferase
Mp	*Myrica pensylvanica*
PAP	phosphatidate phosphatase
PC	phosphatidylcholine
PDAT	phospholipid: diacylglycerol acyltransferase
PM	plasma membrane
RPKM	reads per kilobase of exon model per million mapped reads
TAG	triacylglycerol
TEM	transmission electron microscopy
TLC	thin layer chromatography
TMSi	trimethylsilyl
SAD	stearoyl-ACP desaturase
SD	standard deviation
SE	standard error
SEM	scanning electron microscopy
WRI	Wrinkled

The *sn* (**s**tereospecific **n**umbering) nomenclature is used to denote the position of fatty acids on the glycerol backbone of monoacylglycerols and diacylglycerols. *sn*-2 refers to fatty acids esterified to carbon 2 of glycerol (also called the *beta* carbon). *sn*-1 and *sn*-3 refer to the terminal carbons of the glycerol backbone (also called *alpha* carbons). Methods used in this study do not distinguish between a fatty acid that is esterified to the *sn*-1 or *sn*-3 positions, and therefore they are denoted as *sn*-1/3 throughout the manuscript.

CHAPTER 1

INTRODUCTION

1.1. Overview

Glycerolipids, represent a diverse and multifunctional class of molecules in plants. The diversity is imparted by the number and nature of the molecules that are linked to the hydroxyls of glycerol. All glycerolipids contain at least one fatty acid but these can differ in chain length, saturation of the carbon bonds and addition of polar groups, such as oxygen. Similarly, one to two positions of the glycerol backbones can remain free of functional groups, or can contain non-acyl functional groups, notably carbohydrates and charged molecules (i.e. phosphocholine). These modifications to glycerolipids change their hydrophobicity, polarity, bi-layer forming ability, and chemical reactivity enabling them to participate in many functions including: (1) defining compartmentalization through forming membranes, (2) forming barriers between the plant and its surroundings (i.e. as cutin, waxes and suberin), (3) storing carbon and energy, (4) acting as reaction centers at membranes (e.g. photosynthesis), and (5) acting as signaling molecules.

The overall theme of my dissertation is the biosynthesis and secretion of glycerolipids on the surfaces of aerial plant tissues. All aerial plant surfaces are coated with a hydrophobic lipid barrier called the cuticle (Figure 1). This layer is the primary interface between the plant and its surrounding environment and accordingly has extremely important functions related to a plant's overall response to abiotic and biotic stresses and also in defining tissue shape (Kolattukudy, 2001). Plants produce a wide variety in both the chemical constituents and the quantity of cuticular lipids (Kolattukudy, 1976; Kolattukudy, 2001; Pollard et al., 2008). The cuticle is largely composed of the lipophilic polyester cutin and associated fatty acid-based waxes that are imbedded on top and within cutin. Cutin is insoluble and may be associated with the cell wall,

but the waxes are free and can be extracted by immersing the tissue in an organic solvent, such as chloroform.

Reverse and forward genetics have identified many genes involved in the biosynthesis and secretion or cuticular lipids, but there are still many unknowns (Pollard et al., 2008; Beisson et al., 2012). Some key questions include: (1) The relationship between the synthesis of surface lipids and membranes. (2) The order of reactions from fatty acid modification to lipid secretion from cells. (3) Intermediates in cuticular lipid synthesis, specifically glycerolipids for cutin. (4) How surface lipids are exported from cells. (5) How cutin is assembled outside of the cell and attached to the cell wall. Biochemical studies on surface lipid metabolism may be influenced and limited by the fact that the lipids are produced in a single epidermal cell layer, are most actively synthesized in developing tissues, and that most cutins and waxes in plants accumulate to low levels relative to membrane and seed lipids. Thus, it is challenging to separate the flux of lipids destined for the cuticle from general lipid metabolism, and to visualize cuticular lipid secretion and extracellular assembly.

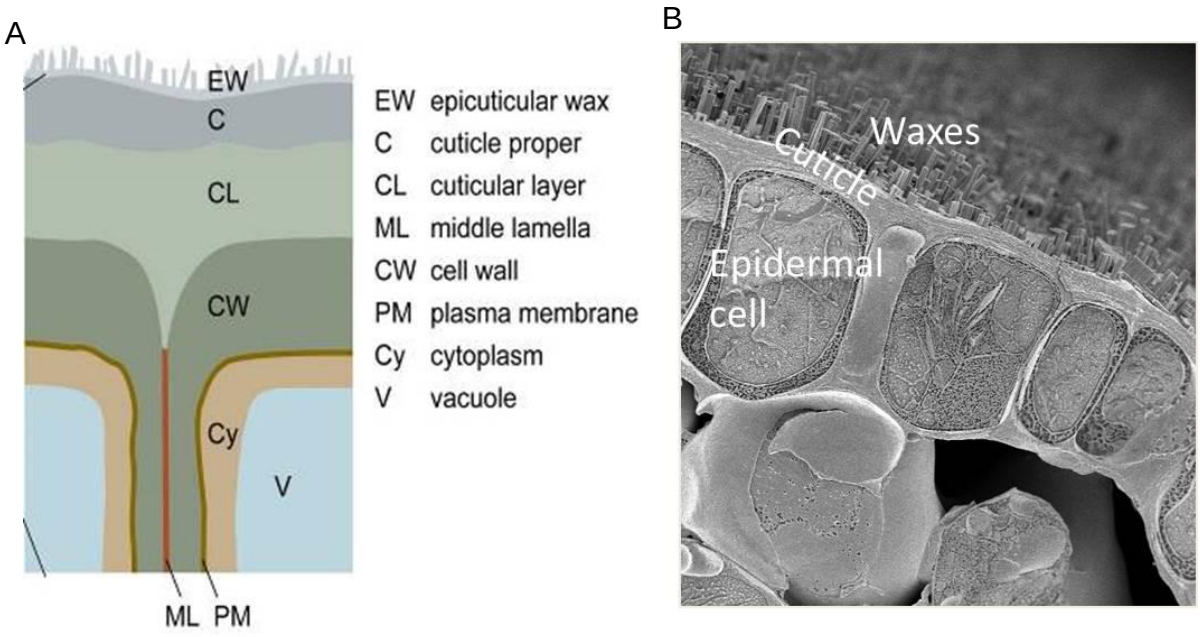

Figure 1: Diagrams of the plant cuticle. (A) Schematic diagram of a plant surface (from Pollard et al, 2008). (B) Cryo-scanning electron micrograph of an Arabidopsis stem (from Lacey Samuels, University of British Columbia).

The fruits of Bayberry (*Myrica* or *Morella pensylvanica*) accumulate up to 30 percent of its dry mass as surface lipids, which is the largest documented surface lipid accumulation in plants. Bayberry provides an attractive model to examine the biochemistry of surface lipid metabolism because; (1) its surface lipids are 10-fold more abundant than any other plant species and, (2) the fact that surface lipids are synthesized continuously on a fully grown tissue allows for an extended period time to study the kinetics of wax synthesis and may simplify quantification. An additional striking and intriguing feature of Bayberry wax is that it is composed almost entirely of triacylglycerol (TAG), diacylglycerol (DAG) and monoacylglycerol (MAG) with saturated fatty acids. This composition contrasts with all other previously characterized plant surface waxes as they contain very long chain (>20 carbons) alkanes, alcohols, aldehydes and wax esters and only trace amounts of glycerolipids. While Bayberry wax and standard surface waxes are both acyl-lipid based, because the final structures are very different Bayberry wax and standard surface waxes are likely synthesized by very different reactions. Instead, the accumulation of glycerolipids DAG, TAG initially suggested that Bayberry wax may be synthesized by a pathway similar to TAG and DAG in oil seeds (i.e. Kennedy pathway). However, extensive evidence will be presented in Chapters 2 and 3 showing that this is not the case and that the biosynthesis of Bayberry TAG proceeds by a pathway never described in plants.

TAG is energetically dense, and large accumulations in vegetative tissue have the potential to increase the overall energy content of plants (Durrett et al., 2008). Furthermore, plants synthesize over 300 different types of fatty acids which are incorporated onto TAGs ("The database of seed oil fatty acids" http://sofa.mri.bund.de/(Badami and Patil, 1981) and many of these have important industrial applications (Jaworski and Cahoon, 2003; Carlsson et al., 2011).

There have been considerable efforts to increase TAG and unusual fatty acid production in plants, but cells often reject large accumulations of unusual lipids (Cahoon et al., 2007; Carlsson et al., 2011). A promising alternative to intracellular lipid accumulation is accumulating the lipids on the surfaces of plants as surface lipids are more resistant to degradation than internal lipids, particularly during plant senescence (Yang and Ohlrogge, 2009). Thus, the potential discovery of pathways and enzymes in Bayberry to synthesize extracellular TAG could represent an alternative approach to produce industrially important, high-value lipids or biofuels with greater stability and yield.

1.2. Objectives

The overall objectives of the work presented in thesis were to characterize the anatomical, biochemical and genetic mechanisms that allow Bayberry to produce such an extremely abundant and unusual surface wax. The techniques used include light and electron microscopy, characterization of the structures and molecular species of its glycerolipids, kinetic radiolabeling with [^{14}C] labeled lipid precursors and a transcriptomic analysis of Bayberry fruits throughout the production of the wax layer. The work is presented in two chapters... Chapter 2 focuses on the characterization of the biochemical pathway that Bayberry uses to produce and secrete its surface wax. In Chapter 3, unique features of the Bayberry transcriptome and anatomy were compared to related plant tissues and hypotheses were developed as to how Bayberry evolved its unique wax layer.

In addition to the work on Bayberry, I also made substantial contributions as a second author to a paper characterizing *sn*-2 specific glycerol-3-phosphate acyltransferases in plants. (Yang et al. 2012 Plant Physiol. 160: 638-652).

In the remaining sections of the introduction, I present an overview of Bayberry plants, and review relevant topics related to the production and secretion of surface lipids and triacylglycerol production in plants.

1.3. A description of Bayberry plants

Bayberry (*Myrica* or *Morella* sp.) is a member of the *Myricaceae* family, in the order *Fagaceae*. The *Myricaceae* family consists of 35-50 species of deciduous shrubs and trees that can be found on every continent, except Australia (Huguet et al., 2005). The species of Bayberry studied in this work is *Myrica pensylvanica* (*Morella pensylvanica*) or Northern Bayberry (Figure 2). *M. pensylvanica* is found in the eastern half of North America, and distributed as far north as Newfoundland, south into the Carolinas and west into Arkansas (Wilbur, 2002). The plant typically grows to heights of 1.5-2 m and can propagate laterally by rhizomes (Hall, 1975). Bayberry has excellent salt tolerance and grows well in sandy and acidic soils, which may be related to its ability to form symbiotic relationships with nitrogen fixing bacteria (*Frankia spp actinomycetes*) (Huguet et al., 2005). *Myrica pensylvanica*, like most *Myricaceae* species, are diecious, meaning they produce male and female flowers on different plants (Hall, 1975). Both flowers are very small and form on catkins that bud early in the season from woody tissue. The female flowers are wind pollinated in early spring and develop a drupe fruit. The size of *Myrica* fruits ranges from 2-5 mm in diameter; the fruits on *Myrica pensylvanica* are on the large end of the spectrum.

The surface wax does not accumulate on the fruit proper, but instead on unusual tubercular protrusions from the fruit exocarp. These structures are called Bayberry knobs (Youngken, 1915; Harlow et al., 1965). Each fruit is completely covered with 200-250 of the

teardrop shaped ~500μm diameter knobs. I estimate that each knob has greater than 10000 cells, making them distinctly different from trichomes. The knobs appear to be a characteristic of *Myricaceae* fruits rather than being a mechanism for the unusual wax production and secretion, as *Myrica rubra* fruits also appear to contain similar knob structures, but not the same abundant layer of wax (Feng et al., 2012). A 1915 PhD thesis from Herber Youngkin (University of Pennsylvania) is the only extensive description of Bayberry knob anatomy and development. He described the interior of the knobs as containing 2-3 "spiral trachea" with "delicate elongate sieve like elements" and "vascular bundles" that run along the outer half of the mesocarp, subtending the knobs and also bulging into the knobs. He further describes the knob mesophyll (i.e. tissue inside the knob) as consisting of two zones: 1) an outer irregular and large celled zone with 12-13 layers, and 2) an inner smaller and rounder celled tissue of many layers. In late July, the knobs develop a reddish color, which may be due to anthocyanins, and also accumulate the thick surface wax layer.

TAG is typically found in large quantities in plants within seeds, some fleshly fruit mesocarps and pollen (Murphy, 2012). To my knowledge, Bayberry fruits are the only documented example of TAG and DAG in plant surface waxes. Furthermore, relative to other TAG compositions in plants, Bayberry surface TAG is unusual in its simplicity and complete saturation. Glycerolipids that have a completely saturated fatty acid composition are resistant to oxidation, and have a high melting point (the melting point of tripalmitate is ~65°C (Gunstone et al., 2007). These properties allow for Bayberry wax to remain intact on the fruit throughout the winter. The high calorie wax that remains on the fruits through the winter is consumed by some bird species (Place and Stiles 1992). Presumably, the thick layer of wax evolved to attract birds which in turn disperse the seeds (Lorts et al., 2008) however, it cannot be ruled out that the

abundant wax layer evolved for other or additional reasons such as desiccation tolerance. Also, owing to the abundance of the wax, its high melting point, and the scents of other natural compounds produced by Bayberry fruits, Bayberry is traditionally used as a source of wax for candle making. A candle I produced from the wax of Bayberry fruits growing on the MSU campus is shown in Figure 2D.

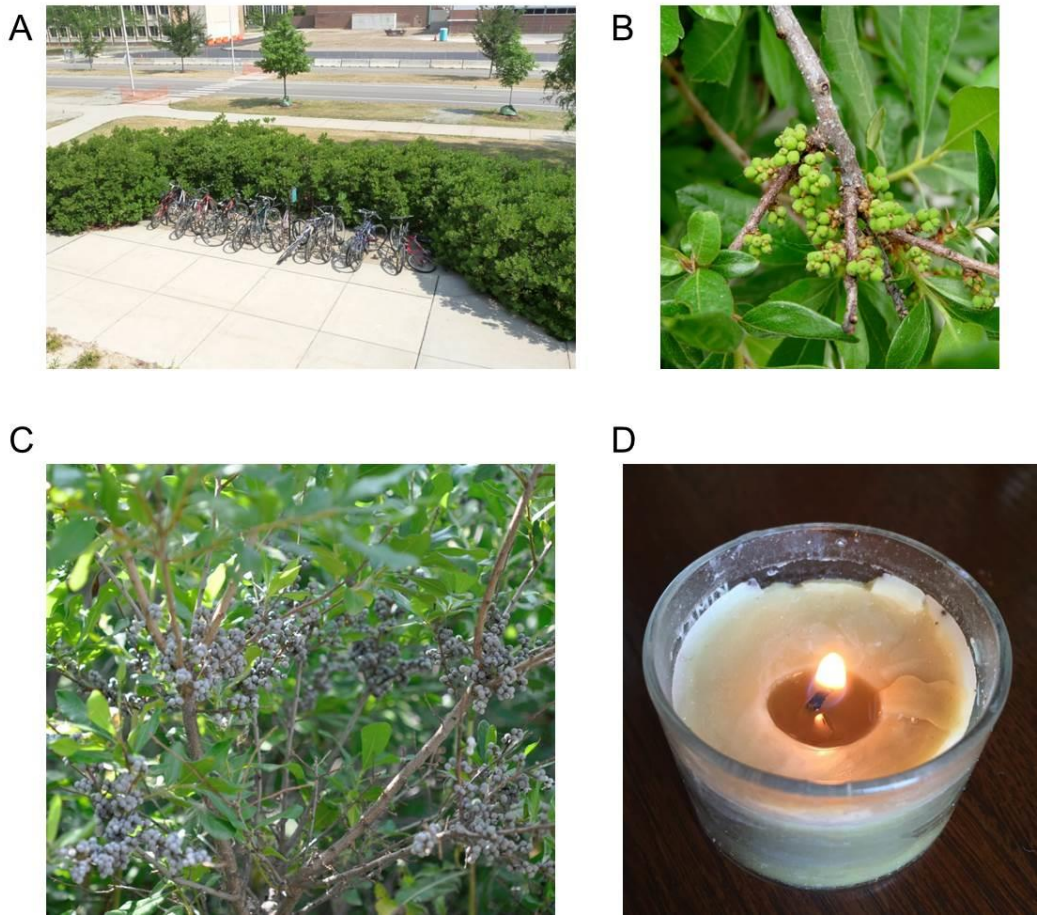

Figure 2: Images of Bayberry plants. (A) Bayberry shrub on Michigan State University campus where most of the plant material for this study was harvested. (B) Clusters of Bayberry fruits prior to surface wax appearance. (C) Mature Bayberry fruits with entire surface wax load. (D) A Bayberry candle produced from wax harvested from the plants in (A).

1.4. Conventional fatty acid and glycerolipid synthesis in plants.

Glycerolipids synthesis is initiated with the synthesis of the fatty acids, which in plants occurs in the plastid by the multi-protein fatty acid synthase (FAS) complex (Ohlrogge and Browse, 1995). The dominant products from FAS are 16:0 and 18:1- acyl groups which are released from the acyl-carrier protein (ACP) of FAS by fatty acid thioesterase proteins (FAT). FATB specifically catalyzes the release of C16:0 and shorter saturated acyl-chains, while the thioesterase FATA releases C18:0 and fatty acids that are desaturated to C18:1 by the soluble stearoyl-ACP desaturase (SAD). In most plants, the majority of fatty acids are exported from the plastid, converted to acyl-CoA's and move to the endoplasmic reticulum (ER) where they are incorporated into glycerolipids and undergo further desaturation.

The synthesis of DAG and TAG in plants can occur by multiple routes (Li-Beisson et al., 2010; Bates et al., 2013). The simplest pathway to TAG is commonly referred to as the Kennedy Pathway, wherein there is sequential acylation by fatty-acyl CoA's on the *sn*-1 and *sn*-2 positions of glycerol-3-phosphate (G3P) to yield phosphatidic acid (PA), followed by removal of the phosphate group to form DAG and a final acylation of the *sn*-3 position of DAG to produce TAG (Figure 3 A). Phosphatidylcholine (PC) is also a major intermediate in the biosynthesis of TAG and membrane lipids. PC can be synthesized by direct conversion of DAG to PC by CDP-choline: DAG cholinephosphotransferase or by acylation of lysophosphatidylcholine (LPC) by LPC acyltransferase (LPCAT) (Bates and Browse, 2012) (Figure 3 B). Incorporation of newly synthesized fatty acids onto LPC is also called the Lands Cycle or acyl-editing pathway and is responsible for over 60% of fatty acid flux into TAG in soybean seeds and over 90% into membrane lipids of pea leaves. (Bates et al., 2007; Bates et al., 2009). In the predominant "eukaryote pathway" to synthesize glycerolipids in plants, fatty acids are desaturated from C18:1

to C18:2 and C18:3 only while esterified to PC in the ER (Ohlrogge and Browse, 1995). Release of unsaturated acyl-CoA's from PC makes them available for acyl transfer to DAG and TAG by the Kennedy pathway enzymes (i.e. DGAT). TAG can also be produced by an acyl-exchange between PC and DAG by PC: DAG acyltransferase (PDAT) (Dahlqvist et al., 2000).

Plants store TAGs and other neutral lipids in lipid droplets (i.e. oil bodies in seeds) (Chapman et al., 2012). The basic structure of lipid droplets is a monolayer phospholipid membrane encircling the neutral lipids contained in a hydrophobic core. Many lipid droplets also contain structural proteins, such as oleosins, which help the lipid droplet maintain a small (2μm) size. Many details of biogenesis of lipid droplets are not clear, but it is thought that neutral lipids accumulate between the ER bilayer, forming a cytosol-facing bulge, which is excised when the droplet reaches a certain size (Chapman et al., 2012). In plants, lipid droplets form wherever neutral lipids such as TAG are produced, (Murphy, 1993, 2012), except for epidermal cells.

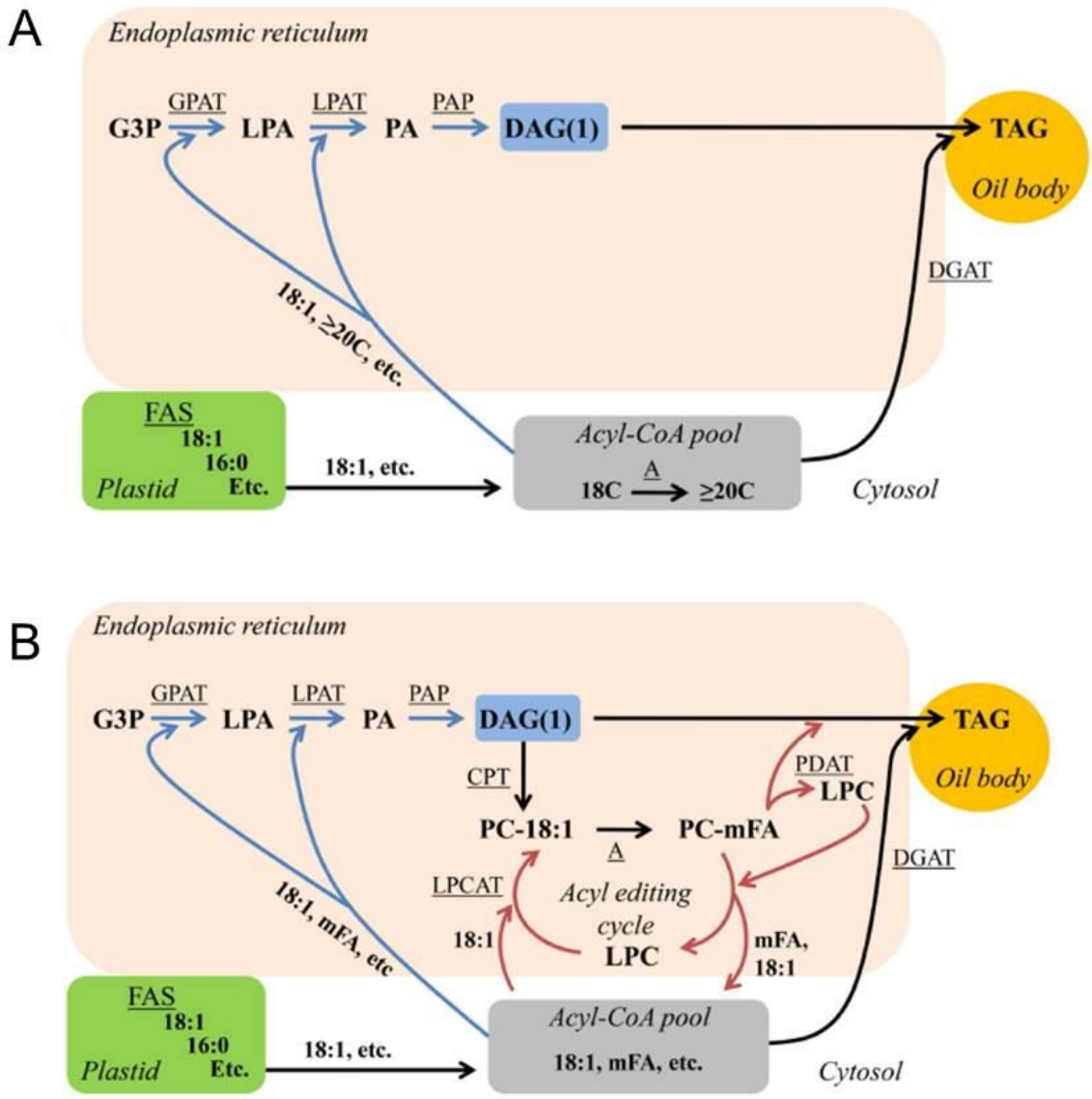

Figure 3: Two pathways for TAG biosynthesis in plants. (Figures from Bates and Browse, 2012). (A) Kennedy pathway. (B) TAG synthesis with acyl-editing. Abbreviations (not in main list) mFA – modified/unsaturated fatty acids, CPT = choline phosphotransferase

1.5. Surface lipid structure and biosynthesis

The primary interface between the plant and its surrounding environment is the cuticle. Accordingly, the cuticle functions to control water loss, influences gas exchange and ion fluxes from the plant, and provides protection from pathogen and insect attacks (Kolattukudy, 2001). The development of the cuticle is thought to be a major contributing factor allowing the evolution of terrestrial plants (Rensing et al., 2008). The cuticle is mostly acyl-lipid based; however, the cuticle also contains phenylpropanoids, isoprenoids, and polysaccharides in its structure (Jetter et al., 2006; Stark and Tian, 2006). The lipid-based structures of the cuticle include (1) an insoluble polyester of hydroxy, dicarboxylic and epoxy fatty acids and glycerol called cutin, (2) a macromolecule related to cutin but with ether and carbon-carbon linkages called cutan, and (3) soluble waxes that are imbedded within and on top of cutin. Constituents of the cuticle are synthesized in the epidermis of aerial plant tissues. In expanding Arabidopsis stems, over half of the fatty acids made by epidermal cells are estimated to be diverted into the production of surface lipids, rather than to membrane lipids (Suh et al., 2005). There appears to be no difference between the biosynthesis of fatty acids for surfaces and membranes, as the same thioesterase FATB contributes to the release of saturated fatty acids for both types of lipids (Bonaventure et al., 2003). However, once fatty acid-CoA's are synthesized, the epidermal cells must separate the fatty acids destined for membranes and surface lipids. While the actual mechanisms are not clear, unlike most membrane lipids, many fatty acyl-CoA's for surface lipids are modified by elongation (to > C20:0), by decarbonylation, or by the addition of polar functionality to the fatty acid. Furthermore, lipids that are destined to be incorporated into cutin are esterified to G3P to form *sn*-2 monoacylglycerol (i.e. *sn*-2 MAG) (Li et al., 2007b; Li et al., 2007a), which is different from membrane lipid synthesis. As discussed below, the synthesis of

sn-2 MAG is catalyzed by a bifunctional *sn*-2 GPAT/phosphatase, an enzyme discovered in our lab and only found in land plants (Yang et al., 2010; Yang et al., 2012).

While Bayberry glycerolipid-based surface wax and conventional plant surface waxes are both soluble and derived from fatty acids, they are quite different in their overall structure. Most plant surface waxes contain very long chain (> C20:0) alkenes, aldehydes, ketones, alcohols and wax esters of fatty acids and alcohols (Samuels et al., 2008). Fatty acids esterified to glycerol are not common components of plant waxes; however, a small amount of *sn*-2 MAG can be found in root-associated waxes (Li et al., 2007a). Instead, the basic structure of Bayberry surface wax is more similar to the insoluble glycerolipid polyester cutin, as they both consist of fatty acids esterified to glycerol (See Figure 4 A for proposed cutin assembly pathway)

While Bayberry wax contains unmodified fatty acids derived directly from FAS, most of the fatty acids in cutin are substituted with functional groups. One of the most common fatty acids in plant cutin is a C16:0 fatty acid that is hydroxylated at its omega and mid-chain positions (i.e. dihydroxypalmitate or DHP). Other common cutin monomers include C18:1 fatty acids containing an acid functional group at its omega position (dicarboxylic acid or DCA) and also epoxylated and trihydroxy C18 fatty acids (Pollard et al., 2008). Cutin is insoluble in part because hydroxy and acid groups allow for chemical bonds (i.e. esters) to form between the fatty acids and likely to polysaccharides in the cell wall (Pollard et al., 2008). Several cytochrome P450 enzymes from CYP86, and CYP77 families have been implicated in the hydroxylation steps (Wellesen et al., 2001; Xiao et al., 2004; Kurdyukov et al., 2006; Molina et al., 2008; Li-Beisson et al., 2009; Li et al., 2010), but some steps have not been determined and it is unclear whether the hydroxylation occurs on a free fatty acid or a CoA activated fatty acid (Pollard et al., 2008; Beisson et al., 2012).

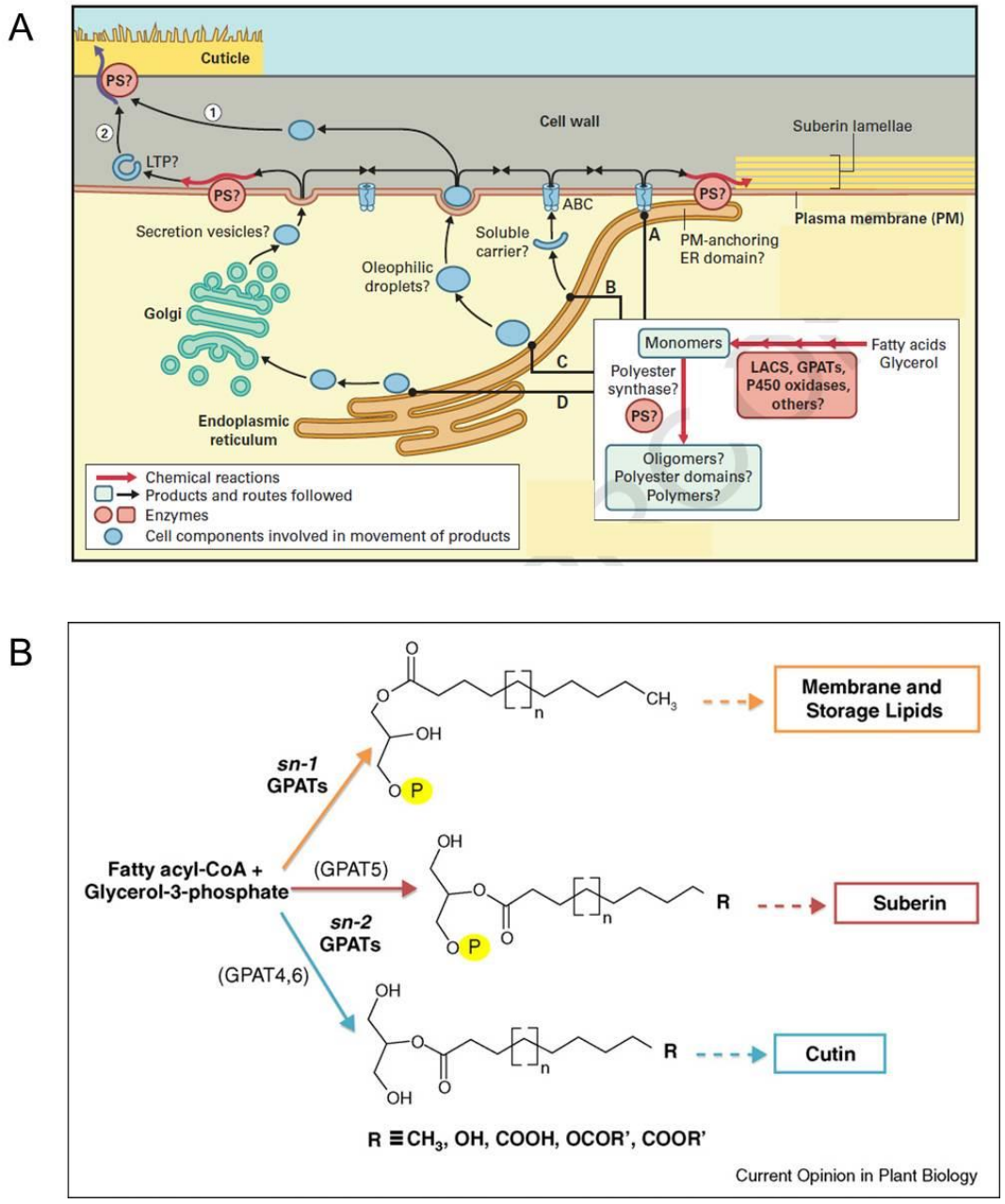

Figure 4: Pathways for cutin synthesis in plants. (A) Proposed pathway for the biosynthesis and secretion of cutin (Adapted from Buchanan et al., 2015). (B) The reactions catalyzed by glycerol-3-phosphate acyltransferases (Figure from Beisson et al., 2012). Abbreviations (not in main list): PS = polyester synthase.

The initial acyltransferase reaction for all glycerolipids is a fatty acyl-CoA esterification to a G3P molecule. In conventional glycerolipid synthesis, the acylation occurs on the *sn*-1 position of G3P to form *sn*-1 LPA and is catalyzed by a plastid or a putative ER localized *sn*-1 specific glycerol-3-phosphate acyltransferase (*sn*-1 GPAT) (Kunst et al., 1988; Cao et al., 2006). In contrast, the G3P acylation step in surface lipid cutin and suberin synthesis is onto the *sn*-2 position of G3P and is catalyzed by members of the *sn*-2 specific glycerol-3-phosphate acyltransferase (GPAT) family (EC 2.3.1.198 http://www.brenda-enzymes.info/enzyme.php?ecno=2.3.1.198) (Figure 4 B). Arabidopsis contains eight *sn*-2 GPATs (Zheng et al., 2003), with most involved in synthesis of different plant extracellular lipids. They include: (1) GPAT5 which is involved in the synthesis of suberin for roots and seed-coats (Beisson et al., 2007), (2) GPATs 4 and 8 which are involved in incorporation of 18:1 DCAs in leaf and stem cutin (Li et al., 2007b), (3) GPAT6 which is important for the incorporation of DHP into cutin (Li-Beisson et al., 2009), particularly in Arabidopsis flowers, and (4) GPAT1 which may be involved in lipid production for the tapetum (Zheng et al., 2003; Yang et al., 2012).

The first experimental indication that the initial step for surface lipid synthesis was different from conventional lipid synthesis was that ectopically expressing suberin-associated GPAT5 in leaves caused the accumulation of *sn*-2 MAG in leaf waxes (Li et al., 2007a). Subsequent *in vitro* assays revealed that GPATs 4, 6, 8, but not GPATs 1 and 5, contained phosphatase activity, producing *sn*-2 MAG (Yang et al., 2010; Yang et al., 2012). All enzymatically characterized GPATs (1, 4, 5, 6, and 8) prefer to acylate the *sn*-2 position of G3P, compared to the *sn*-1 position, and many prefer to use fatty acyl-CoAs containing omega hydroxy and carboxylic acid functionalities over normal fatty acyl-CoA's (Yang et al., 2014).

sn-2 MAGs can be secreted from plant cells and may serve as the primary backbone for cutin and/or the delivery molecule of fatty acids outside of the plant cell to be incorporated into cutin (Beisson and Ohlrogge, 2012). First, the fact that ectopic overexpression of suberin-associated GPAT5 allowed for the accumulation of *sn*-2 MAGs in leaf wax (Li et al. 2007a) indicated that *sn*-2 MAG can be secreted from epidermal cells. Second, when GPAT5 was co-overexpressed with a root expressed cytochrome P450-dependent fatty acyl oxidase (CYP86A1) involved in suberin production, suberin-like fatty acids were incorporated into leaf cutin (Li et al. 2007b). Together, these results suggested that fatty acids on *sn*-2 MAG can be incorporated into the cutin polyester and that the acyl transfer occurs extracellularly. Subsequent *in vitro* evidence revealed that an extracellular localized GDSL-motif enzyme from tomato (named *cutin deficient 1* or CD1), and an Arabidopsis homolog, can catalyze the transesterification of cutin-like fatty acids from *sn*-2 MAG onto the omega-hydroxy position of another cutin-like fatty acid (Yeats et al., 2012; Yeats et al., 2014). Tomato CD1 was originally identified because it caused a >90% reduction in total cutin monomers and a small amount of *sn*-2 MAG was detected in the soluble waxes (Girard et al., 2012; Yeats et al., 2012). Thus, the authors claimed that enzyme is the "cutin synthase" responsible for the extracellular assembly of cutin. While, the Arabidopsis homolog to CD1 exhibited the same activity *in vitro*, gene knockouts were not as severely disrupted in cutin, suggesting that additional enzymes, including other GDSL-motif enzymes, may be involved in cutin assembly or the incorporation of different fatty acids into cutin (i.e. 18:1 DCA's) (Yeats et al., 2014). It has also been proposed that cutin may be partially assembled non-enzymatically (Dominguez et al., 2015).

In addition to *sn*-2 GPATs and GDSL-motif enzymes, an annotated HXXXD motif (or BAHD) acyltransferase named "defective in cuticular ridges" (DCR) was demonstrated to be

important for DHP incorporation into the cutin polyester (Panikashvili et al., 2009). *dcr* knockout plants displayed a 70-80% reduction in DHP in flower and leaf cutin, but were not affected in the major leaf cutin monomer 18:1 DCA. Based on the acyltransferase activity of other related HXXXD enzymes, and the intracellular localization of DCR, the authors proposed that it may be involved in intracellular concatenation of CoA activated cutin monomers to create an oligomer which is then secreted and incorporated into extracellular cutin. *In vitro* assays with a variety of fatty acyl-CoA's and phenylpropanoid-derived molecules (which are substrates for other HXXXD enzymes) as acyl-donors and acceptors, did not produce any products (Panikashvili et al., 2009). However, subsequent *in vitro* assays, done by another group, demonstrated that DCR possessed MAG (forming DAG) and DAG (forming TAG) acyltransferase activity with unsubstituted fatty acyl-CoA's as the acyl-donors (Rani et al., 2010). Nevertheless, it is not clear whether DCR functions as a fatty acid acyltransferase *in vivo*, as DAG and TAG have not been identified as intermediates in cutin synthesis and the authors did not test cutin-like fatty acyl-CoAs and *sn*-2 MAG as substrates for DCR. Furthermore, enzymes of this family have broad substrate specificity and may be performing another reaction *in vivo* (Molina and Kosma, 2015).

1.6. Secretion of lipids to plant surfaces

Surface lipids must be transferred from their site of biosynthesis in the cell, then transported to the cell membrane, transverse the amphipathic cell membrane, and then move through the hydrophilic cell wall (Samuels et al., 2008). There are several proposed mechanisms for surface lipid transport, which are briefly reviewed below to provide context for consideration of mechanisms of Bayberry wax secretion.

1.6.1. Movement from the endoplasmic reticulum to the plasma membrane

The delivery of cuticular lipids to the plasma membrane (PM) may involve the secretory system, ER and PM fusion sites, protein carriers, oil-body mediated transport, or a combination of these mechanisms (Pollard et al., 2008; Samuels et al., 2008). McFarlane et al. (2014) identified a Golgi transport mutant which affected surface wax accumulation; however, it was not clear whether the Golgi is directly involved in wax transport or whether the mutation affected another molecule required for surface wax production. In epidermal cells rapidly synthesizing cutin, osmiophilic globules, which are diagnostic of lipid aggregations, were shown by transmission electron microscopy to fuse with the PM (Hoffmann-Benning and Kende, 1994) ; however, it has not yet been established if the globules contain cuticular lipids.

Intracellular movement of TAG, and movement of TAG through the PM have not been described in plants; however, there are some relevant examples in nature. In the symbiotic relationship between a photosynthetic *Zooxanthella* and the sea anemone *Condylactis giganta*, the *Zooxanthella* was visually and biochemically shown to synthesize 3.5μm diameter TAG-containing lipid droplets and deliver it into the tentacle tissue of the anemone (Kellogg and Patton, 1983; Patton and Burris, 1983). In another example, TAG- containing lipid droplets are released from mammalian epithelial cells by being enveloped by the PM, creating a tripartite membrane structure, which is then released into the surrounding extracellular space (Heid and Keenan, 2005). In Arbuscular mycorrhizal fungi, its intraradical mycelium transfers TAG contained in lipid bodies to its extraradial mycelium, and the lipid bodies were shown to move through the cells with the cytoplasmic stream (Bago et al., 2002).

1.6.2. Movement through the plasma membrane

In all biological kingdoms, ABC transporters have been implicated in the transport of lipids and other lipophilic substances through cell membranes.(Deeley et al., 2006; Davidson et al., 2008; Roston et al., 2014) although some research supporting passive diffusion has been reported (Hamilton et al., 2001). ABC transporters are ATP driven pumps with two transmembrane domains and two cytosolic domains. The subunits are encoded by one or two genes, which form homo- or heterodimers or act as full transporters (Kang et al., 2011). The plant genome encodes for more than 100 putative transporters, which can be organized into 8 families. ABC transporters have a number of important roles in plants such as intracellular lipid movement, detoxification of cells, biotic and abiotic stress tolerance, secretion of molecules for interaction with other cells and the environment, and cuticular lipid assembly (Kang et al., 2011). Members of the ABCG subfamily are associated with cutin and wax production (Kang et al., 2011). Cer5 (or ABCG12) was the first transporter identified that affected cutin load. The mutant was reduced in surface wax by over 50% compared to wild-type, and the epidermal cells of mutant plants contained sheet-like inclusions, which the authors proposed were surface lipids that were unable to be secreted (Pighin et al., 2004). Subsequently, it was discovered that ABCG12 forms a heterodimer with ABCG11 affecting only surface wax production, while ABCG11 forms a homodimer for cutin production (Bird et al., 2007; McFarlane et al., 2010). Other ABCG half transporters are required for the accumulation of cutin in Arabidopsis flowers (Panikashvili et al., 2011), potato tuber suberin (Landgraf et al., 2014), suberin in Arabidopsis seed coat and pollen walls (Yadav et al., 2014) and at least 2 full-size transporters have been associated with cutin accumulation (Bessire et al., 2011; Chen et al., 2011). It is important to note that despite clear reductions in wax and cutin in ABCG transporter mutants, the proteins

have never been demonstrated to transport specific cuticular lipids in reconstituted *in vitro* assays. Therefore, it not certain which molecules are transported, or even whether ABCG transporters actually transport lipids or transport another molecule required for surface lipid production.

1.6.3. Movement through the cell wall

Once lipids have been transported through the cell membrane, they have to move through the hydrophilic cell wall. This may occur through channels or pores, diffusion, protein mediated, or a combination thereof (Kunst et al., 2006). Lipid transfer proteins (LTPs) are a large class of extracellular proteins that are thought to carry lipids through the cell wall. LTPs have been implicated in this function because they are among the most abundant extracellular localized proteins, have a hydrophobic binding core and can interact with lipids (Thoma et al., 1993; Thoma et al., 1994; Pyee and Kolattukudy, 1995; Kader, 1996; Suh et al., 2005; Cameron et al., 2006; Yeats et al., 2010). While LTPs have cellular export sequences, they were first cited as intracellular lipid shuttles and may have a function inside cells (Arondel and Kader, 1990; Pagnussat et al., 2012). Only one LTP, named LTPG1, caused a decrease in cuticular wax load when knocked-out in Arabidopsis (Debono et al., 2009; Lee et al., 2009). LTPG1 is different from other LTPs because it has a GPI domain which anchors it to the PM; thus, the protein may not directly act as a carrier of lipids through the cell wall (Debono et al., 2009). Mutants in other LTP genes caused phenotypes suggestive of involvement in the secretion of substances, from pollen cells (Zhang et al., 2010; Huang et al., 2013), glandular trichomes (Choi et al., 2012) and roots (Lei et al., 2014). In addition, LTPs may be involved in cell wall expansion (Nieuwland et al., 2005), pathogen defense (Lindorff-Larsen et al., 2001; Bakan et al., 2006) and desiccation

tolerance (Cameron et al., 2006). While LTPs are small enough to be able to diffuse through the primary cell wall and mutant studies support a role in that process, there is no direct evidence that they actually transport cuticular lipids (Kunst et al., 2006).

1.7. Examining translational properties in alternative pathways for glycerolipid production and secretion

Prior to my work on Bayberry, the only data published regarding Bayberry wax was its abundance, the fact that it accumulates on the surface of fruits, and that it contained MAG, DAG and TAG (Harlow et al., 1965; Hawthorne and Miller, 1987). Based on that earlier background data, I considered multiple hypotheses regarding the possible biochemical pathways that Bayberry may have evolved to synthesize its unique surface wax. Specifically, the accumulation of TAG with normal saturated fatty acids (i.e. C16:0) suggested that the wax is synthesized by a pathway similar to TAG synthesis in oil-seeds (i.e. the Kennedy pathway). However, DAG and MAG are not detected as substantial components of seed lipids, and in plants, MAG is not an intermediate for *de novo* TAG synthesis. In contrast, the fact that the wax accumulates only outside of the cells suggests that Bayberry wax may be synthesized by reactions analogous to the production of extracellular glycerolipids, specifically cutin. However, the overall structure and fatty acid composition of cutin and Bayberry wax are different. In nature, there are other pathways and enzymes associated with the synthesis of TAG or related glycerolipids, which were also considered as possible reactions for Bayberry wax assembly.

1.7.1. sn-2 MAG as an intermediate for TAG synthesis

sn-2 Monoacylglycerol (MAG) accumulates to up to 4% of the mass of Bayberry surface wax. In addition to serving as a substrate for cutin synthesis in plants, *sn*-2 MAG is also an important intermediate for TAG accumulation in some mammalian cells. In order for calories from dietary TAG to be absorbed by mammals, the TAG is digested by pancreatic lipase in the intestine into free fatty acids (FFA) and *sn*-2 MAG. MAG and FFA are then absorbed by the intestinal enterocyte cells where an acyl: CoA monoacylglycerol acyl transferase (MGAT) catalyzes the incorporation of acyl-CoA onto *sn*-2 MAG to form DAG, which is then acylated again by DGAT to form TAG (Yen et al., 2002). The resynthesis of TAG from *sn*-2 MAG by these reactions is especially important to preserve unsaturated fatty acids and for synthesis of lipoproteins in intestines for fat transport (Yen et al., 2002). The mammalian MGAT1 (which is related to plant DGAT2) has been introduced into plants as an alternative pathway for TAG synthesis (Petrie et al., 2012). Also in plants, peanut cotyledons were reported to have a soluble MGAT enzyme. However, since the only known *de novo* synthesis of MAG in plants is through the *sn*-2 GPAT's for surface lipid synthesis (Yang et al., 2012), the physiological function of a seed MGAT enzyme may not be for *de novo* synthesis of TAG, but instead for re-acylation of MAG derived from degraded TAG (Tumaney et al., 2001; Vijayaraj et al., 2012).

1.7.2. Transacylase enzymes for TAG synthesis

Diacylglycerol acyltransferase (DGAT) enzymes catalyze transfer of fatty acyl-CoA's onto the *sn*-3 position of DAG to form TAG. However, there are several examples of acyl-CoA independent reactions involved in TAG synthesis in plants and animals. In plants, fatty acids from the *sn*-2 position of PC can be transferred to the *sn*-3 position of DAG, forming TAG and

lysophosphatidylcholine (LPC). This acyl-CoA independent reaction is catalyzed by the PC:DAG acyltransferase (PDAT) and is particularly important for incorporating desaturated fatty acids into the *sn*-3 position of TAG (Dahlqvist et al., 2000). In addition to PDAT, activity for a DAG:DAG transacylase, forming TAG and MAG, was identified in safflower microsomes and may contribute to some TAG synthesis in seeds (Stobart et al., 1997). However, an enzyme for that activity has not been discovered.

Mammalian cells can also synthesize TAG through acyl-CoA independent transacylases. Many of these reactions are catalyzed by lipase-like enzymes (Yamashita et al., 2014). While the name "lipase" may infer that the enzymes degrade lipids (i.e. lipolysis), under some conditions the same enzyme can catalyze the reverse reaction, resulting in synthesis or remodelling of lipids (Akoh et al., 2004). Related to this, lipase enzymes are used industrially for the inter-esterification of fat (i.e. in cocoa butter synthesis) to obtain different chemical properties (Schmid and Verger, 1998). Conditions that favor synthesis reactions by lipases include low pH and low water environments (Schmid and Verger, 1998). These are conditions that exist in the plant apoplast, and the adjoining cuticle where cutin may be assembled by extracellular lipases (Beisson et al., 2012)

The class of lipase-like enzymes that have become associated with surface lipid synthesis are the GDSL-motif lipases/transacylases. Recently, such enzyme was identified as a "cutin synthase" in tomato (CD1), and also displayed the same activity in Arabidopsis (Yeats et al., 2012; Yeats et al., 2014). *In vitro* assays revealed that CD1's primary activity is the extracellular acyl-CoA independent transesterification of MAG to create a cutin-like polyester. Interestingly, and of importance to this thesis, minor products in assays with CD1 and *sn*-2 MAG were DAG and TAG (Yeats et al., 2012). GDSL-motif enzymes are highly expressed in epidermal cells (Suh

et al., 2005) and are abundant proteins in extracellular spaces (Yeats et al., 2010; Ge et al., 2011). There are over 100 genes annotated as GDSL-motif enzymes in the Arabidopsis proteome, thus, it is possible that more than one GDSL-motif enzyme can catalyze the extracellular assembly of cutin and suberin glycerolipids. In addition to CD1, there are two other examples of GDSL-motif enzymes in plants that catalyze synthesis reactions, although not with lipids. TGLIP from *Tanacetum cinerariifolium* catalyzes the transfer of a chrysanthemoyl-CoA to pyrethrolone to synthesize pyrethrin I (Kikuta et al., 2012). In tomato, a GDSL-motif enzyme was identified that catalyzes the acyl-CoA independent synthesis of caffeoylglycearate and caffeoylgalactarate form chlorogenate (Teutschbein et al., 2010). Interestingly, the protein retained synthesis ability even after the removal of the serine residue important for lipase activity. Although there are many other GDSL lipase-motif enzymes in plants, a very small number have been studied and the few that have been characterized reveal a diverse array of functions (Volokita et al., 2011).

1.7.3. Similarities between the production of Bayberry wax and synthesis and secretion of TAG estolides

For successful pollination, the surfaces of stigmas must be receptive to and bind pollen. To accomplish this, many stigmas are coated with a viscous mixture of proteins and carbohydrates and also lipid polyesters called estolides (i.e. wet stigmas) (Cresti et al., 1986; Wolters-Arts et al., 1998). In the wet stigmas of petunia flowers, lipid estolides are essential for pollen tube growth (Wolters-Arts et al., 1998). The stigma exudate was shown by microscopy to be produced and released by cell rupture from multiple stigma cell layers, as opposed to just the surface cells (Konar and Linskens, 1966; Mackenzie et al., 1990). The estolides are similar in structure to cutin in that it is a polyester of omega hydroxy- fatty acids that are esterified to each

other and to a glycerol backbone. However, unlike cutin, the estolides are soluble, linear, and contain only 4-8 omega hydroxy fatty acids esterified to 2-3 positions of a glycerol molecule (i.e. like DAG and TAG), and are capped with a non-hydroxy fatty acid (Matsuzaki et al., 1983; Koiwai and Matsuzaki, 1988).

Intermediates in the assembly of TAG estolides and enzymes required for the assembly of TAG estolides are not known. However, a P450, similar to P450s used to hydroxylate cutin monomers (CYP86 family), is important for the accumulation of hydroxy fatty acids in TAG estolides in petunia stigmas (Han et al., 2010). This suggests that enzymes involved in cutin assembly may also be used for estolide synthesis.

1.8. The use of [^{14}C] labeled compounds to study lipid metabolism

Significant progress in plant biochemistry has been greatly aided by development of radioactive isotopes (i.e. ^{14}C, ^{3}H, ^{35}S, ^{32}P, ^{33}P) that can be used as 'tracers' for metabolic reactions and pathways. Biochemical pathways and reactions have been elucidated by feeding and then measuring the incorporation of isotopically labeled compounds into intact tissues, isolated organelles, or used in enzyme assays. As one of many examples, the crucial discoveries of Calvin and Benson relied on incubations with [^{14}C]-labeled bicarbonate to discover the carbon fixation reactions of photosynthesis. [^{14}C] is a particularly useful tracer to study metabolism because carbon occurs in almost all molecules, it is safe, relatively easy to detect, has an extremely low natural abundance, and has a long half-life (5730 years) (Allen et al., 2015). In lipid metabolism, [^{14}C]-acetate, [^{14}C]-glycerol and [^{14}C]-fatty acids have been the precursors most used to study membrane and storage lipid synthesis in leaves and oil seeds and to infer metabolic precursor-product relationships, pool sizes and fluxes (Roughan and Slack, 1982;

Harwood, 1988; Bates and Browse, 2012; Allen et al., 2015). [^{14}C]-acetate rapidly enters plastids and is activated into acetyl-CoA which is used as a substrate for FAS, while [^{14}C]-glycerol is phosphorated and labels the glycerol backbones of lipids.

Key information about metabolic pathways can be inferred by the order and the relative time it takes for a labeled substrate to accumulate linearly in each compound of a pathway. For example, in the hypothetical pathway A→B →P (Figure 5), A is considered a precursor to B if [^{14}C] in A saturates at approximately the same time as linear labeling is detected in compound B, and the time it takes for this to occur corresponds to the pool size of compound A (Allen et al., 2015). Pool sizes of intermediates can be calculated by the equation: lag time = ln2/k, where k = rate of lipid accumulation / substrate pool (Segel, 1968) (Figure 5).

The mechanism of fatty acid incorporation into glycerolipids has been determined by radiolabelling a number of different oil seeds of different fatty acid compositions (Bates and Browse, 2012; Allen et al., 2015). In general, and relevant to the interpretation of labeling experiments in this thesis on Bayberry, saturated/monounsaturated and polyunsaturated fatty acids flux though different metabolic pools prior to their incorporation into TAG. In most oilseeds, the fatty acids produced from plastid FAS are C16:0, C18:0 and C18:1; but glycerolipids contain a large amount of polyunsaturated 18:2 and 18:3 fatty acids. In the predominant "eukaryotic" glycerolipid assembly pathway, FAD2 and FAD3 desaturate 18:1 fatty acids on PC to 18:2 and 18:3 (Ohlrogge and Browse, 1995). Initial incorporation of 18:1 into PC for desaturation may occur through acyl-editing (Bates et al., 2007; Bates et al., 2009; Tjellstrom et al., 2012) or by DAG to PC conversion (Lu et al., 2009). Regardless of the mechanism, in tissues that contain 18:2 and 18:3 fatty acids, [^{14}C]-acetate labeled fatty acids are initially incorporated into [^{14}C]-PC at high levels, relative to DAG and TAG. However, in plants that

accumulate TAGs with primarily saturated and monounsaturated fatty acids (e.g. *Cacao*, *Cuphea*, avocado mesocarp) newly synthesized fatty acids do not appear as abundantly on PC, presumably because they do not require desaturation (Stobart and Stymne, 1985; Griffiths et al., 1988; Bafor et al., 1990; Griffiths and Harwood, 1991; Bates and Browse, 2012). Instead, newly synthesized fatty acids enter a common acyl-CoA pool where they then have an equal chance of reacting with G3P, lysophosphatidic acid (LPA) or DAG via the Kennedy pathway and thus produce [^{14}C]-DAG and -TAG at equal initial rates. Therefore, if Bayberry wax is synthesized by a conventional TAG synthesis pathway, PC would not be highly labeled.

Despite the use and value of [^{14}C]-labeled lipid substrates in understanding membrane and oil-seed lipid synthesis, very few similar studies have been done on the biosynthesis of surface lipids. This may be because it is difficult to separate the surface lipid synthesising epidermal cells from the mesophyll cells that are synthesizing lipids for membranes. The first documented use of [^{14}C] acetate to study surface lipid metabolism was by Kolattukudy (1965) investigating the biosynthesis of leaf waxes in *Brassica oleracea.* He observed that after 4 h of labeling, approximately 4% of the added acetate was in leaf wax, with major component C29 alkanes incorporating greater than 90% of that radioactivity. He also examined cutin synthesis by labeling leaf discs from beans and peas with [^{14}C]-acetate and [^{14}C]-labeled fatty acids. Both labeled compounds were detected in the cutin within 30min to 1h with no noticeable lag; after 4h 6-7% of the label from acetate and 15-18% of the label from fatty acids were detected in cutin (Kolattukudy, 1970; Kolattukudy and Walton, 1972). Considering entire leaves were labeled in those studies, and not epidermal peels, cutin appears to be a significant destination for fatty acids in leaves. Despite the considerable flux of lipids into cutin, the cutin-like fatty acids (i.e. omega and mid-chain oxygenated) were not detected in any soluble lipid pools (i.e. membrane lipids,

PC, DAG) (Kolattukudy and Walton, 1972). This suggests that the pools of fatty acids destined for the surface lipids are separated from the lipid pools destined for membrane synthesis. There have been no studies examining how glycerol is incorporated into the cutin polyester.

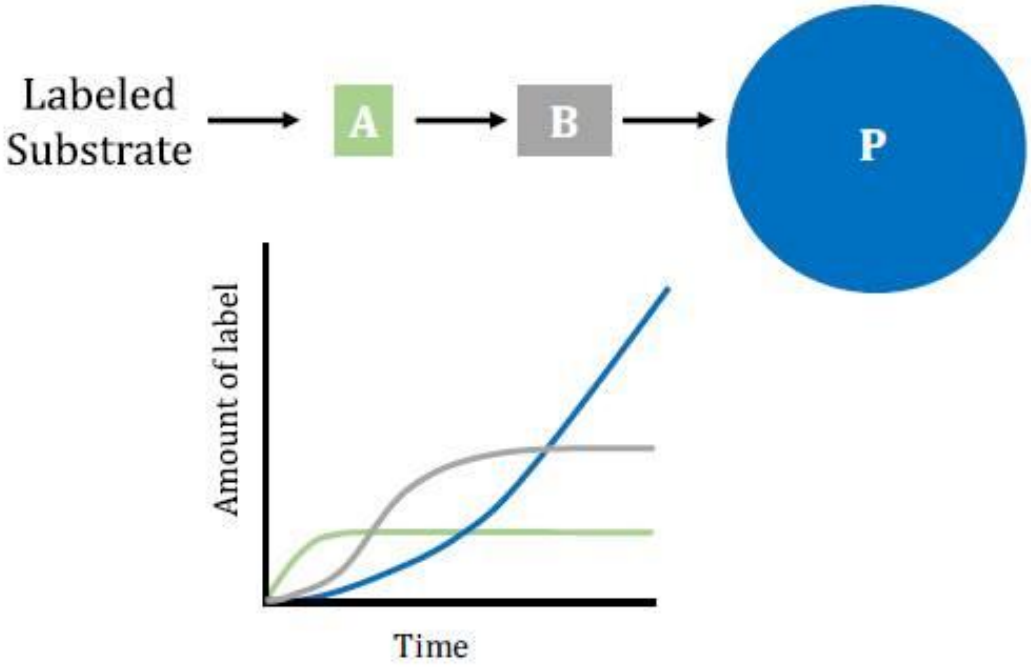

Figure 5: Excepted labeling results in a liner metabolic (A→ B → P) pathway with a continuous pulse of a labeled substrate. The labeled substrate first enters intermediate pool A. As pool A is filling to its fixed size (i.e. compounds incorporating label), there is a lag in incorporation of label into compound B. When pool A reaches a steady state (i.e. indicating filling), label in pool B increases linearly. The same relationship is observed between pool B and product (P). Label continuously accumulates in P until the pulse of labeled substrate ends. Figure from Allen et al., (2015).

1.9. The power of transcriptomics in deciphering lipid metabolism

Qualitative and quantitative assessments of unique and industrially important plant traits from a diverse range of species have been made possible because of developments in high-throughput sequencing of cDNA produced from mRNA (Ohlrogge and Benning, 2000; Weber, 2015). Initially this approach was called EST sequencing, where a few hundred or thousand randomly selected clones from a cDNA library were sequenced by the Sanger method (i.e. dideoxy terminator) and also counted. However sequencing cDNA clones introduces many biases (i.e. because of the cloning steps) and only works well for highly abundant transcripts (Ohlrogge and Benning, 2000). Today, massively parallel methods of sequencing (i.e. next generation sequencing or NGS), such as 454 sequencing and Illumina HiSeq, are able to generate hundreds of thousands to millions of reads with deep converge from fragmented cDNA, and importantly without a cloning step. The sequence data is then assembled *in silico* into contigs representing the genes expressed in the tissue, and number of reads per sequence can be counted to obtain transcript abundance. This high-throughput method had led to the discovery of new enzymes, unknown regulators, and helped understand the underlying genes that may be required for the expression of a trait (Weber, 2015). While the ultimate determinant of a plant trait are the levels of the proteins, in most cases, and especially for highly abundant transcripts, the abundance of mRNA and protein are well correlated (Ponnala et al., 2014). Furthermore, cDNA sequencing can be done with higher throughput, more sensitivity and at a lower cost than proteomics (Weber, 2015).

One of the earliest examples of gene discovery from cDNA sequencing was the discovery of the hydroxylase for ricinoleic acid biosynthesis in castor (van de Loo et al., 1995). Their approach for gene discovery was successful because castor endosperm triacylglycerol contains

85-90% ricinoleic acid, and accordingly the hydroxylase was one of the most highly expressed genes in the tissue. Measuring transcript abundance by sequencing cDNA clones was done on genes involved in lipid metabolism (Mekhedov et al., 2000). More recently, NGS of cDNAs derived from lipid producing tissues has been used to understand the mechanisms that allow for differences in oil composition and quantities in plants. Notably, the expression of lipid genes have been compared between plants that accumulate oil in different tissues (i.e. embryos, endosperms, arils, mesocarps) and also between genetically related species which differ in oil quantity and quality (Bourgis et al., 2011; Troncoso-Ponce et al., 2011; Kilaru et al., 2015). Those studies have identified regulatory genes, the genetic basis behind different oil compositions, how different tissues accumulate oil, and the pathways by which reduced carbon is assembled into fatty acids (Bourgis et al., 2011; Troncoso-Ponce et al., 2011; Kilaru et al., 2015). More recently, NGS has also led to the identification of genes involved in the synthesis of unusual oils, such as acetyl-TAG in Euonymus (Durrett et al., 2010), and thioesterases from *Cuphea* responsible of the synthesis of short chain fatty acids in TAG (Kim et al., 2015**).** There have also been some efforts to use NGS to identify genes involved in the production of surface lipids wax and cutin (Mintz-Oron et al., 2008; Matas et al., 2010; Matas et al., 2011; Alkio et al., 2014).

In addition to studying lipid metabolism, NGS sequencing has proved very useful in identifying enzymes of specialized metabolism. Some important examples include: (1) comparison of C3 and C4 and intermediary species to identify genes important for the evolution of C4 crops (Brautigam et al., 2014), (2) discovery of enzymes for the synthesis of monoterpene alkaloids (Gongora-Castillo et al., 2012), (3) discovery of genes required for the domestication of tomato (Koenig et al., 2013), (4) understanding xyloglycan biosynthesis in *Nasturitum* (Jensen et

al., 2012), and (5) discovery of an acyltransferase to introduce ester linkages in lignin from *Angelica sinensis*, which was transformed into poplar to produce a more digestible lignin (Wilkerson et al., 2014).

Obtaining a good gene expression resource often relies on being able to isolate the correct cell type, sequencing multiple developmental stages, and comparing results to genetically-related tissues. In many cases, for molecules that are produced in large amounts, the biosynthetic genes tend to be some of the most abundantly expressed genes the tissue (Schilmiller et al., 2010; Tissier, 2012). Indeed, Bayberry knobs secrete up to 30% of its DW in surface wax and highest expressed sequences were associated with acyl-lipid metabolism (Chapters 2 and 3).

CHAPTER 2

A NOVEL PATHWAY FOR TRIACYLGLYCEROL BIOSYNTHESIS IS RESPONSIBLE FOR THE ACCUMULATION OF VERY ABUNDANT GLYCEROLIPIDS ON THE SURFACE OF BAYBERRY (*MYRICA PENSYLVANICA*) FRUITS

Submitted to The Plant Cell (October, 2015)

Authors: Jeffrey P. Simpson and John B. Ohlrogge

2.1. Acknowledgements

We are grateful to Henrik Tjellstrom and Mike Pollard for help with labeling and lipid analysis, and Patrick Horn for critical reading of this the manuscript (all of Michigan State University (MSU)). We thank the MSU Center for Advanced Microscopy's Abby Vanderberg and Melinda Frame for sample preparation and assistance with SEM and confocal microscopy, respectively. Mathias Schuetz (University of British Columbia) also helped with confocal microscopy and Starla Zemelis (MSU) provided guidance for fixation of Bayberry tissue for microscopy. Adam Rice (MSU) performed the differential scanning calorimetry analysis of Bayberry wax. RNA sequencing was performed by the DOE Joint Genome Institute (JGI), with special assistance from Kerrie Barry, Erika Lindquist and Anna Lipzen. Transcriptome assembly and databases were provided by Nick Thrower (MSU) and Curtis Wilkerson (MSU). We also thank Kurt Stepnitz (MSU) for assistance with time-lapse photography and the MSU Grounds department for maintenance of the Bayberry shrubs. This work was supported by Department of Energy–Great Lakes Bioenergy Research Center Cooperative Agreement DE-FC02-07ER64494. J.P.S. received a National Science and Engineering Research Council of Canada (NSERC) post graduate fellowship (PGS-D3).

2.2. Abstract

Bayberry fruits synthesize an extremely thick and unusual layer of crystalline surface wax that accumulates to 30% of fruit dry weight, the highest reported surface lipid accumulation in plants. The composition is also striking, consisting of completely saturated triacylglycerol, diacylglycerol and monoacylglycerol with palmitate and myristate acyl chains. To gain insight into the unique properties of Bayberry wax synthesis we examined the chemical and morphological development of the wax layer, monitored wax biosynthesis through [^{14}C]-radiolabeling, and sequenced the transcriptome. Radiolabeling identified *sn*-2 MAG as the first glycerolipid intermediate. The kinetics of [^{14}C]-DAG and [^{14}C]-TAG accumulation and the regiospecificity of their [^{14}C]-acyl chains indicated distinct pools of acyl donors and that final TAG assembly occurs outside of cells. The most highly expressed genes were associated with production of cutin, whereas transcripts for conventional TAG synthesis were >50-fold less abundant. The biochemical and expression data together indicate that Bayberry surface glycerolipids are synthesized by a previously unknown pathway for TAG synthesis that is related to cutin biosynthesis. The combination of a unique surface wax and massive accumulation may aid understanding of how plants produce and secrete non-membrane glycerolipids, and also how to engineer alternative pathways for lipid production in non-seeds.

2.3. Introduction

The aerial surfaces of plants are covered with a variety of soluble and insoluble lipids that together constitute the cuticle. Waxes are a component of the plant cuticle, and together with the glycerolipid polyester cutin provide plants with their primary interface with the external environment. The most common surface waxes found on plants are derived from fatty acids modified to form very-long-chain hydrocarbons, alcohols, aldehydes, ketones and wax esters of fatty acids and alcohols (Samuels et al., 2008). However, the wax that accumulates on the surfaces of the fruits of some species of North American Bayberry plants (*Myrica* or *Morella* sp.) are strikingly unusual in abundance and composition. The surface density of Bayberry wax determined in this study is 9 μg wax cm^{-2}, which is ten to one thousand fold higher than other plant species (Kolattukudy, 1976; Baker, 1982; Jetter et al., 2006) making it the highest reported accumulation of surface wax in the plant kingdom. Furthermore, Bayberry fruit wax is composed almost entirely of the glycerolipids triacylglycerol (TAG) and diacylglycerol (DAG) with small amounts of monoacylglycerol (MAG). Adding to its distinctiveness, the fatty acids in the surface lipids are entirely saturated, primarily palmitic (C16:0) and myristic (C14:0). Despite these unique features Bayberry is rarely cited as a massive accumulator of surface wax, or as a plant tissue that produces large amounts of glycerolipids. In the past 100 years there have been four studies examining the morphology and composition of Bayberry fruits and its surface wax – a thesis by H. Youngken (1915) and three brief reports on the chemical composition of the surface wax (McKay, 1948; Harlow et al., 1965; Hawthorne and Miller, 1987). The thick unusual wax layer is attractive to and digestible by some species of birds and may have evolved as a seed dispersal mechanism (Fordham, 1983) (Place and Stiles, 1992). Owing to the striking abundance

and exclusively saturated fatty acid content that confers a high melting point to the wax, a traditional use of Bayberry wax is to make holiday candles (Williams, 1958)

To our knowledge TAG, DAG and MAG have never been reported as abundant constituents in the surface waxes of other plant species and details of the accumulation of DAG and TAG as major components of Bayberry surface wax have not been described. In plants, TAG is most abundantly produced in seeds, pollen and the mesocarps of some fleshy fruits (i.e. avocado, oil palm, olive). The simplest pathway to produce TAG in those tissues involves two acylations of glycerol-3-phosphate (G3P) with fatty acyl-CoA to produce phosphatidic acid (PA). After phosphate removal, the resulting DAG is further acylated to yield TAG (Chen et al., 2015) that is then sequestered into oil bodies or lipid-droplets within the cytoplasm (Chapman et al., 2012). Although Bayberry is exceptional in its massive extracellular accumulation of TAG and DAG, plants do accumulate extracellular lipids containing glycerol in the form of cutin and suberin. Extracellular or surface lipids are synthesized and secreted from the single layer of epidermal cells on the outer plane of aerial tissues. Aerial epidermal lipid metabolism is largely devoted to the production and secretion of lipids, with 2/3 or more of all acyl chains synthesized in this cell monolayer destined to become wax or cutin (Suh et al., 2005). However, in contrast to seeds and other TAG accumulating plant tissues, surface lipids do not accumulate within epidermal cells and unlike the fatty acids of membrane and storage lipids, most fatty acids in cutin and suberin are modified by omega and mid-chain oxygenations which allows inter-esterification reactions to form a lipophilic and insoluble polymer (Pollard et al., 2008; Samuels et al., 2008).

Epidermal cells clearly evolved mechanisms to separate membrane fatty acids from the unusual fatty acids that form the cuticle, and also the ability to secrete the lipids through the cell

membrane, cell wall and onto external surfaces. Because Bayberry accumulates on its fruit surface very large quantities of glycerolipids that are typically intracellular, it was not clear how these lipids are exported and whether the TAG and DAG are synthesized by reactions similar to oil seeds or perhaps by a previously undescribed pathway. The objective of this study was to identify similarities or differences between Bayberry wax production and conventional surface lipid and intracellular glycerolipid production. Research on plants that produce such large amounts of surface lipids may provide insights into the molecular features and biochemical pathways for plant surface lipid secretion. In addition, studying Bayberry wax triacylglycerol production may help elucidate mechanisms for non-polar lipid production, particularly in non-seed tissues. We initiated this work by examining changes in fruit anatomy, details of the chemical structures secreted by Bayberry fruits, and quantifying the accumulation of wax through an entire growing season. Biochemical pathway analysis by [^{14}C]-labeling, and transcript analysis by RNA-seq revealed features of Bayberry wax accumulation that are strikingly different from conventional TAG production. Together, these results indicate that the extracellular glycerolipids in Bayberry wax, including TAG, are synthesized by a novel pathway that is different from any previously defined TAG biosynthesis pathway in plants. An increased understanding of this process may prove useful in engineering plants for secretion of high value lipids, particularly those that have toxic or negative consequences when accumulated inside cells.

2.4. Results and discussion

2.4.1. Bayberry surface wax accumulates to the highest levels reported for plants and is composed entirely of saturated glycerolipids

Mature Bayberry fruits are covered with a strikingly thick layer of surface wax (Figure 6). As with most other soluble waxes on the surfaces of plants (Jetter et al., 2006), Bayberry wax can be removed by immersing the fruits for a short time (30 seconds) in an organic solvent, such as chloroform, without removing typical internal membrane lipids (Figure 16). Gravimetric determination of surface wax from mature Bayberry fruits yielded 10.0 (± 1.2) mg fruit $^{-1}$. This is 32% of the entire fruit dry weight (DW) (Table 1), is comparable to 25% from an earlier report (Harlow et al., 1965), and when calculated based on fruit surface area is 8.7 mg cm^{-2}. The amount of surface wax on mature Bayberry fruits is higher than any levels of surface lipid reported for the plant kingdom and possibly in nature (Kolattukudy, 1976; Baker, 1982; Jetter et al., 2006).

The composition of chloroform soluble surface waxes was analyzed by thin-layer chromatography (TLC) and by high-temperature GC-FID. TLC identified the major components of the wax as triacylglycerol (TAG) and diacylglycerol (DAG) with minor bands aligning with monoacylglycerol (MAG) and free fatty acid (FFA) standards (Figure. 6A). Analysis of intact lipids by GC-FID confirmed TAG, DAG and MAG as the major components of mature Bayberry surface wax and indicated a molar ratio of 30:62:8 between them (Figure 17). Common plant surface waxes (i.e. alkanes etc.) were not detected on the TLC plate or in the GC-FID chromatogram and gravimetric quantification (10.0 mg fruit^{-1}) of the surface wax was very similar to the GC FID quantification (10.7 ± 1.9 mg fruit^{-1}). To our knowledge Bayberry is the only plant reported to contain almost exclusively glycerolipids in its surface wax. Also intriguing

was that we could only detect saturated fatty acid species in TAG, DAG and MAG; predominantly C16:0 (>75%) and C14:0 (< 25%) with trace amounts of C18:0 (<1%). TAG or DAG containing such a high percentage of C16:0 fatty acids, with no unsaturated fatty acids, has also never been reported for plants (Badami and Patil, 1981; Banerji et al., 1984; Gunstone et al., 2007).

2.4.2. Bayberry wax accumulates continuously through eight weeks of fruit maturation

Cuticular lipid production (i.e. wax and cutin) by epidermal cells involves the coordinated action of intracellular lipid synthesis, trafficking of lipids within the cells, and movement of the cuticular lipids through the cell membrane and the cell wall (Beisson et al., 2012). The cuticular lipid layer is established during the initial stages of tissue development and cuticular lipid synthesis is highest in young expanding tissue (Suh et al., 2005). Because of the unique composition and abundance of Bayberry surface wax, we asked whether its mechanism of surface wax production is similar to conventional cuticular lipid production and secretion (Samuels et al., 2008). Figure 6 presents images of the developmental progression of Bayberry fruits by light microscopy (B) and scanning electron microscopy (SEM) (C). Surface wax became first visible to the naked eye approximately one month after pollen production by the male flowers. At that time, the fruits were green, fully exposed from the flower bracts, and appeared to be fully developed. The surface wax initially appeared in small separated clusters on the fruit surface, but gradually spread to cover the entire surface of the fruits and thickened considerably. This process extended over approximately eight weeks, after which the wax layer persisted on the fruits through the fall and winter months. SEM images of the fruits prior to wax detection show a smooth surface devoid of any of the crystals that appear later in the season

(Figure 6 C). At the earliest stages of wax accumulation, sharp crystals congregated in the junctions between the epidermal pavement cells and as the season progressed the fruit surface became completely covered with the greyish-white wax coating. The ultrastructure of the layer was fissured and crust-like. In this regard, mature Bayberry wax appeared similar to many succulents that accumulate thick layers of wax (Barthlott et al., 1998).

The quantity and composition of the surface wax determined by GC-FID throughout 160 days of development, beginning approximately two weeks after pollen production (Figure 6 D). In agreement with the images, surface wax was not detected in the youngest fruits analyzed (days 1 – 12). By day 14, glycerolipids were detected in the surface wax and the highest amount of surface wax occurred approximately 70 days after initial detection (day 90 of this analysis). Three distinct periods of accumulation were identified during this analysis; Stage 1) days 1-19 when 2% of the wax was deposited; Stage 2) days 19-45, when 15% of wax was deposited; Stage 3) days 45 – 90 when the remaining 83% of the wax was deposited, The mean daily rate of wax accumulation during stage 3 was 3 µg g FW^{-1} or 200 µg $fruit^{-1}$. Interestingly, the fruits approached their maximum fresh weights prior to the majority of the wax being deposited (Figure 18). This indicates that most of the wax on Bayberry fruits was deposited on fully formed fruit tissues, rather than accumulating through the initial stages of fruit development like cutin and most conventional surface waxes (Suh et al., 2005; Jetter et al., 2006). During a fourth stage, from days 90-159, there was a 5-10% loss in surface wax, which may be attributable to some shedding of the wax layer, animal or insect feeding, or microorganism degradation.

Table 1: Wax accumulation on Bayberry fruits and knobs based on different fruit measurements. Wax and fruit parts were measured gravimetrically.

	In a single fruit	**In a single knob**
Total wax	9.8 mg	0.043 mg
Wax per surface area	8.7 mg cm^{-2}	---
Wax per fresh mass	15 %	28 %
Wax per dry mass	31 %	56%

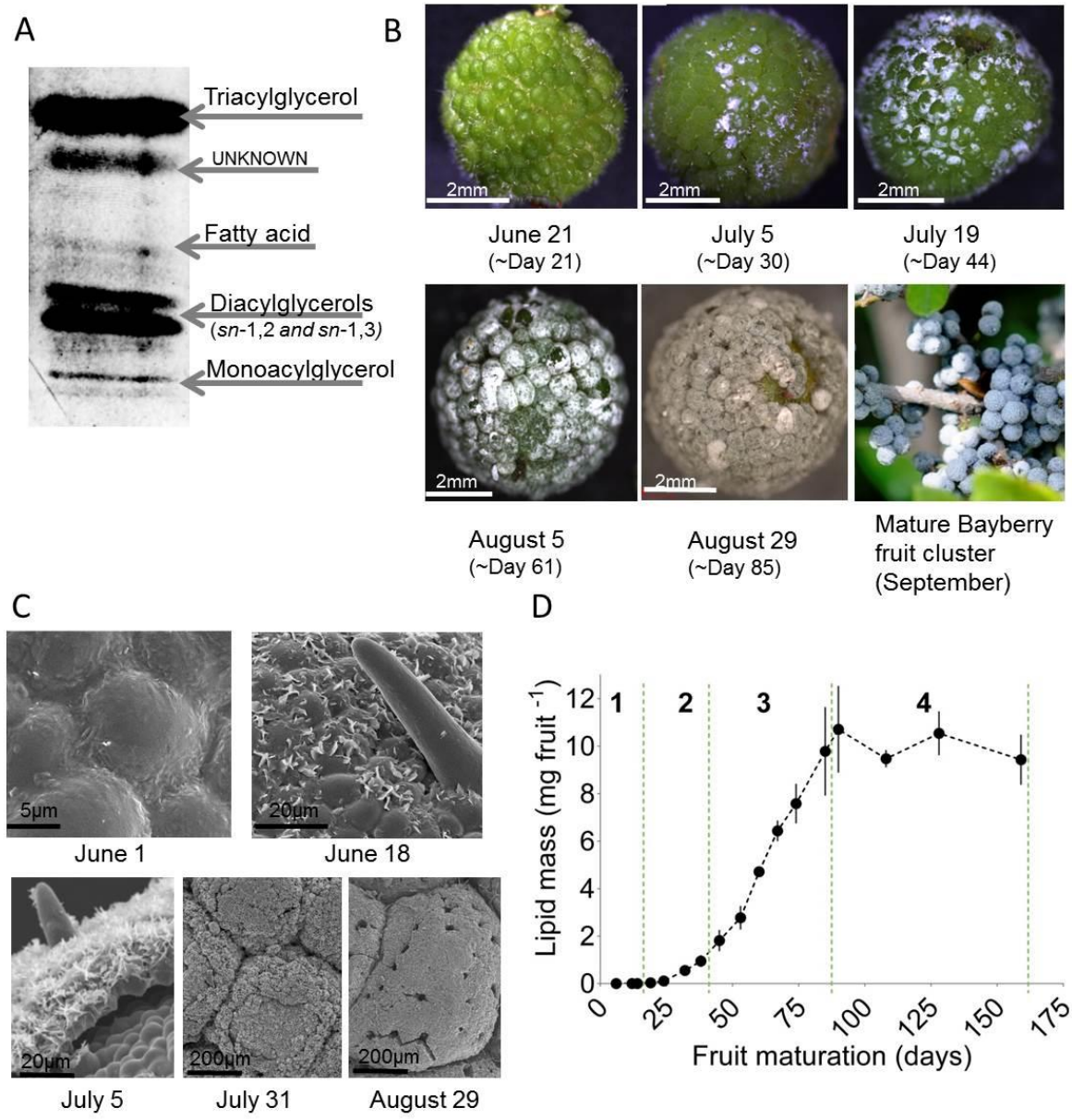

Figure 6: Progression of wax accumulation on the surfaces of Bayberry fruits through development. (A) Thin layer chromatography separation of mature Bayberry wax. After development the plate was sprayed with primuline and viewed under UV. (B) Light microscopy images through the growth season. (C) Scanning electron microscopy images of Bayberry fruits. (D) Mass of glycerolipids in Bayberry wax through the season, determined by GC-FID. Stages of wax accumulation are designated by the dotted green lines. Each point represents the mean of 3-4 replicates ±SE.

2.4.3. Bayberry surface wax is produced by “knobs”: An unusual multicellular tissue that extends from the fruit exocarp

The wax that accumulates on the surface of Bayberry fruits appears on three sides of multicellular structures that extend from the surface of the fruit proper (exocarp) (Figure 7 A). These structures are referred to as “knobs” (Harlow et al., 1965). The fruit (drupe) is five mm in diameter and its entire surface is covered with 200-250 knobs. Each knob is approximately ~500 µm in diameter, contains greater than 10,000 cells, and is connected to the fruit proper by a vascular system that runs along the circumference of the fruit into each knob (Figure 7 B). The large size and uniform distribution of the knobs on the fruit make them distinctly different from other surface protrusions in plants, such as trichomes. Non-wax producing *Myricaceae* species (i.e. *Myrica rubra*) also appear to have knobs, suggesting these structures are a feature of the fruits of the *Myricaceae* family (Feng et al., 2012)rather than specific for a large accumulation of surface wax.

To investigate cellular and subcellular sites associated with the massive production and secretion of surface wax by Bayberry, the neutral lipid fluorescent dyes Nile Red or BODIPY493/503 were applied to freshly-harvested intact fruits and cross sections of the fruits and were imaged by confocal microscopy (Figure 7 C to F). At both early and mid-stages of development, staining by both dyes was strongest around the knobs, and not within any structures of the fruit proper (Figure 7 C and D). This is unlike oil palm, olive, or avocado which accumulate lipids as a major component of their fruit mesocarp. There was also very little lipid staining within the inner interstitial layers of the knobs. Moreover, we did not detect any stained subcellular structures characteristic of lipid droplets, or other defined structures indicative of accumulation of lipids within the knob cells. Staining fruits after rapid removal of wax by

dipping in chloroform also did not expose intercellular or interstitial lipids that might not have been visible due to the strong signal from the lipids on the immediate surface (Figure 7 F). Together, these results indicate that the wax, or neutral lipid precursors, do not accumulate to detectable levels within the cells or interstitial spaces.

Each knob produces and secretes approximately 40 µg of wax, which is greater than 50% of its dry weight (DW) (Table 1). The crystallization temperature of extracted Bayberry wax, as determined by differential scanning calorimetry, was greater than 40°C (Figure 19), which is much higher than other plant oils that accumulate within cells (Gunstone et al., 2007). Presumably, if these surface glycerolipids accumulated within the knob cells they might exist as a solid, potentially restricting further movement to the surface, and also affecting cell function.

The gradual accumulation of surface wax and the apparent lack of significant lipid storage inside the fruit tissues indicates that Bayberry surface wax is actively secreted from the knobs through development, rather than released as a senescence-related disintegration of outer layers of the fruit. The lack of storage within knob cells is in contrast to other TAG accumulating plant tissues. For example, extracellular triacylglycerol estolides on the surface of ‘wet’ stigmas and lipids that coat pollen appear to initially accumulate inside cells, and are deposited on the surface when cells rupture (Konar and Linskens, 1966; Murphy, 2001). Instead, the mechanism that Bayberry employs is similar to the deposition of conventional surface lipids, where lipids do not accumulate within cells (Pighin et al., 2004) and are exported from the cells to the surface immediately after synthesis.

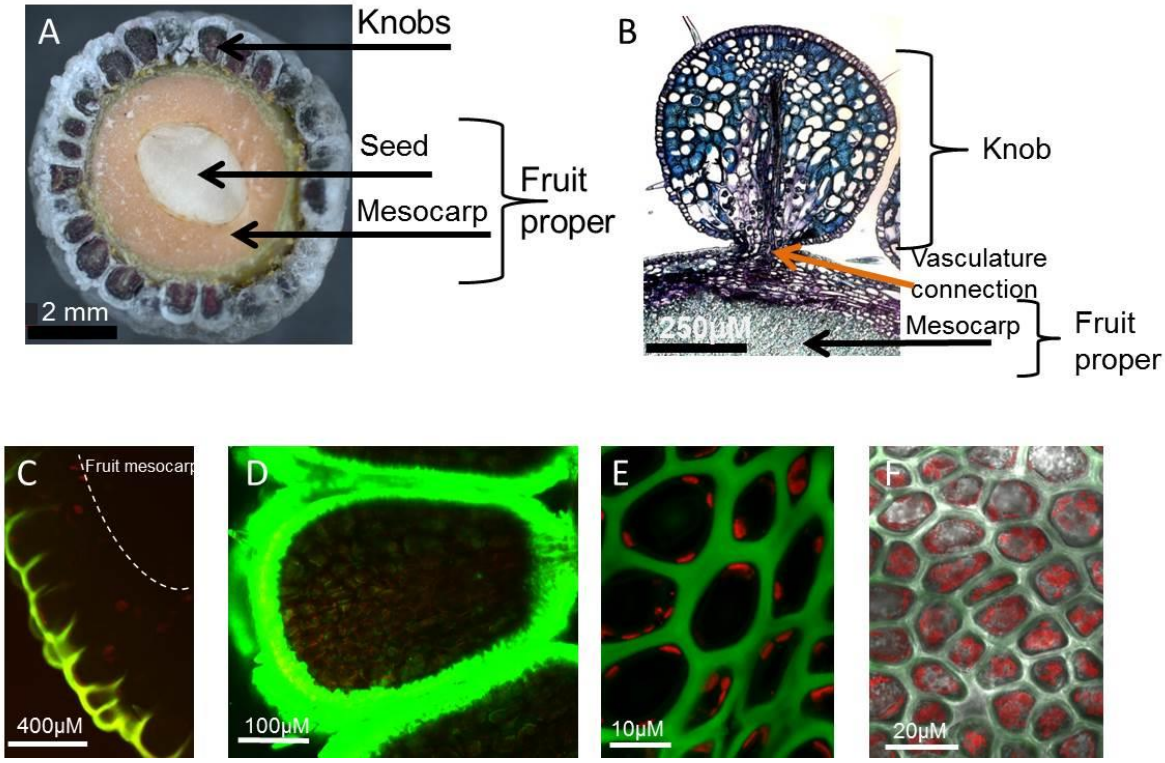

Figure 7: Structure of Bayberry knobs and localization of the surface wax. (A) Cross section of a mature Bayberry fruit. (B) Paraffin embedded cross section stained with toluidine–blue shows the connection of a single Bayberry knob to the fruit proper. (C to F) Confocal fluorescence images of Bayberry fruits stained for neutral lipids with Nile red (C, E) or BODIPY 493/503 (D, F). Green color in images is lipid and red color is chlorophyll florescence. (C) Cross section of a young Bayberry knob and fruit (~5% final wax load). (D) Cross section of a Bayberry knob in mid-development (~50% final wax load). (E) Top-down view into knob epidermal cells. (F) Similar view into knob epidermal cells, but after surface wax removed from the fruits. Note the reduction of interstitial fluorescence from the stained lipids in F compared to E, and that both appear not to contain neutral lipids within cells.

2.4.4. The distribution and structure of surface glycerolipids throughout development provides an initial suggestion of a pathway to synthesize TAG for Bayberry wax that is different from oil seeds

TAG was the only lipid detected in Bayberry surface wax at the earlier stages of development and was the most abundant surface glycerolipid throughout stages 1 and 2 (Figure 8 A; Table 3). However, DAG accumulation gradually overtook TAG mid-way through wax production and at maturity DAG was two-times more abundant than TAG in the surface wax. DAG and TAG exhibited similar rates of accumulation in the wax from about 40 to 60 days, with both peaking between days 53-60, but, from days 60-90 the rate of TAG accumulation declined (Figure 20). The accumulation of DAG to greater levels than TAG is unusual for a tissue that accumulates large levels of TAG. For example, in oilseeds TAG represents >95% of total glycerolipids with DAG constituting less than 5% of the lipids at maturity (Slack et al., 1980).

The increasing levels of DAG through the season occurred without any reduction in total TAG levels suggesting that DAG was derived from new synthesis, and not due to degradation (lipolysis) of TAG already present in the surface wax. Consistent with this suggestion, FFA, the other product of lipolysis was present only at trace levels in the wax. Instead, we tentatively concluded that DAG accumulated late in the season because its rate of production may have exceeded the capacity of the final acylation of DAG to TAG. The reduction in the rate of TAG synthesis might be due to a limited supply of acyl-donors, and/or a physical restriction for TAG synthesis due to the increasing level of crystalline surface wax.

Also intriguing, and in sharp contrast to oil seeds, was that MAG accumulated to 4% of the mass of the surface wax (Figure 8). The kinetics of MAG accumulation was similar to DAG in that it was detected and produced at its highest rate late in the wax accumulation period

(Figure 20). The regiospecificity of the acyl chain of MAG, determined by GC-FID, was primarily in the *sn*-2 position of the glycerol backbone at all stages of development (i.e. *sn*-2 MAG) (Figure 21 A). Additional analysis by GC-MS confirmed the identity of the isoforms and revealed a molar ratio of *sn*-2 MAG : *sn*-1/3 MAG of 7:1 for both C16:0-MAG and C14:0-MAG (Figure 21 B).We were unable to find any reports on the accumulation of MAG in oil seeds(Slack et al., 1980) or other oil accumulating plant tissues. However, *sn*-2 MAG is produced as an intermediate for the biosynthesis of the surface glycerolipid polymer cutin and accumulates as a component of root waxes (Li et al., 2007a; Pollard et al., 2008; Yang et al., 2010).

Together, the accumulation of MAG and DAG and the enrichment of acyl chains in the *sn*-2 position of MAG implied that Bayberry DAG and TAG synthesis differs from conventional TAG synthesis in plants. Furthermore, the kinetics of *sn*-2 MAG and DAG accumulation in the wax is consistent with a role as intermediates for TAG synthesis, as opposed to products of lipolysis.

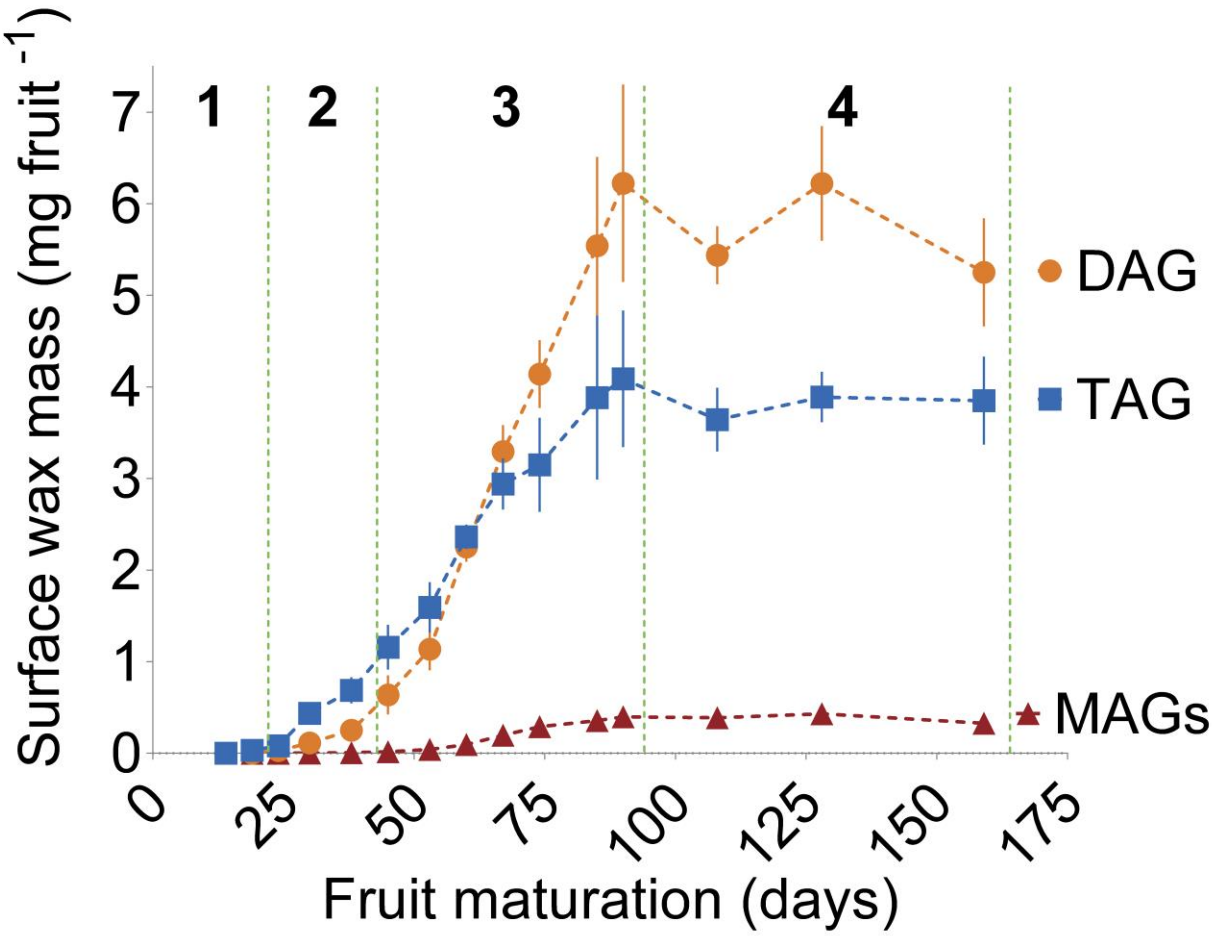

Figure 8: The mass per fruit of the glycerolipids found in Bayberry wax during fruit maturation. Stages, as defined in Figure 1 D, are designated by the dotted green line. Each point in the graphs represents the mean of 3-4 replicates ±SE.

2.4.5. [^{14}C]-Glycerol radiolabeling supports a pathway from *sn*-2 MAG → DAG → TAG

To investigate how Bayberry synthesizes its unusual surface wax, we incubated knob tissue with radiolabeled precursors of lipids, [^{14}C]-acetate and [^{14}C]-glycerol, and monitored their incorporation into glycerolipids through time. [^{14}C]-glycerol is converted into glycerol-3-phosphate (G3P), the initial molecule that is acylated to produce glycerolipids, while [^{14}C]-acetate enters fatty acid synthesis and labels newly synthesized fatty acids (Slack et al., 1977). Both labels have been used extensively to study membrane and storage lipid synthesis in leaves and oil seeds and to infer metabolic precursor-product relationships, pool sizes and fluxes (Harwood, 1988; Bates and Browse, 2012; Allen et al., 2015), but have not been used to identify pools of glycerolipid intermediates for cuticular lipid synthesis.

Knobs isolated from freshly harvested fruits were incubated for up to 11 h with [^{14}C]-glycerol and [^{14}C]-incorporation into lipids was analyzed by TLC at five time points. In agreement with the composition of the surface wax, [^{14}C]-MAG, -DAG and -TAG were abundantly labeled, representing 80-90% of the [^{14}C]-glycerol incorporated into lipids throughout the time course (Table 4). To identify the position of the acyl group on glycerol, the *sn*-1/3 and *sn*-2 isoforms of [^{14}C]-MAG were separated by borate impregnated TLC (Thomas et al., 1965). Consistent with the identification of *sn*-2 MAG in Bayberry wax (Figure 21), over 80% of the newly synthesized [^{14}C]-MAG occurred as the *sn*-2 isoform (Figure 22). These data point toward *sn*-2 MAG, as an intermediate in the pathway to produce Bayberry surface DAG and TAG. Other [^{14}C]-lipids, notably phosphatidylcholine (PC), which is extensively labeled in leaf or seed incubations (Slack et al., 1977, 1978) represented less than 10% of the total radioactivity (Table 4).

We next asked whether *sn*-2 MAG is radiolabeled in a pattern consistent with its participation as an intermediate for Bayberry DAG and TAG synthesis. Because some [^{14}C]-glycerol can enter glycolysis and subsequently label acyl chains (Slack et al., 1977, 1978) radiolabel specifically in the glycerol backbone of MAG, DAG and TAG was determined (see Table 5 for acyl-chain vs glycerol labeling results). At the earliest time point collected (30min), [^{14}C]-MAG represented ~85% of the [^{14}C]-glycerol backbone of glycerolipids and [^{14}C]-MAG increased through 90 min, after which it remained at a steady state (Figure 9). [^{14}C]-glycerol incorporation into DAG lagged behind MAG through the first 90 min of labeling, but afterwards [^{14}C]-DAG became the most abundant radiolabeled lipid. Since MAG represented less than 1% of the glycerolipid mass of the tissue at this stage of development, these kinetics are consistent with the filling of a precursor pool of [^{14}C]-MAG, followed by [^{14}C]-MAG acylation to form [^{14}C]-DAG. [^{14}C]-TAG was labeled after [^{14}C]-MAG and [^{14}C]-DAG, with a substantially longer lag time, and [^{14}C]-TAG continually increased through the remainder of the 11h labeling period. The labeling of TAG is consistent with a model of glycerol backbone flux from [^{14}C]-DAG into [^{14}C]-TAG. Of note, after 11h, radiolabel in [^{14}C]-DAG was still 4-5 fold more abundant than [^{14}C]-TAG, despite the fact that the rate of TAG accumulation in the wax at this stage of development was greater than DAG (see Figure 20 days 40-45). This long lag in [^{14}C]-TAG accumulation also suggested that there was a very large DAG intermediate pool used as the substrate for TAG synthesis, and that this pool was not completely filled with radiolabeled DAG even after 11h.

Together, the kinetics of [^{14}C]-glycerol incorporation demonstrated that *sn*-2 MAG is an initial glycerolipid intermediate in the production of DAG, and DAG is further acylated to form TAG. The lack of PC produced, immediate synthesis of *sn*-2 MAG, and the long lag in TAG

labeling is strikingly different from oilseed labeling experiments (Slack et al., 1977; Bates et al., 2007; Bates et al., 2009) and is the first report of plants producing *sn*-2 MAG as an intermediate for DAG and TAG synthesis.

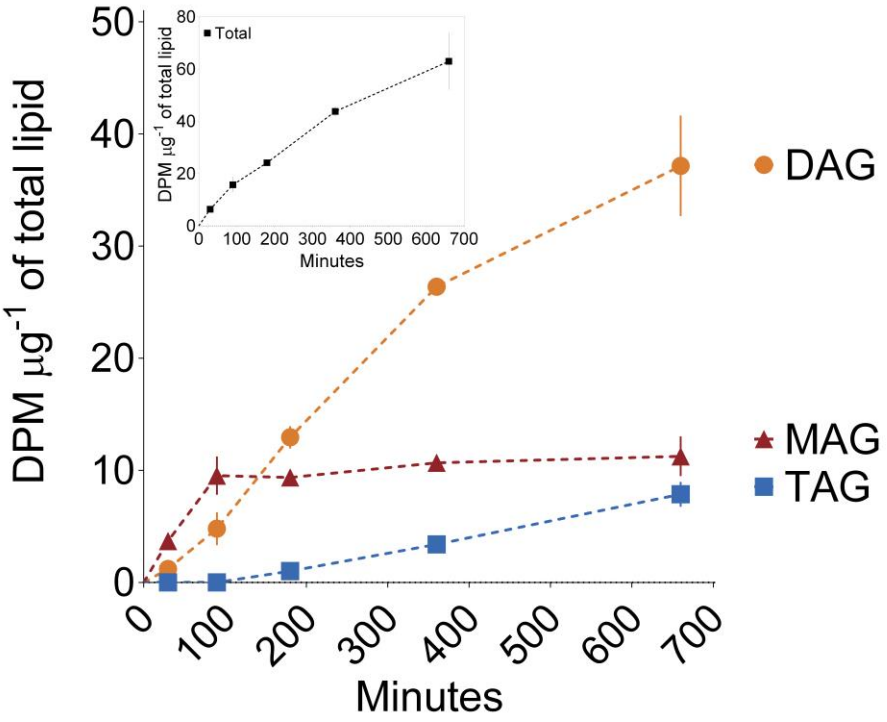

Figure 9: Time course of incorporation of [^{14}C]-glycerol into glycerol backbones of MAG, DAG and TAG. The insert presents the total radioactivity incorporated into glycerol backbone. The data are expressed as the mean of 2 replicates ± range. DPM was normalized to the total lipid content in the tissue at each time point.

2.4.6. [^{14}C]-acetate labeling indicates acyl chains enter *sn*-2-MAG prior to incorporation into DAG and TAG

The kinetics of [^{14}C]-glycerol incorporation (Figure 9) provided information on the flux of the glycerol backbone into MAG, DAG and TAG. To understand the kinetics of acyl chain incorporation into glycerolipids, Bayberry knobs were incubated with [^{14}C]-acetate for 5 min to 11 h. As with [^{14}C]-glycerol, [^{14}C]-MAG, -DAG and -TAG represented the majority of [^{14}C]-acetate incorporated into lipids. [^{14}C]-PC was never more abundant than [^{14}C]-MAG, particularly at the earliest time points, and represented less than 10% of total [^{14}C] incorporation (Table 4). Notably, and unlike results from most oilseed labeling experiments (Bates et al. 2009; Allen 2015), the initial kinetics of [^{14}C]-acyl chain incorporation was very similar to the [^{14}C]-glycerol incorporation. [^{14}C]-*sn*-2 MAG was again the most abundantly labeled lipid at the initial time-points (5 to 60 min) and there was a 60 to 90 min lag in radiolabel incorporation into [^{14}C]-DAG and a much longer lag for [^{14}C]-TAG synthesis (Figure 10 A and B). The time-course experiments (Figure 10) were repeated numerous times over two separate growing seasons with tissue of different ages with similar results. Minor differences in the abundance and the incorporation kinetics likely represent differences in development and in the uptake of label.

The rapid initial incorporation of [^{14}C]-acetate into the acyl chain of *sn*-2 MAG provided additional evidence that MAG is an early intermediate in Bayberry surface wax production However, the lag in acyl chain incorporation into [^{14}C]-DAG and the even longer lag in [^{14}C]-TAG production, relative to [^{14}C]-MAG, is not consistent with TAG labeling results for plants which accumulate primarily saturated and monounsaturated fatty acids (e.g. *Cacao*, *Cuphea*, avocado mesocarp) (Stobart and Stymne, 1985; Griffiths et al., 1988; Bafor et al., 1990; Griffiths and Harwood, 1991; Bates and Browse, 2012). In these tissues, rather than initial incorporation

into PC, newly synthesized fatty acids apparently enter a common acyl-CoA pool where they have an equal chance of reacting with G3P, lysophosphatidic acid (LPA) or DAG via the Kennedy pathway and thus produce [^{14}C]-DAG and [^{14}C]-TAG at similar initial rates.

The fatty acyl-CoA pools in plants are very small and would introduce a lag of less than one minute (Larson and Graham, 2001; Tjellstrom et al., 2012). In Bayberry, the labeling of [^{14}C]-MAG with no discernable lag is consistent with acylation of G3P by acyl-CoA. However, the substantial lag time in acyl-chain labeling of [^{14}C]-DAG and even longer lag time for [^{14}C]-TAG implied that the fatty acid donor pools for these acylation reactions are distinct from G3P acylation to synthesize MAG, and also from each other. One possibility is that acyl chains are incorporated into DAG and TAG via reactions that are acyl-CoA independent. Regardless, the incorporation of acyl chains into Bayberry fruit DAG and TAG appears to be different from previously reported pathways for TAG synthesis in plants.

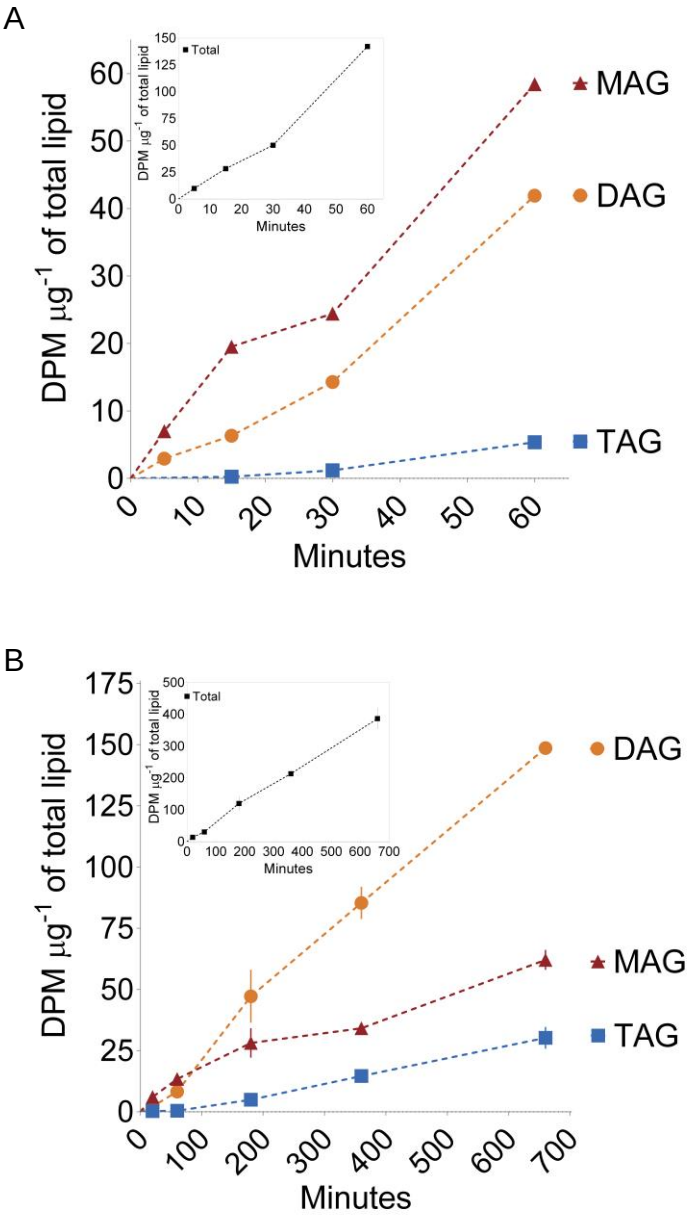

Figure 10: Time course of incorporation of [^{14}C]-acetate into acyl-chains of MAG, DAG and TAG. (A) Incorporation into acyl chains through 60 min of labeling. (B) Incorporation into acyl chains through 11 h of labeling. The insert in each graph presents the total radioactivity incorporated into the organic fraction at each time point. The data are expressed as the mean of 2 replicates ± range. DPM was normalized to the total lipid content in the tissue at each time point.

2.4.7. Evidence for DAG biosynthesis by an acyl-CoA independent transacylase

The substantial lag prior to linear accumulation of [^{14}C]-acetate labeled fatty acids into [^{14}C]-DAG suggested that there was a pool of precursors or intermediates, larger than the pool of fatty acyl-CoAs, and that contributed acyl chains to MAG to form [^{14}C]-DAG. To further examine possible reactions for DAG biosynthesis, we analyzed the distribution through time of [^{14}C]-acyl chains on the *sn*-1/3 and *sn*-2 positions of DAG after incubations with [^{14}C]-acetate. The regiospecific localization of [^{14}C]-acyl chains was determined by digesting acetylated *sn*-1,2 (2,3) DAG with pancreatic lipase (Christie and Han, 2010) followed by TLC analysis of the resulting FFA (representing acyl chains from the *sn*-1/3 positions of DAG) and MAG (representing the *sn*-2 acyl chain of DAG).

Unexpectedly, the results from the digestion of DAG revealed that after both short (15 to 60 min) and long labeling incubations (up to 5 days), [^{14}C]-acyl chains were distributed almost equally between the *sn*-1/3 and *sn*-2 positions of its glycerol backbone (Figure 11). An equal distribution of [^{14}C] in the *sn*-1/3 and *sn*-2 positions of DAG, as observed here, would not occur if the acyl-donor had significantly less or greater specific activity than the [^{14}C]-*sn*-2 MAG acyl-acceptor (Figure 23). Instead, the equal distribution of [^{14}C] on both acyl chains of DAG indicated that [^{14}C]-DAG was synthesized by acylation of the [^{14}C]-*sn*-2 MAG precursor at its *sn*-1 (or 3) position by a [^{14}C]-acyl-donor with a very similar specific activity. The equal distribution of [^{14}C]-acyl chains at both positions of DAG was established within 15 min of labeling, which was before the intermediate [^{14}C]-MAG pool had filled (i.e. reached maximum specific activity or steady-state). The identity of the acyl-donor to [^{14}C]-*sn*-2 MAG to produce [^{14}C]-DAG is not directly determined by these experiments, but some inferences can be made. Because MAG represented almost all of the [^{14}C]-labeled compounds at the earliest time points,

and as discussed earlier, the acyl-donor is likely not acyl-CoA, a simple interpretation consistent with these data is that the acyl-donor was another molecule of [^{14}C]-*sn*-2 MAG. In this scenario, based on the almost equal distribution of acyl chains at *sn*-1/3 and *sn*-2 positions of DAG, the *sn*-2 MAG acyl-donor may be from the same intermediate pool of *sn*-2 MAG that provided the glycerol backbone and *sn*-2 acyl-chain of DAG. This reaction can be considered a MAG:MAG transacylation. We note that an acyl-CoA independent MAG:MAG transacylation that is catalyzed by phospholipase A2 (iPLA2) has been described in animals (Waite and Sisson, 1973; Jenkins et al., 2004; Gao and Simon, 2005), but not for plants.

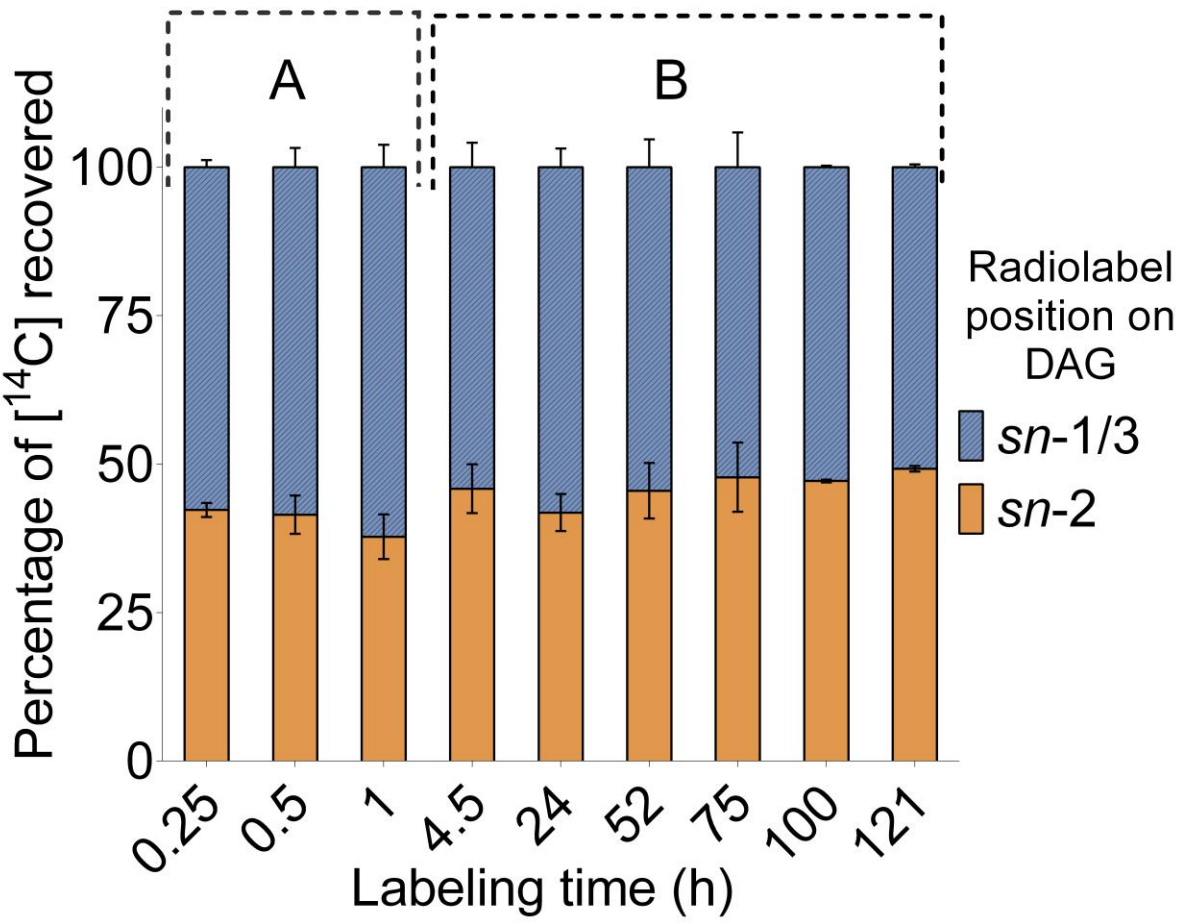

Figure 11: Distribution of [^{14}C]-acyl chains on the *sn*-1/3 and *sn*-2 positions of [^{14}C]-DAG. Two separate incubations with [^{14}C]-acetate were analyzed: (A) Up to 1h labeling of dissected knobs, and (B) Up to 5 days of labeling with whole fruits. After incubations with labeled substrates, [^{14}C]-lipids were extracted and separated by TLC. [^{14}C]-DAG was recovered, acetylated and digested with pancreatic lipase to determine the locations of the [^{14}C]-acyl chains on glycerol of DAG. Each bar is the mean from two independently collected labeled Bayberry tissues ± range.

2.4.8. Evidence for TAG synthesis by an acyl-CoA independent mechanism

To evaluate the reaction mechanism and possible acyl-donor for TAG synthesis, we also determined the positional distribution of [^{14}C]-acyl chains on its glycerol backbone by digestion with pancreatic lipase. Unexpectedly, the positional labeling of acyl chains of [^{14}C]-TAG differed markedly from [^{14}C]-DAG (Figure 12). After 30 minutes of [^{14}C]-acetate labeling, radiolabel could only be detected in the *sn*-1/3 positions of TAG, and at 60 min 90% of label was derived from the *sn*-1/3 positions. Surprisingly, even after 5-days of continuous incubation with [^{14}C]-acetate, acyl chains in the *sn*-1/3 positions were still at least 4-fold more highly labeled than [^{14}C] at the *sn*-2 position of TAG. This indicated that the [^{14}C]-acyl donor pool had a consistently higher [^{14}C]-per acyl chain (i.e. specific activity) compared to the DAG backbone (i.e. acceptor) pool. Clearly, most of the [^{14}C]-TAG synthesized was derived from an unlabeled DAG, rather than from the newly synthesized [^{14}C]-DAG molecules, even after 5 days of labeling. This result indicates that the biosynthetically active DAG pool involved in TAG synthesis is very large.

As discussed above, the kinetics of [^{14}C]-acetate incorporation into DAG and TAG was very different from other plant tissues with a high content of saturated and monounsaturated fatty acids. Specifically, in those examples acyl-CoA provides the acyl chains for DAG and TAG and the reactions are catalyzed by CoA dependent acyltransferase enzymes (i.e. LPAAT, DGAT 1 and 2). In contrast, labeling results for Bayberry wax synthesis point towards acyl-CoA independent reactions for DAG and TAG synthesis. Other examples of acyl-CoA independent reactions for TAG synthesis in plants include the enzyme phospholipid: diacylglycerol acyltransferase (PDAT) that produces TAG via PC donating an acyl chain from its *sn*-2 position onto DAG (Dahlqvist et al., 2000). However, PDAT was not considered as a significant source

of acyl chains for Bayberry TAG because PC was not abundantly labeled, and PDAT expression was barely detectable (see RNA-seq results). The labeling data were also not consistent with TAG synthesis by a DAG:DAG transacylase, as occurs in animal cells (Lehner and Kuksis, 1993; Yamashita et al., 2014) and also in safflower microsomes (Stobart et al., 1997). Specifically, a DAG:DAG transacylase would catalyze an exchange of acyl chains between two molecules of [^{14}C]-DAG. However, in Bayberry, because both acyl chains of [^{14}C]-DAG were equally labeled, the DAG:DAG transacylase reaction would result in the retention of label in TAG from the *sn*-2 position of the acceptor DAG. In this case, both *sn*-1/3 and *sn*-2 positions would be labeled, resulting in a ratio close to 2:1 of [^{14}C] in the *sn*-1/3 and *sn*-2 positions of [^{14}C]-DAG. This distribution is in contrast to the consistently > 4:1 ratio observed in [^{14}C]-TAG produced by Bayberry (Figure 10). A reaction mechanism that is supported by both the labeling kinetics of *sn*-2 MAG and by lack of label in other compounds, is TAG synthesis by acylation of DAG with a [^{14}C]-acyl chain derived from [^{14}C]-*sn*-2 MAG (Figure 24) schematically outlines the alternative scenarios for TAG labeling).

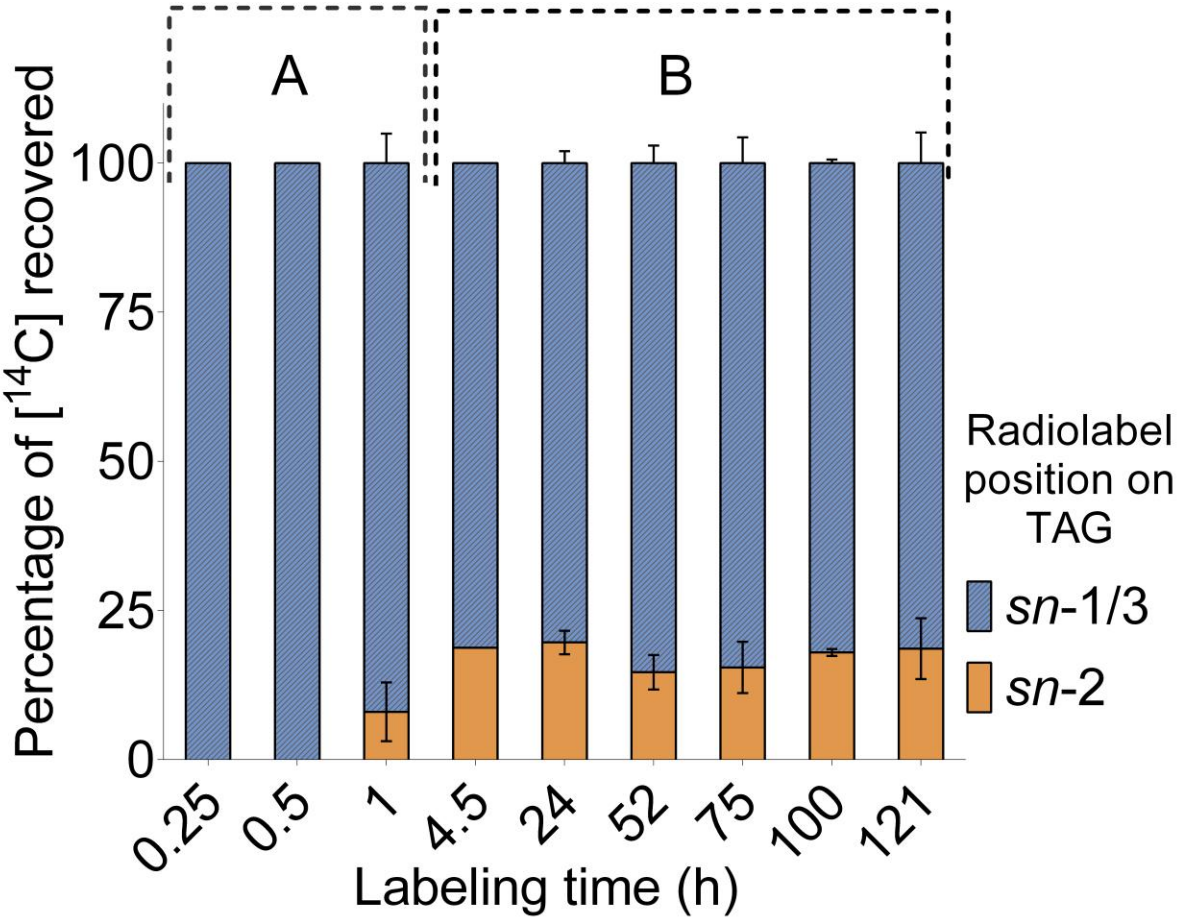

Figure 12: Distribution of [^{14}C]-acyl chains on the sn-1/3 and sn-2 positions of [14C]-TAG. Two separate incubations with [^{14}C]-acetate were analyzed: (A) Up to 1h labeling of dissected knobs, and (B) Up to 5 days of labeling with whole fruits. After incubations with labeled substrates, [^{14}C]-lipids were extracted and separated by TLC. [^{14}C]-TAG was recovered and digested with pancreatic lipase to determine the locations of the [^{14}C]-acyl chains on *sn*-1/3 and *sn*-2 positions of glycerol. Each bar is the mean from two independently collected labeled Bayberry tissues ± range.

2.4.9. Evidence for extracellular *sn*-2 MAG and DAG pools for extracellular TAG synthesis

The accumulation kinetics and regiospecificity of [^{14}C]-acyl chains into DAG and TAG indicated they were synthesized from independent acyl-donor pools (Figure 10). However, the labeling also suggested that the acyl-donor for both DAG and TAG synthesis may be *sn*-2 MAG. This implies that two independent pools of biosynthetically active *sn*-2 MAG exist in Bayberry. Since it has been previously demonstrated that *sn*-2 MAG is secreted from epidermal cells to the surface (Li et al., 2007a) and *sn*-2 MAG is an acyl donor for cutin polyester synthesis via a GDSL-motif enzyme (Yeats et al., 2012), by analogy we considered that TAG synthesis in Bayberry may occur outside of the cell by acylation of DAG by secreted *sn*-2 MAG.

To examine the possibility of two distinct metabolic pools of *sn*-2 MAG (intra and extracellular), the distribution and abundance of [^{14}C]-glycerolipids in the extracellular wax and the knob tissue were compared. Intact Bayberry fruits were incubated for 1h to 5 days with [^{14}C]-acetate, and at each harvest time the surface lipids were separated from knob tissue associated lipids by dipping fruits in chloroform for 30 seconds. The results clearly demonstrated that [^{14}C]-MAG existed at comparable levels in both the extracellular lipids and the lipids that remained in the knob tissue after wax removal (Figure 13). In contrast, [^{14}C]-DAG and [^{14}C]-TAG were found predominately in the extracellular surface wax extract. Furthermore, although MAG is a very minor (0.5-1% wax mass) component in the surface wax at these developmental stages, [^{14}C]-MAG represented a much higher proportion of the [^{14}C]-glycerolipids in the extracellular wax extract (up to 70%). Therefore, these experiments provide evidence for an extracellular and intracellular pool of biosynthetically active [^{14}C]-*sn*-2 MAG but that [^{14}C]-DAG is predominantly extracellular.

Two additional observations support this interpretation: (1) The fact that the majority of [^{14}C]-acyl chains in [^{14}C]-TAG are in the *sn*-1/3 positions (Figure 12) indicated that the DAG pool used for TAG synthesis was not completely filled with [^{14}C]-DAG, even after 5 days of continuous labeling. If the biosynthetically active DAG pool were completely filled with [^{14}C]-DAG molecules there would have been an increased proportion of [^{14}C]-acyl chains in the *sn*-2 position of TAG. Instead, these data indicate that the [^{14}C]-DAG molecules in the active DAG pool were diluted substantially by a large amount of unlabeled DAG molecules, implying that the active DAG pool is very large. Therefore, we conclude that the biosynthetically active DAG pool exists outside of the cells because a large DAG pool inside cells was not detected by neutral-lipid specific staining (Figure 7), and major accumulation of DAG inside the cells would be expected to disrupt lipid bilayers (Goni and Alonso, 1999). Moreover, in the case of di16:0 DAG, with a melting point of 48°C, a large accumulation of intracellular DAG may crystalize within cells hindering export to the surface. (2) The rate of DAG and MAG accumulation increased or remained high late in the season (stage 3) whereas the TAG accumulation rate decreased (Figure 20). In relation to the observed labeling kinetics, the increased levels of surface wax may diminish the final acylation for TAG synthesis, whereas intracellular reactions to synthesize MAG and DAG remain less affected.

2.4.10. Exogenously added *sn*-2 MAG is incorporated into DAG and TAG

The kinetics of [^{14}C]-acetate incorporation into labeled acyl chains together with the distribution of the acyl chains on the glycerol backbone suggested that acyl-CoA independent reactions participate in DAG and TAG synthesis and that *sn*-2 MAG may act as an acyl donor. To directly test the capability of Bayberry knobs to incorporate radiolabel from *sn*-2 MAG into

DAG and TAG, knobs were incubated with [^{14}C]-*sn*-2 MAG for 5 to 30 min (Figure 14). Radiolabeled DAG and TAG were both detected within 5 minutes and [^{14}C]-DAG increased through time. Reverse phase (RP) TLC of the radiolabelled DAG and TAG isolated from the incubations confirmed their identities. [^{14}C]-DAG and [^{14}C]-TAG synthesis in these incubations was 3-4 fold higher than in parallel control incubations with avocado mesocarp. Thus, these results provide direct evidence that Bayberry knobs can synthesize [^{14}C]-DAG and [^{14}C]-TAG from [^{14}C]-*sn*-2 MAG.

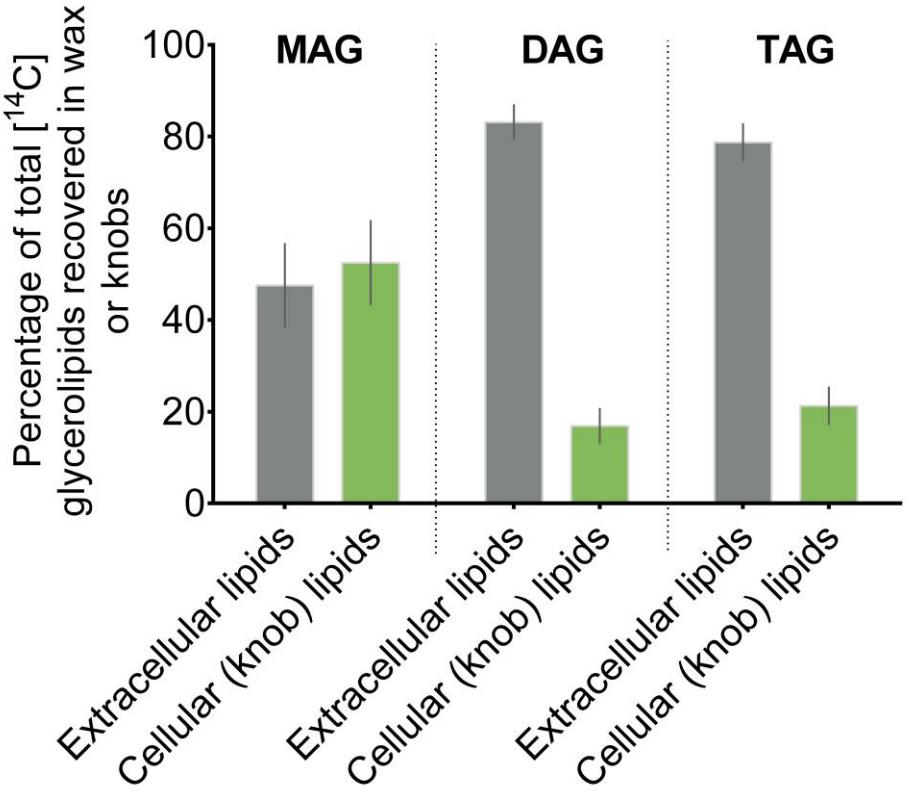

Figure 13: Distribution of [^{14}C]-glycerolipids recovered in the extracellular wax lipids, and the tissue after wax extraction (i.e. the cellular or knob lipids). Clusters of 5-10 fruits were submerged in labeling buffer containing 200 µCi [^{14}C]-acetate after which surface wax was removed by dipping labeled fruits in chloroform. The remaining lipids in the tissue were extracted with 3:2 hexane isopropanol. The relative percentage of MAG, DAG or TAG that was incorporated into the surface wax or the knob lipids is presented. Each bar reports the percentage of the glycerolipid in the respective fractions averaged over 9 time-points from two independent experiments (± SE). Data were pooled to account for variation in incorporation of label into intact fruit clusters and in the extractability of labeled wax within and between experiments. The time-course data are presented in Figure 25. As described in that figure, TAG and DAG detected in the cellular knob lipids is attributed to residual, un-extracted surface wax, and not due to intracellular synthesis.

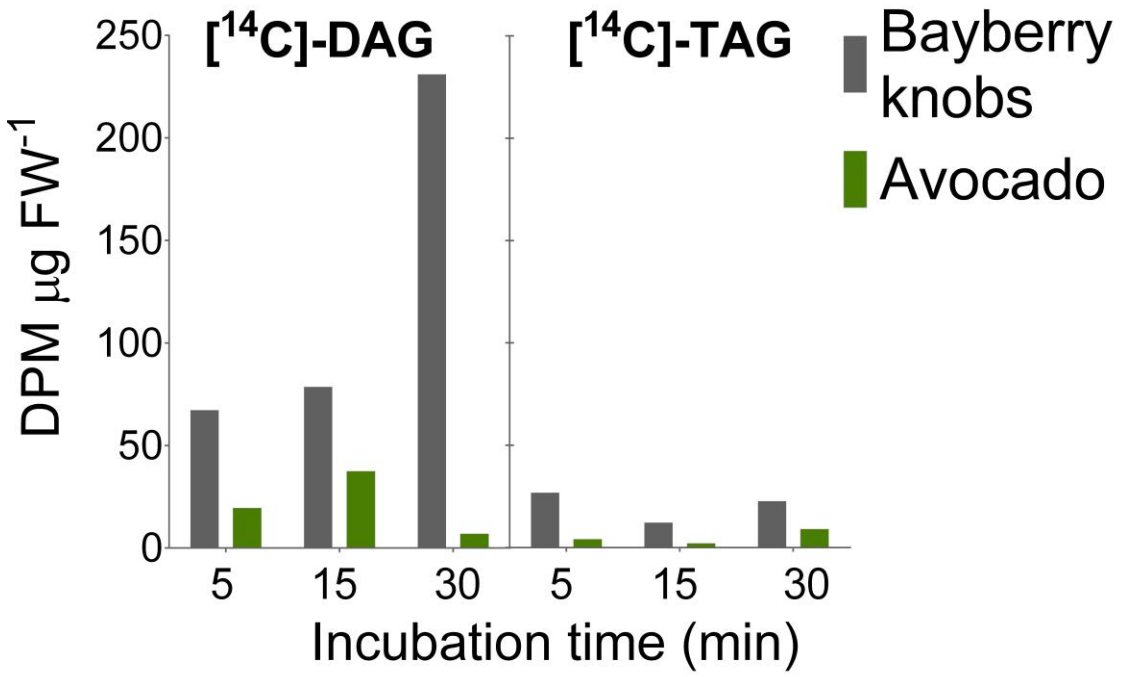

Figure 14: Synthesis of [^{14}C]- DAG and [^{14}C]- TAG by Bayberry knobs (gray) or avocado mesocarp tissue (green) from [^{14}C]-*sn*-2 MAG. Each bar represents the total DPM recovered from a lipid extract of the tissue and incubation media. Data were normalized to the tissue fresh weight. This experiment was repeated and incubation was extended to 3h. Similar trends were observed at the initial time points (1h) but avocado DAG and TAG production accelerated after 1h.

2.4.11. Genes related to biosynthesis and secretion of surface lipids are very highly expressed in Bayberry knobs

To identify possible enzymes and proteins expressed during Bayberry surface wax production, transcript profiles from seven developmental stages of Bayberry knobs were analyzed by RNA-seq. In the knobs, there was strikingly high expression of transcripts that are annotated as being associated with acyl-lipid and cutin synthesis. Overall, thirteen out of the top 55 most highly expressed annotated transcripts from Bayberry knobs were associated with acyl-lipid metabolism (Table 2). This high expression of acyl-lipid related transcripts exceeds castor (60% oil) and even oil palm mesocarp (90% oil), where less than 10 of the 50 most highly expressed genes are acyl lipid associated (Bourgis et al., 2011; Troncoso-Ponce et al., 2011).

The identities of these very highly expressed transcripts in Bayberry knobs are illustrative of its highly specialized lipid metabolism. First, the most abundantly expressed acyltransferases, were annotated as *sn*-2 glycerol-3-phosphate acyltransferase (*sn*-2 GPAT) (Zheng et al., 2003; Beisson et al., 2007); an HXXXD-motif acyltransferase closely related to Arabidopsis DEFECTIVE IN CUTICULAR RIDGES (DCR) (Panikashvili et al., 2009); and GDSL-motif lipase/transacylases related to CUTIN DEFICIENT 1 (CD1) (Yeats et al., 2012). The putative or known activities of the three acyltransferases in other plant species are generally consistent with the lipid structures produced for Bayberry surface wax, with the enzymatic reactions predicted by the labeling data and with the extracellular localization of the glycerolipids (see below). Furthermore, transcripts associated with these three cutin-associated acyltransferases were expressed at levels 50-fold higher than transcripts associated with acyltransferases for known TAG assembly pathways in plants (e.g. GPAT9, LPAAT, DGAT, PDAT). Moreover, none of the 'conventional' TAG-associated acyltransferases were ranked among the top 1400 most highly

expressed transcripts of Bayberry knobs (Table 2). Second, Bayberry surface glycerolipids are exceptional in that over 99% of the fatty acids are saturated. In agreement, the most highly expressed transcript among the fatty acid synthesis pathway encoded a predicted acyl-ACP thioesterase B (FATB), the enzyme that releases saturated fatty acids from ACP. Third, the secretion of waxes and cutin precursors (including *sn*-2 MAG) to the plant surface requires ATP binding cassette transporters of the G subfamily (ABCG) and is believed to be coordinated with lipid transfer proteins (LTPs)(Samuels et al., 2008). Accordingly, transcripts assigned to an ABCG transporter and three LTPs were among the most highly expressed transcripts in Bayberry knobs

Based on previous knowledge from other plants, and the labeling and biochemical data above, we hypothesize that the very highly expressed cutin-associated acyltransferases, *sn*-2 GPAT, DCR, and GDSL-motif lipase/transacylase, could provide insights into biosynthetic mechanisms for Bayberry wax synthesis. First, unlike the GPAT reaction that acylates the *sn*-1 position of G3P to initiate intracellular TAG synthesis, the *sn*-2 GPATs are bifunctional enzymes that acylate the *sn*-2 position of G3P, and remove the phosphate to produce *sn*-2 MAG. Among the three *sn*-2 GPAT clades previously characterized (Li et al., 2007a; Li-Beisson et al., 2009; Yang et al., 2010), the highly expressed Bayberry GPAT transcripts were most closely related to genes required for cutin biosynthesis (Arabidopsis *sn*-2 GPAT 4/8 and 6 isoforms) and were less related to suberin associated or other members of the *sn*-2 GPAT family (Figure 27 A). Furthermore, their expression increased through the development of the wax layer (Figure 26 A).

Next, the most abundant transcript that encodes an enzyme in Bayberry knobs was a close homolog to the Arabidopsis HXXXD (BAHD) acyltransferase *defective in cuticular ridges* (DCR) (Figure 26 C, 27 C). Arabidopsis DCR is a soluble, cytosolic enzyme that is essential for

production of dihydroxy16:0 rich cutin (Panikashvili et al., 2009). *In vivo* substrates for DCR were not identified, however, it was proposed that DCR may be involved in intracellular concatenation of the cutin polyester (Panikashvili et al., 2009; Molina and Kosma, 2015). Although DCR has diacylglycerol acyltransfrase activity *in vitro* (Rani et al., 2010) flax DCR could not complement the Arabidopsis *dgat1* knockout mutant (Pan et al., 2013) and DAG or TAG have not been identified as intermediates in cutin production. That DCR was the most highly expressed of all enzyme transcripts in Bayberry knobs and is temporally correlated with wax production implies that the enzyme has a key role in surface wax production in Bayberry.

Finally, transcripts encoding two highly expressed annotated GDSL-motif enzymes (referred to here as MpGDSL1 and MpGDSL2) may also catalyze the assembly of Bayberry glycerolipids. Although often annotated as "lipase', GDSL-motif enzymes can catalyze transacylase reactions, which are typically favoured under acidic, and low-water environments (Schmid and Verger, 1998; Akoh et al., 2004). Such conditions exist at aqueous-aliphatic interphases within the apoplast surrounding epidermal cells, where the final assembly of the cutin polyester is thought to be catalyzed by extracellular localized GDSL-motif or related lipase-like enzymes (Beisson et al., 2012; Beisson and Ohlrogge, 2012; Yeats et al., 2012). MpGDSL1 was most highly expressed at the first two stages of RNA analysis, but decreased to very low levels during the remainder of the time course. MpGDSL2 was highly expressed at all stages of wax accumulation (Figure 26 B). The predicted MpGDSL1 protein is most closely related to CD1 (74% identical; 87% similar), the "cutin synthase" identified in tomato (Yeats et al., 2012) (Figure 27 B). Interestingly, a minor reaction in CD1 assays was the production of DAG and TAG (Yeats et al., 2012). The other highly expressed protein with a GDSL-motif

(MpGDSL2) is 53% similar to CD1, but falls into another clade for which no members have been characterized.

Table 2: Rank (out of approximately 10000 contigs annotated to an Arabidopsis loci) and expression (RPKM) of the highest expressed acyl lipid-related contigs in Bayberry knobs. The ranks were determined from the total RPKM summed across 7 developmental stages. Each gene is annotated according to its Arabidopsis homolog.

Expression rank	Total RPKM	Arabidopsis homolog	Pathway /reaction
TOP LIPID-RELEATED TRANSCRIPTS			
1	72,750	Lipid transfer protein (LTP) type 1 (AT2G38540)	Lipid secretion
3	34,303	DCR/PEL3/HXXXD acyltransferase	Cutin synthesis
7	23,603	*sn*-2 GPAT4/8	Cutin synthesis
11	11,809	*sn*-2-GPAT6	Cutin synthesis
21	7,777	GDSL2-motif lipase/transacylase (AT3G16370)	Cutin synthesis
23	7,726	LTP_2 (AT3616307)	Lipid secretion
29	6,847	Keto-acyl CoA synthase (KCS) 10	Fatty acid elongation
30	6,819	KCS19	Fatty acid elongation
33	6,564	LTP_2 (AT3G18280)	Lipid secretion
36	5,828	GDSL1-motif lipase/transacylase (CuS1/SiCD1)	Cutin synthesis
40	5,354	ABCG Transporter 1 (WBC1)	Lipid secretion
43	4,947	Acyl-ACP thioesterase B (FATB)	Fatty acid synthesis
46	4,655	Acyl carrier protein (ACP) 4	Fatty acid synthesis
TRANSCRIPTS FOR CONVENTIONAL TAG SYNTHESIS			
1476	359	Putative diacylglycerol acyltransferase 3 (DGAT3)	
1509	352	Lysophosphatidic acid acyltransferase 3 (LPAAT3)	
2391	223	Phosphatidylcholine : diacylglycerol acyltransferase 1 (PDAT1)	
3642	138	Diacylglycerol acyltransferase 2 (DGAT2)	
4220	114	*sn*-1 g*lycerol-3-phosphate* acyltransferase 9 (GPAT9)	
		* DGAT1 AND LPAAT 2, 4 were not detected	

2.4.12. A model for Bayberry wax biosynthesis

Based on a combination of molecular species analysis of glycerolipids, microscopy, radiolabeling by [^{14}C]-acetate, [^{14}C]-glycerol, and [^{14}C]-MAG, and transcript analysis, we propose a sequence of intra- and extracellular reactions that result in the massive accumulation of glycerolipid surface wax on Bayberry fruits (Figure 15). Fluxes of glycerol and acyl chains are also presented in Figure 28. Most aspects of the pathway are in sharp contrast to glycerolipid synthesis in oil seeds and other TAG accumulating plant tissues. Instead we propose that Bayberry has evolved a novel pathway for soluble glycerolipid synthesis in plants. The key observations that support this model are: (1) The continuous eight-week accumulation of surface wax coupled with the light and microscopic images of the fruits clearly indicate that components of the surface wax are not stored within the cells, and instead point towards the knob cells actively secreting neutral lipids to their surface throughout development. (2) Bayberry wax contains a high proportion of DAG (~65%) and up to 4% *sn*-2 MAG, which are not significant constituents of oil seeds. Instead, *sn*-2 MAG is an intermediate in the synthesis of the surface glycerolipid cutin and thus initially suggested that Bayberry surface wax may be synthesized by enzymatic reactions related to cutin, and not conventional TAG synthesis reactions. (3) The kinetics of [^{14}C]-glycerol labeling confirmed that *sn*-2 MAG is an initial intermediate, and also revealed that the glycerol backbone flux proceeds from *sn*-2 MAG →DAG→TAG. (4) [^{14}C]-acetate labeling indicated that newly synthesized acyl chains also flux from *sn*-2 MAG to DAG and then to TAG with increasing lag times similar to [^{14}C]-glycerol labeling. This was not expected, and indicated that the acylation of each position on the glycerol backbones of MAG, DAG and TAG utilizes different pools of acyl chain donors. (5) Analysis of the regiospecific distribution of [^{14}C]-acyl chains on DAG and TAG supports a model where DAG and TAG are

synthesized by acyl-CoA independent mechanisms and, as discussed, *sn*-2 MAG is a likely acyl-donor for both reactions. (6) Radiolabeled *sn*-2 MAG appears rapidly in both the knob cells and in the extracellular wax lipids. This indicated that Bayberry contains two separate pools of *sn*-2 MAG that are potential acyl donors for the transacylase reactions; an intercellular MAG pool used for DAG synthesis (via a proposed MAG:MAG transacylase) while the extracellular MAG pool is used for TAG synthesis outside of the cells (via a proposed MAG:DAG transacylase). Furthermore, the very long lag times from both acetate and glycerol radiolabeling of TAG indicate a very large DAG precursor pool that is too large to exist entirely within the knob cells. (7) RNA-seq of Bayberry knobs revealed that a striking proportion of highly expressed transcripts are associated with the production and secretion of the surface lipid polyester cutin. The very high expression of transcripts encoding cutin-related acyltransferases and very low or undetectable expression of transcripts for acyltransferases previously identified for TAG synthesis support the biochemical analysis and radiolabeling results that the biosynthesis of the unique surface wax on Bayberry fruits utilizes reactions and intermediates analogous to the synthesis of the insoluble surface glycerolipid cutin. Specifically, the highly expressed bifunctional *sn*-2 GPATs may produce *sn*-2 MAG. The intercellular HXXXD-motif DCR enzyme was the highest expressed enzyme in Bayberry knobs and may contribute to intracellular DAG synthesis. Finally, secretion of both MAG and DAG may provide a substrate for the extracellular localized GDSL-motif enzymes to catalyze a transacylase reaction forming TAG, which is analogous to models for cutin assembly (Yeats et al., 2012; Yeats et al., 2014).

While the data clearly identify a novel pathway to produce TAG in plants and suggest a combination of intracellular and extracellular reactions with *sn*-2 MAG as a primary acyl-donor, some aspects of the proposed model are uncertain and a number of questions remain.

Specifically, despite the fact that most of the radioactivity was recovered in MAG, DAG and TAG, we cannot rule out that there is another intermediate or acyl-donor, other than *sn*-2 MAG, for DAG or TAG acylation reactions. Although [^{14}C]-*sn*-2 MAG added to knobs was a substrate for DAG and TAG synthesis, more direct evidence for the reactions could be provided by enzyme assays after purification of the enzymes highly expressed in Bayberry knobs. However, we were unable to detect enzymatic activity when Bayberry DCR or GDSL-motif enzymes were heterologously expressed in *E. coli*, yeast, or transiently in tobacco. Thus, we could not directly demonstrate which enzymatic reactions are catalyzed by the DCR and GDSL-motif enzymes. GDSL-motif enzymes have broad substrate specificity (Akoh et al., 2004) and the highly expressed GDSL-motif enzymes in Bayberry might be active in both intra and extracellular synthesis of Bayberry DAG and TAG. Indeed, related lipase-like enzymes in animals can catalyze an acyl-CoA independent formation of DAG and TAG (Yamashita et al., 2014). DCR was the highest expressed enzyme, but the reaction mechanism by which it contributes to the assembly of Bayberry wax is not clear. Although Bayberry wax does not contain hydroxy-fatty acids as do the cutin monomers impacted in *dcr*, the structure of *sn*-2 MAG and DAG are chemically analogous in that their glycerol backbone possess free hydroxyls. In a previous study, Arabidopsis DCR was expressed in *E. coli* and yeast and exhibited diacylglycerol acyltransferase activity (DGAT), and also monoacylglycerol acyltransferase (MGAT) activity (Rani et al., 2010). However, radiolabeling kinetics together with the positional distribution of [^{14}C]-acyl chains of Bayberry wax implied that DAG and TAG are not synthesized by acyl-CoA-dependent acyl transferases. That DCR is the highest expressed intracellular enzyme strongly suggests that it contributes to intracellular DAG synthesis proposed here, and future work should explore the possibility of DCR catalyzing a CoA independent transacylase reaction, and/or identify other

enzymatic partners or cofactors for additional reactions catalyzed by DCR. Regardless of the absence of direct *in vitro* evidence for the proposed enzyme reactions, this study has clearly identified that plants can synthesize TAG by a novel pathway involving *sn*-2 MAG as an intermediate and enzymes related to cutin biosynthesis.

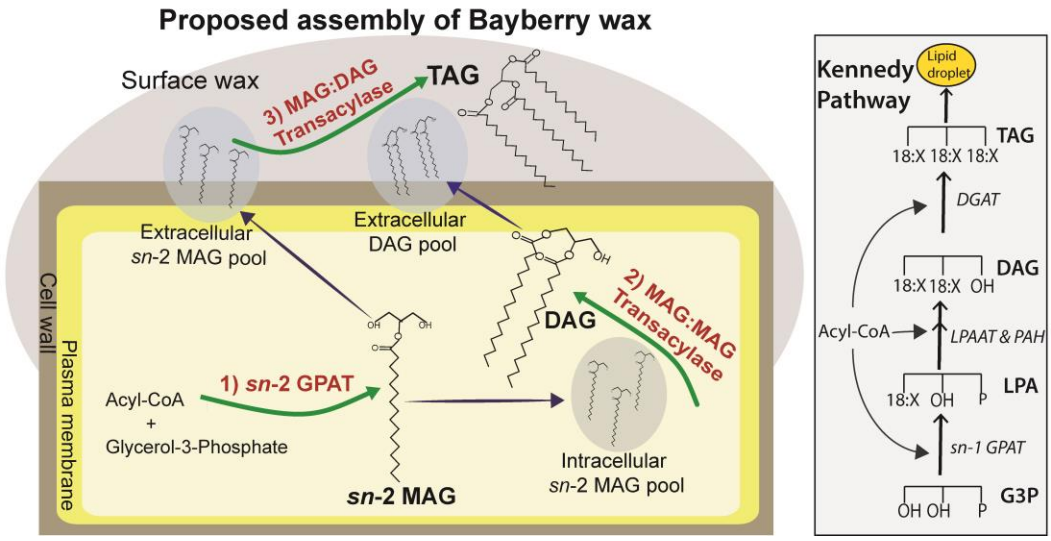

Figure 15: Proposed model for Bayberry surface wax biosynthesis. The pathway shown is supported by multiple lines of evidence (see text) including lipid structural analysis, radiolabeling and the identity of very highly expressed acyltransferase transcripts in Bayberry knobs (*sn*-2 GPAT, DCR, GDSL-motif). The pathway begins with acylation of G3P by 16:0-CoA and synthesis of *sn*-2 MAG catalyzed by bifunctional *sn*-2 GPAT (1). The intracellular pool of *sn*-2 MAG is then used as a substrate for DAG synthesis by a putative MAG:MAG transacylase (2). The DAG product and a portion of the *sn*-2 MAG are transported outside of cells. TAG synthesis occurs when *sn*-2 MAG donates an acyl chain to DAG through a proposed extracellular MAG:DAG transacylase (3). The MAG:MAG transacylase and MAG:DAG transacylase reactions proposed here are based on radiolabeling data and have not been demonstrated by direct assays with purified enzymes. (B) The Kennedy pathway for TAG synthesis is also presented to illustrate the contrasting reactions of oil seed TAG synthesis to Bayberry surface wax synthesis**.**

2.5 Conclusions

Bayberry fruit accumulates the largest known quantity of surface wax among plants, is the only plant reported to contain almost entirely TAG and DAG in its surface wax, and is the only example of TAG synthesis from exclusively saturated fatty acids with chain lengths greater than C12:0. We conclude that Bayberry wax glycerolipids are synthesized by a combination of intracellular and extracellular reactions via enzymes related to biosynthesis of the insoluble surface glycerolipid cutin. However, Bayberry wax is quite different from cutin in its structure and the fact that the fatty acids are not modified or linked together or to the cell wall as an insoluble polyester. Seed dispersal is a driving force for evolution of the very large diversity of fruit structures and composition (Lorts et al., 2008). By providing a high calorie food source for birds, the glycerolipids on the surface of Bayberry fruits presumably increase seed dispersal resulting in a selective advantage for evolution of the massive surface wax layer (Fordham, 1983; Place and Stiles, 1992). Bayberry knobs clearly upregulated the expression of a very specific subset of genes associated with cutin production and saturated fatty acids to achieve its extraordinarily specialized metabolism.

Bayberry could be a useful model to study surface lipid production and secretion in addition to TAG synthesis in non-seed tissues. The fact that Bayberry produces surface lipids at many fold higher levels than other plant species may allow for improved visualization and biochemical analysis of the mechanism for surface lipid secretion and also a better understanding of how surface lipid synthesis interacts with other lipid metabolism in plant cells. Secondly, the genes and enzymatic reactions to synthesize and secrete soluble surface glycerolipids represents an entirely new plant system to study and also manipulate lipid synthesis in plants. Many efforts to produce higher-value lipids and increase quantities of lipids in crop species have been stymied

by deleterious effects on cell metabolism and pathway bottlenecks (Bates and Browse, 2011; Carlsson et al., 2011). Bayberry provides an example where modifications in surface lipid pathways, specifically in genes used to produce cutin, can enable the plant to synthesize extracellular TAGs. Future work should address what specific gene modifications are required to secrete DAG and TAG, and understand how they might be introduced in other plants as a strategy to engineer accumulation of potentially deleterious lipids. Furthermore, the mechanism Bayberry employs to secrete lipids might also be useful to secrete other valuable hydrocarbons.

2.6. Materials and methods

2.6.1. Plant material and collection

Myrica pensylvanica fruits were collected from three separate stands of plants on the campus of Michigan State University (42°43N, 84°23W). Experiments were done on tissue harvested from 2011 to 2015. Fruit development was comparable each year, although we noticed that fruits developed earlier (~1-2 weeks) in 2012 when spring temperatures were warm. Fruits were used fresh (i.e. within minutes after collection from plants) or were immediately frozen in liquid nitrogen and stored at -80°C for later analysis. Intact knobs were either dissected from the fruits by gently scraping them with a syringe needle, or, when the fruits hardened the knobs were removed be gently grinding the whole fruit with a motor and pestle or Polytron.

2.6.2. Wax and lipid extraction

Surface wax was extracted by immersing whole intact Bayberry fruits in 5-20mL (depending on the number of fruits used) of chloroform for 20s-30s. Testing of various extraction times indicated that 20-30s releases >90% of the available surface wax monomers. The chloroform fraction with the soluble waxes was separated from the fruits, and the solvent was removed under N_2. In some experiments, after surface lipid extraction, the knob lipids or whole fruit lipids were recovered by quenching the tissue in 85 °C isopropanol for 10 min, grinding with a Polytron and following the 3:2 Hexane: isopropanol extraction method (Hara and Radin, 1978). After drying under N_2, surface wax and internal lipid extractions were re-dissolved in 1mL of toluene or hexanes or chloroform, capped under N_2 and stored at minus 20°C until further analysis.

2.6.3. Lipid quantification by GC-FID

The glycerolipids of Bayberry wax were analyzed by gas chromatography (GC) with FID detection using a high-temperature DB-5 column (length 30 m x 0.25mm id, 0.1 μm film thickness, Agilent). To facilitate better separation of hydroxyl-containing compounds (i.e. FFA, MAG and DAG) in the wax, samples were derivitized overnight at 50°C with bis-N,N-(trimethylsilyl) trifluoroacetamide (BSTFA) in pyridine and toluene as co-solvent. Derivitized samples were then dried under N_2 and immediately and re-dissolved in 1:1 *n*-heptane: toluene (1:1 v/v). The GC temperature program was: inlet temperature of 380 °C, oven temperature of 250 °C for 3 min and then ramped to 370 °C at 10 °C min^{-1} and held for 15 min. Because the response factors for intact TAG decreases as the carbon number increases, correction factors were applied by creating standard curves using saturated TAG standards from Tri13:0 to Tri 20:0 (Christie, 2011).

In addition to intact glycerolipid analysis, some lipid samples were quantified based on their transmethylated fatty acid content (i.e as FAMEs). Samples were transmethylated in 1mL of 5% H_2SO_4 (v/v), supplemented with 300μL of toluene, at 85°C for 2h. FAMEs were extracted once with 2mL of hexane, and the solvent was evaporated under N_2. FAMEs were then re-dissolved in *n*-heptane and analyzed by gas chromatography according to Li-Beisson et al. (2010).

For all lipid quantification, appropriate glycerolipid or FAME internal standards were added during the extraction, and also prior to analysis.

2.6.4. Microscopic analysis of Bayberry tissue

Visualization of Bayberry fruits was performed with standard light microscopy, scanning electron microscopy (SEM) and confocal fluorescence microscopy. To characterize the developmental progression of Bayberry fruits, fresh and paraffin fixed tissue were photographed using a dissecting or compound light microscope with an attached digital camera. Fixation of Bayberry fruits was done essentially as described in (Karlgren et al., 2009). Sections were cut to thickness of 10-20µm, attached to a microscope slide and stained with toluidine blue for 5-10 minutes (Brundrett et al., 1991).

For SEM, whole fruits were frozen in liquid nitrogen followed by freeze drying (Electron Microscopy Sciences Model EMS750X). Dried samples were mounted on aluminum stubs using carbon suspension cement and high vacuum carbon tabs. Samples were then coated with gold (~20 nm thickness) and osmium (~10 nm thickness) and examined in a JEOL 6610LV SEM (tungsten hairpin electron emitter) scanning electron microscope.

For confocal microscopy, freshly harvested fruits were hand-sectioned in half and stained with 2 $\mu g\, mL^{-1}$ BODIPY 493/503 (excitation wavelength 488 nm, detected between 505-545nm) or Nile red (excitation wavelength 559 nm, detected between a 570-640nm). Stained and unstained control samples were then mounted in 5% glycerol and viewed under a Olympus FluoView FV1000 Confocal Laser Scanning Microscope configured on an IX81 automated inverted microscope using a 100x UPlanSApo (NA 1.4) objective. Chlorophyll autofluorescence was also collected using an excitation wavelength or 488nm and collected between 655-755nm. All images obtained were analyzed using FluoView FV1000 FV10-ASW Advanced Software version 4.2.

2.6.5. Radiolabeling of Bayberry fruits with [^{14}C]-acetate or [^{14}C]-glycerol

Radiolabeling was conducted with both dissected knobs and intact whole fruits. Freshly harvested tissue was incubated in buffer containing 20mMol MES (pH 5.7), 0.1M sorbitol, 0.1X MS salts, 0.01% tween, 1g of sucrose and either 200 µCi [1-^{14}C] of acetate (specific activity 52 mCi mmol^{-1}, Perkin Elmer) or 16 µCi [^{14}C-(U)] glycerol (specific activity 150 mCi mmol^{-1}, Perkin Elmer). The dissected knobs were incubated in 5-10mL of buffer, while whole fruits were incubated in 20-25mL of buffer. The tissue was gently shaken at room temperature under 50-100µE of white light. At each harvesting time, a portion of the tissue was removed from the buffer, and lipids were extracted as described above. To account for different amounts of knob tissue harvested at different time points, radioactivity was normalized based on the total fatty acids content of respective lipid extracts, or when whole fruits were labeled, to the number of fruits harvested. Total radioactivity in lipids was quantified by scintillation counting (LS 6500, Beckman Coulter). In some incubations with whole fruits, surface wax was first extracted from the fruits with chloroform, and then lipids were extracted from the knobs, as described above.

Radiolabeled lipids were separated on 20cm X 20cm K6 TLC plates by developing the TLC plate first to 12-14 cm in chloroform: methanol: acetic acid: water (85:15,10.3.5, v/v/v/v) to separate polar lipids, followed by neutral lipid separation by developing the TLC plate to its full length in hexane: diethyl ether: acetic acid (70:30:1, v/v/v). Labeled lipids were identified and quantified by autoradiography of TLC plates exposed in a Bio-Rad cassette for 3 to 24 hours and using a PMI FX Phosphoimager (Bio-Rad). Labeled lipid classes were positively identified by co-migration with non-labeled standards.

For [^{14}C]-glycerol-labeled lipids, the amount of label in the acyl groups was compared to the backbone. Bands were eluted from TLC plants using chloroform: methanol: water (5:1:1

v/v/v), then transmethylated followed by scintillation counting of the separated organic and aqueous phases.

2.6.6. Regiospecific analysis of the radiolabeled acyl chains

Regiochemistry of acyl chains in DAG and TAG was performed as previously described (Christie and Han, 2010). Briefly, 1,2 (2,3)- DAG or TAG was purified by TLC. DAG was then acetylated with acetic anhydride and methanol at 50°C overnight, and the acetyated DAG was re-purified by TLC (hexane: diethyl ether:acetic acid -70:30:1, v/v/v). A dried mixture of acetylated Bayberry DAG or TAG containing 100µg of unlabeled C18:1 was incubated in 900µL of 1M Tris-HCL (pH 8.0) 125 µL of 2.2% $CaCl_3$, 250 µL of 0.25% bile salts and 25 µL of hexanes. The hexanes and FAME were added to aid in solubilization of the completely saturated Bayberry lipid mixtures (Brockerhoff, 1965). The reaction was pre-incubated in an orbital shaker at 400RPM at 42°C for 15min, then 0.5mg of pancreatic lipase was added. After a 4min incubation with the enzyme, the reaction was immediately quenched with 1mL of 6M HCl and 1mL of ethanol, and then extracted 3-times with diethyl ether. Lipids were dried under N_2 and separated by TLC and analyzed as described above.

2.6.7. Synthesis of [^{14}C]-*sn*-2 MAG substrate and incubation with Bayberry fruits

[^{14}C]-Myristoyl-*sn*-2MAG was prepared by pancreatic lipase digestion of trimyristin [1-^{14}C] (specific activity 55 mCi mmol^{-1}, American Radiochemicals) as described above, except that the digestion time was extended to 15min and the reaction quenched by adding 2mL of 5% boric acid in 50% ethanol to minimize acyl-migration in MAG (Thomas et al., 1965) Digested lipids were then separated by TLC impregnated with 5% boric acid, and [^{14}C]-*sn*-2 MAG was

eluted from the TLC, and used in an assay within 1 day. Approximately 12% of the [^{14}C]-TAG added was recovered in [^{14}C]-*sn*-2MAG.

A standard assay contained approximately 0.7 μCi of [^{14}C]-*sn*-2MAG in 500μL of labeling buffer added to knobs dissected from one Bayberry fruit. This equated to a concentration of 60μM *sn*-2 MAG per assay. At each time point the knobs and surrounding media were collected and lipids were extracted using 1:2 chloroform:methanol.

2.6.8. RNA-seq of Bayberry knob tissue

RNA was extracted from Bayberry knobs through seven stages of wax development, from when surface wax was undetectable to approximately 50% of its final production. Knobs were collected by gently scraping the fruit with a syringe needle. For comparison, RNA from young and mature Bayberry leaves were also extracted for sequencing. Triplicate biological replicates were collected at one stage of fruit development, three time points were collected in duplicate, and three time points were collected with one replicate. Total RNA was extracted from knobs and leaves using a method similar to Meisel et al. (2005). For each extraction, knobs or leaves were first ground to a fine powder in liquid N_2, followed by adding hot (~65°C) extraction buffer which was vigorously mixed with the tissue and then incubated at 65°C for 10min. The extraction buffer contained 2% (w/v) CTAB, 2M NaCl, 0.05% (w/v) spermidine, 100mMol Tris-HCl (pH 8.0), 25mMol EDTA, 3% (v/v) β-mercaptoethanol, and 3% (w/v) PVPP at a ratio (w/v) of tissue to buffer of 1:10. The mixture was allowed to cool to room temperature and insoluble material was removed by two extractions with 24:1 Chloroform: isoamyl-alcohol (10000xg for 20min at room temperature). The aqueous layer containing the nucleic acids was precipitated twice; once with ethanol containing 50μg mL^{-1} glycogen (Ambion) at minus 20°C overnight

followed by a second overnight precipitation with 2.5M lithium chloride in 100µL of RNAse free water at 4°C. The concentrated RNA was treated with DNAse (Ambion) and then purified using the RNeasy MinElute kit (Invitrogen). The purity of the RNA was assessed with an Aligent 2100 Bioanalyzer.

A total of 14 RNA samples from knobs and leaves were sequenced at the Joint Genome Institute (Walnut Creek, CA). For each sample, stranded cDNA libraries were generated using Illumina mRNA sample preparation protocols. Briefly, mRNA was extracted from 10 µg of total RNA with magnetic beads containing poly-T oligos. mRNA was then fragmented with divalent cations and high temperature and then reverse transcribed using random hexamers and SSII (Invitrogen) followed by second strand synthesis. The cDNA was then treated with end-pair, A-tailing, adapter ligation, and 10 cycles of PCR. qPCR was then used to determine the concentration of the libraries.

The cDNA was subjected to paired-end sequencing using an Illumina HiSeq, obtaining a read length of 150nt. The data was computed using a combination of CLC workbench (version 7.5. www.clcbio.com) and Trinity software package (version r20140413). Briefly, reads were screened against the silva rRNA database (Quast et al., 2013) and trimmed on quality and adapter sequence using the Trim Sequences program from CLC Genomics Workbench. Reads were normalized with Trinity's *in silico* normalization package and assembled in stranded orientation. *De novo* transcriptome assembly was done with a sample that contained a mixture of RNA from knobs from seven developmental stages and from two stages of leaves (Grabherr, 2011). Contigs were annotated against the Arabidopsis proteome (TAIR 10.0) with BLASTX. Arabidopsis was selected because annotations of its proteins are the most authoritative and well supported by data (Li-Beisson et al., 2010). Reads from each time-point and leaves were mapped

against the *de novo* assembly and quantified using the Genomics Workbench RNA-Seq Analysis program (Similarity fraction: 0.8, Length fraction: 0.75). RPKM for each contig, top Arabidopsis homolog and assembly statistics for each library can be found in Supplemental File 1**.** The sequencing details can be found at NCBI under BioProject number PRJNA250987 and the data can be downloaded from Joint Genome Institute (JGI) Genome portal (http://genome.jgi.doe.gov/) under project ID 1007578.

2.6.9. Phylogenetic tree construction

Multiple alignments and the phylogenetic trees were constructed with bioinformatic tools available at www.phylogeny.fr, using the default settings (MUSCLE 3.7 was used for multiple alignment, Gblocks 0.91b was used for alignment refinement, and PhyML 3.0 was used to generate the phylogenies) and trees were modified with MEGA6. The non- Bayberry sequences used for each tree are and sequence identifiers are as follows: (A) GPATs (all from Arabidopsis (At)): GPAT1 (At1g06520), GPAT2 (At1g02390), GPAT3 (At4g01950), GPAT4 (At1g01610), GPAT5 (At3g11430), GPAT6 (At2g38110), GPAT7 (At5g06090), GPAT8 (At4g00400). (B) GDSL motif enzymes: Tomato (Si) CD1/CuS1(Solyc11g006250), CGT (E7AIM3); *Agave americana* (Aga) SGNH hydrolase (Q5J7N0); AtCuS1 (At3g04290), AtCDEF1 (At4g30140), At3g16370; *Jacaranda mimosifolia* JNP1 (EU350954); *Physcomeitrella pattens* (Pp) CuS1 (Pp1s34 96V6.1). (C) DCR and other HXXXD-motif acyl transferases: *Linum usitatissimum* (Lu) DCR1 (AHA57444), DCR2 (Lus10039256); At DCR (At5g23940), CER26 (At4g13840), CER2 (AT4G24510), HCT (At5g48930), ASFT (At5g41040), FACT (At5g63560) and At3G62160; Rice (Os) PMT (LOC_Os01g18744).

APPENDIX

2.7. Supplemental figures for chapter 2

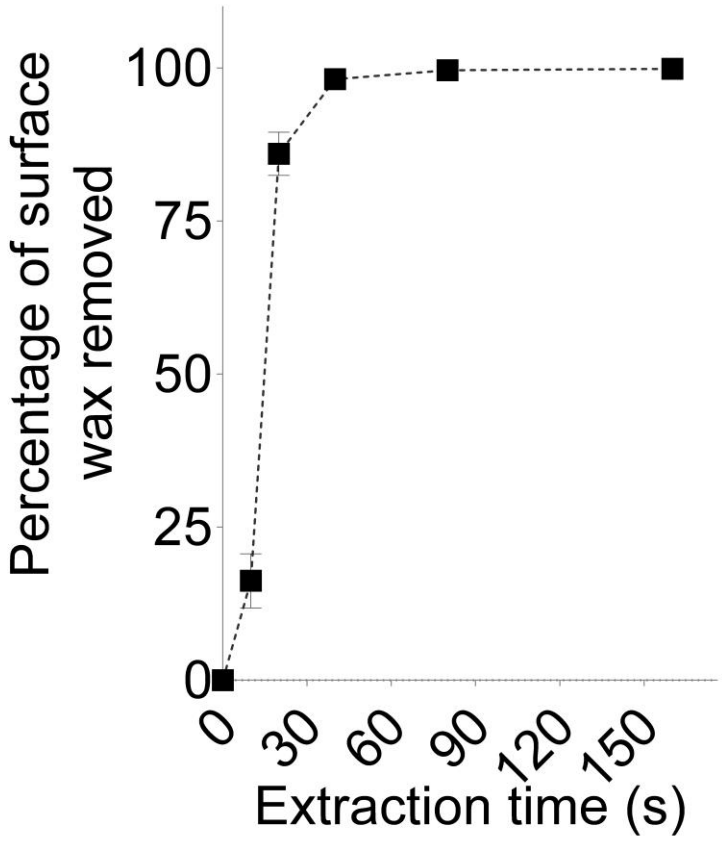

Figure 16: Extraction of Bayberry surface wax by chloroform. Each point represents percentage of the maximum wax (determined as fatty acids) that was removed from the surface of Bayberry fruits through 10-160 seconds of continuous immersion in chloroform (2 independent extractions, ± range). No unsaturated fatty acids were detected in any sample through the time course.

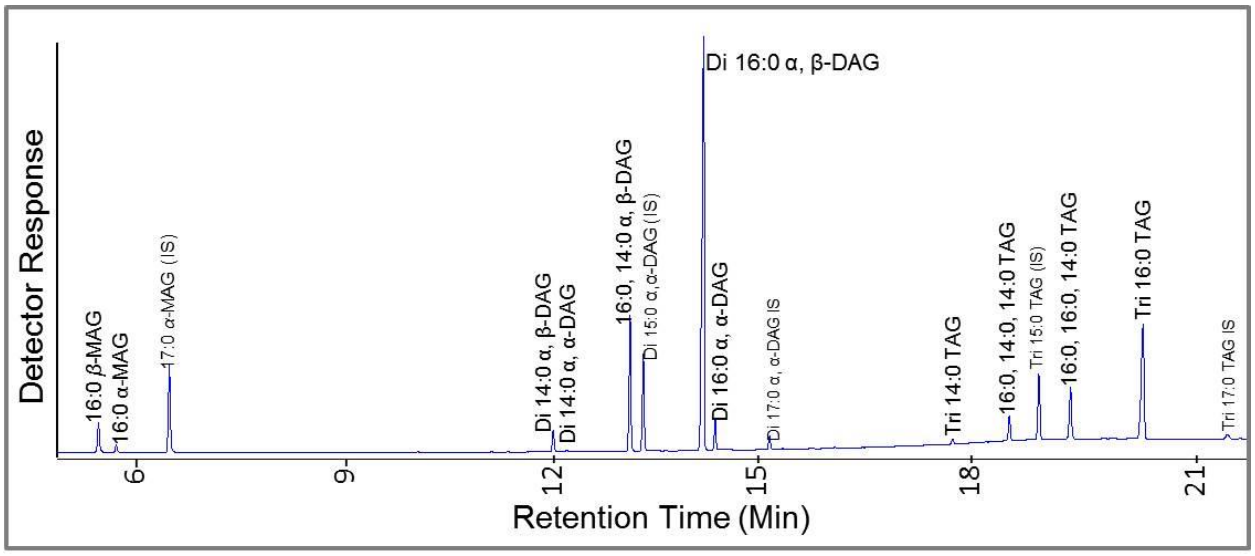

Figure 17: A representative GC-FID separation, using DB5-HT column, of Bayberry surface wax with added internal standards (IS). Alpha (α) refers to acyl chains in the *sn*-1 or 3 positions of glycerol, and beta (β) refers to the acyl chain in the *sn*-2 position of glycerol.

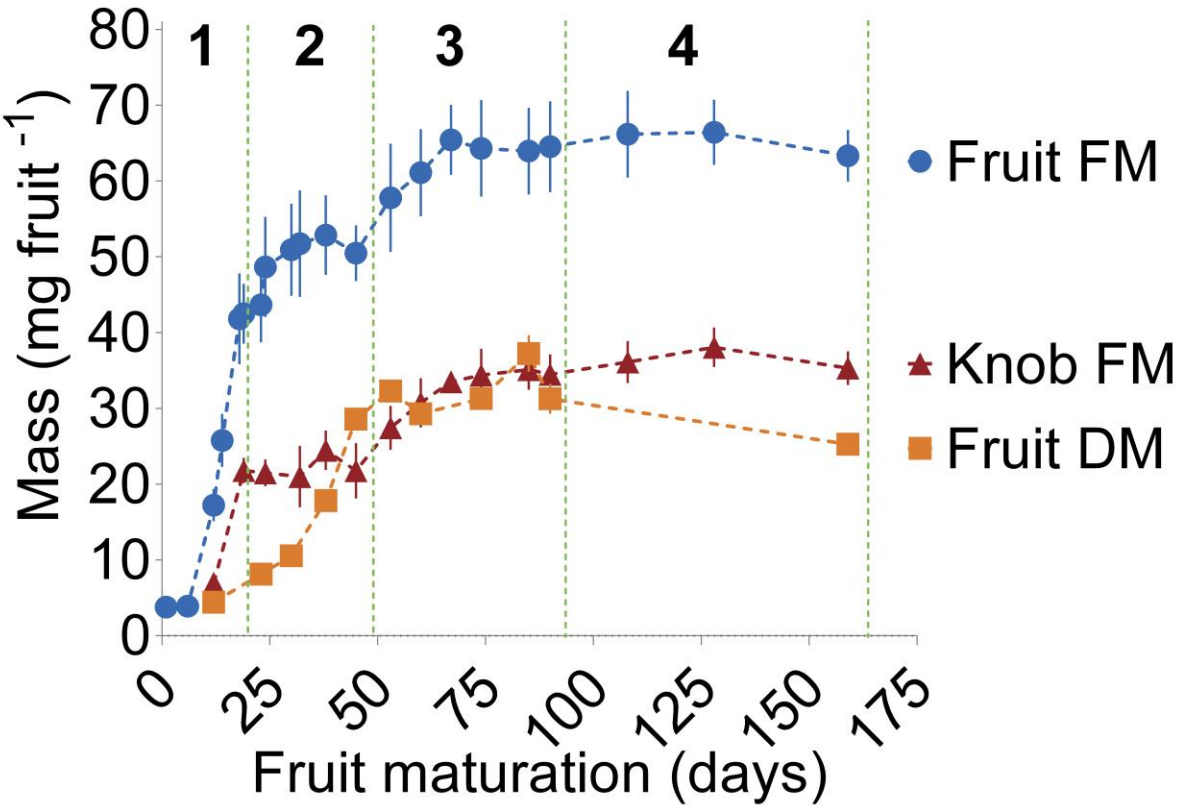

Figure 18: Mass of Bayberry fruit parts through development. Stages of wax accumulation are designated by dotted green lines. Fruit fresh mass (FM) and dry mass (DM) includes the mass of the whole fruit with the intact wax layer. Knob FM is the mass of the knobs with the wax layer. To best approximate the mass of the knobs, the whole fruit mass was subtracted from the mass of the fruit proper (i.e. without knobs and wax). Each point represents the mean value from 3-4 replicates ±SE.

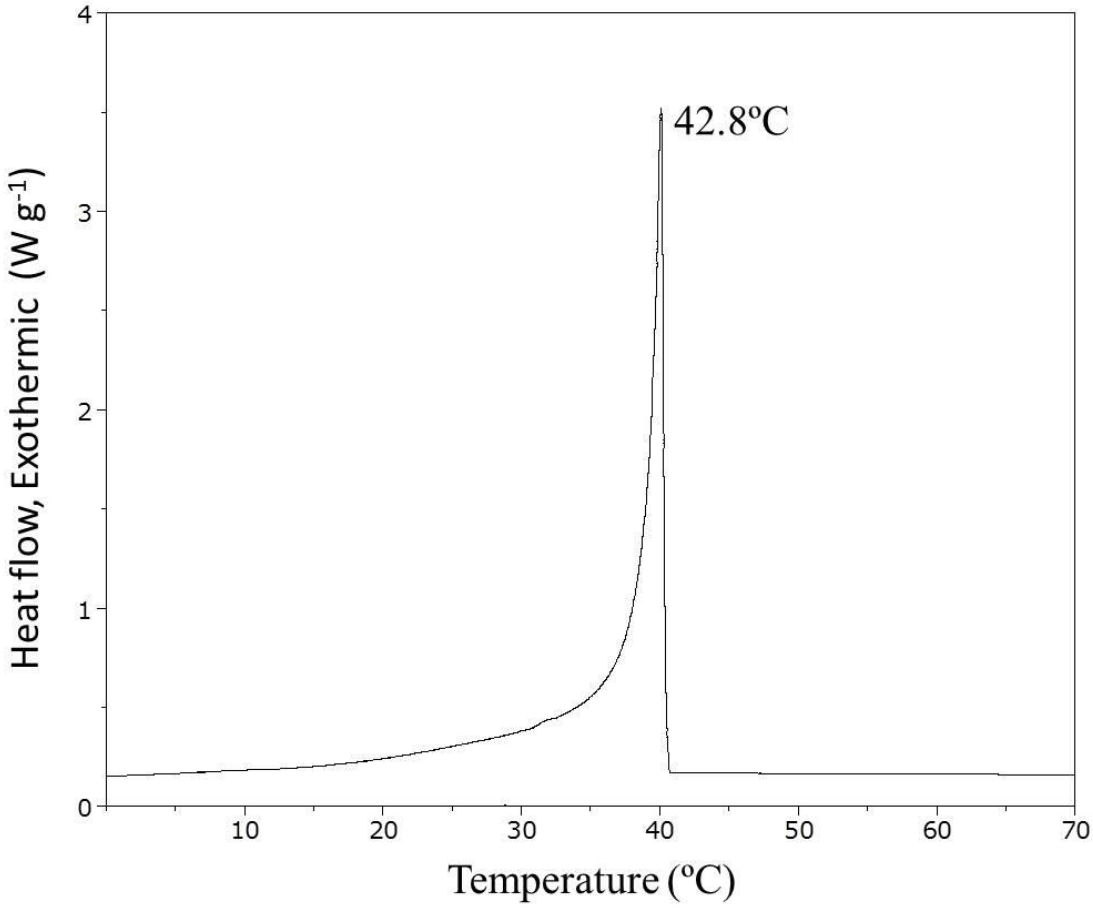

Figure 19: Crystallization temperature of purified Bayberry wax determined by differential scanning calorimetry. The crystallization temperature is the peak of the major exotherm upon cooling.

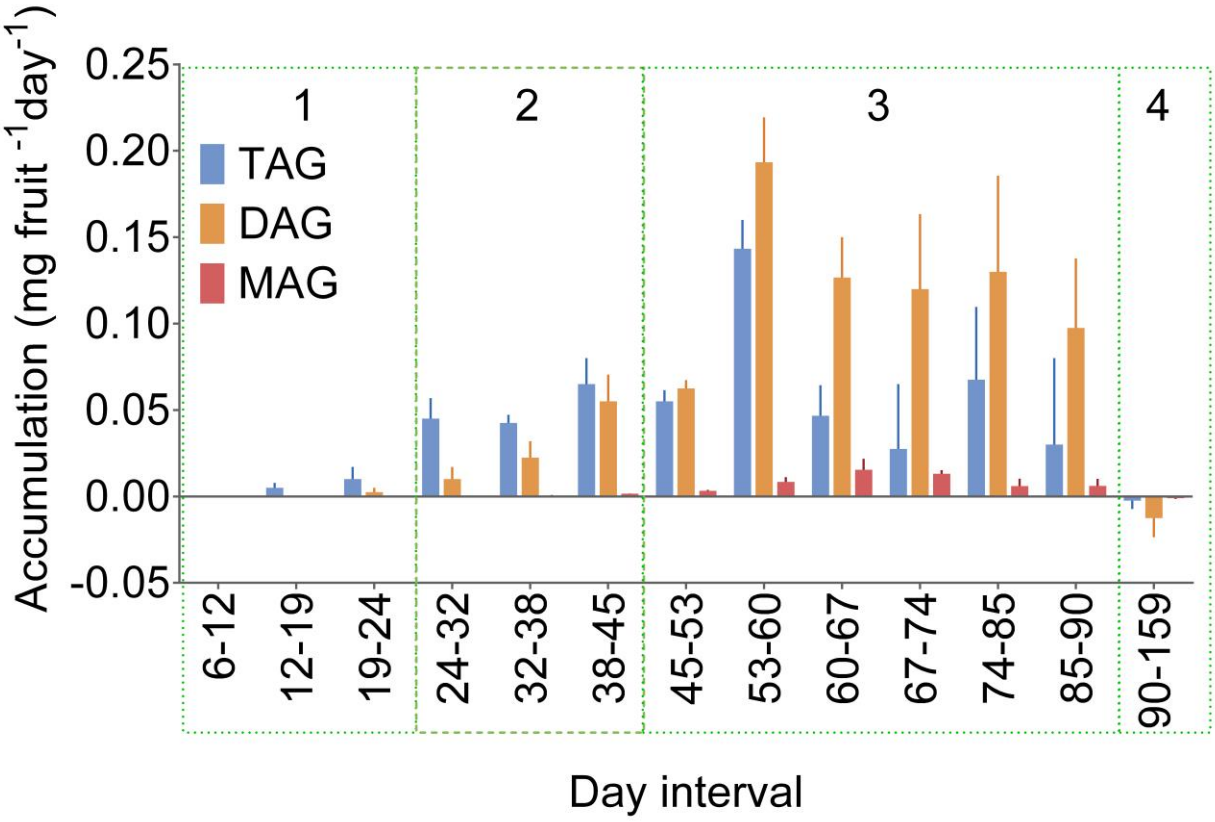

Figure 20: Rates of accumulation of each glycerolipid class in the surface wax through development. Each bar represents the mean value from 3-4 replicates ±SE. Stages of wax accumulation are designated by the dotted green lines.

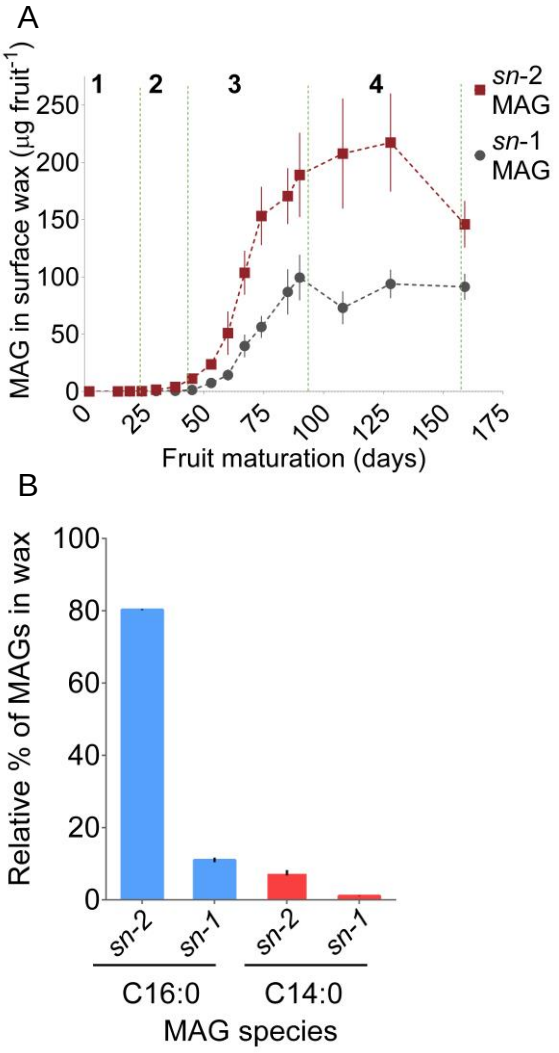

Figure 21: Monoacylglycerols in Bayberry wax occur predominately as the *sn*-2 isomer. (A) Accumulation of *sn*-2 and *sn*-1 MAG through development of the fruit. Stages are denoted by the dotted green line and each point on the graph is the mean of 3-4 separate wax extraction ± SE. (B) Relative percentages of C16:0 and C14:0 *sn*-1/3 MAG and *sn*-2 MAG isoforms in the surface wax at day 60. The isomers were identified by GC/MS and normalized to a *sn*-1 C17:0-MAG internal standard added to the extracted surface wax. The extracted surface wax was derivitized with BSTFA and analyzed within 1 day of chloroform extraction. Each bar represents the mean of 3 separate extractions ± SD.

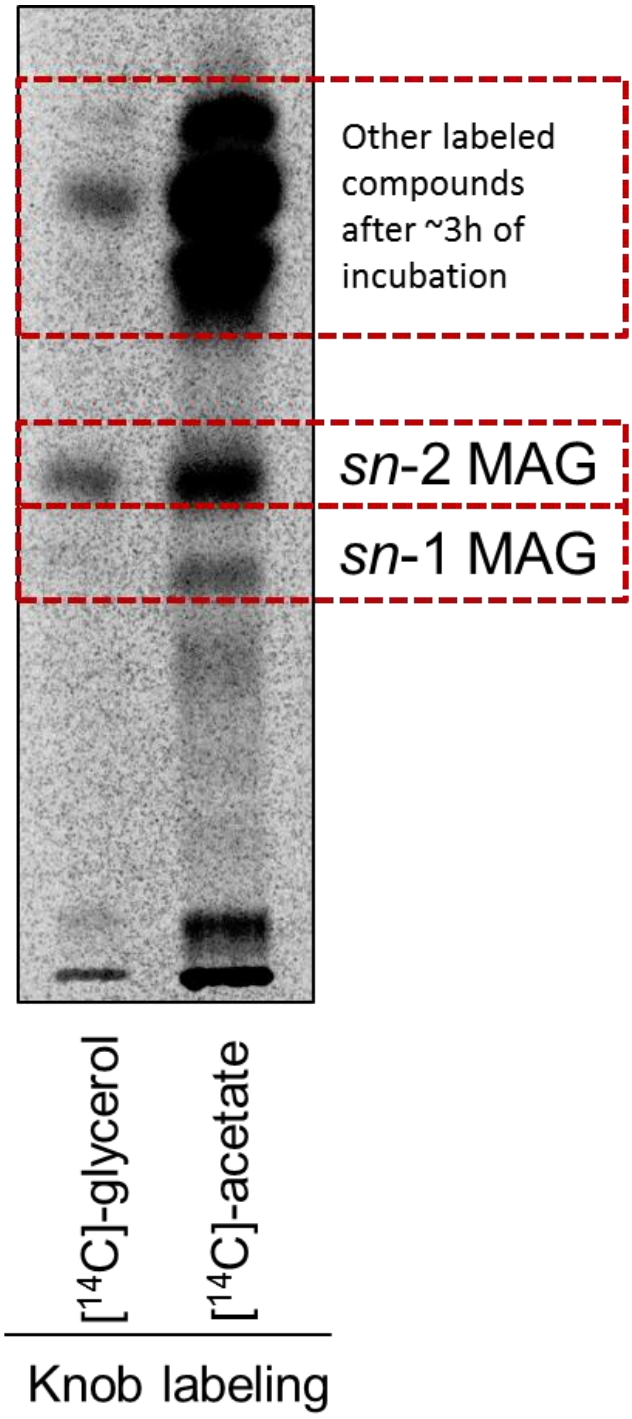

Figure 22: TLC separation of MAG isoforms after labeling Bayberry knobs for 3h with [^{14}C]-glycerol or [^{14}C]-acetate. The TLC plate contained 5% boric acid and was developed in chloroform: acetone (85/15 v/v).

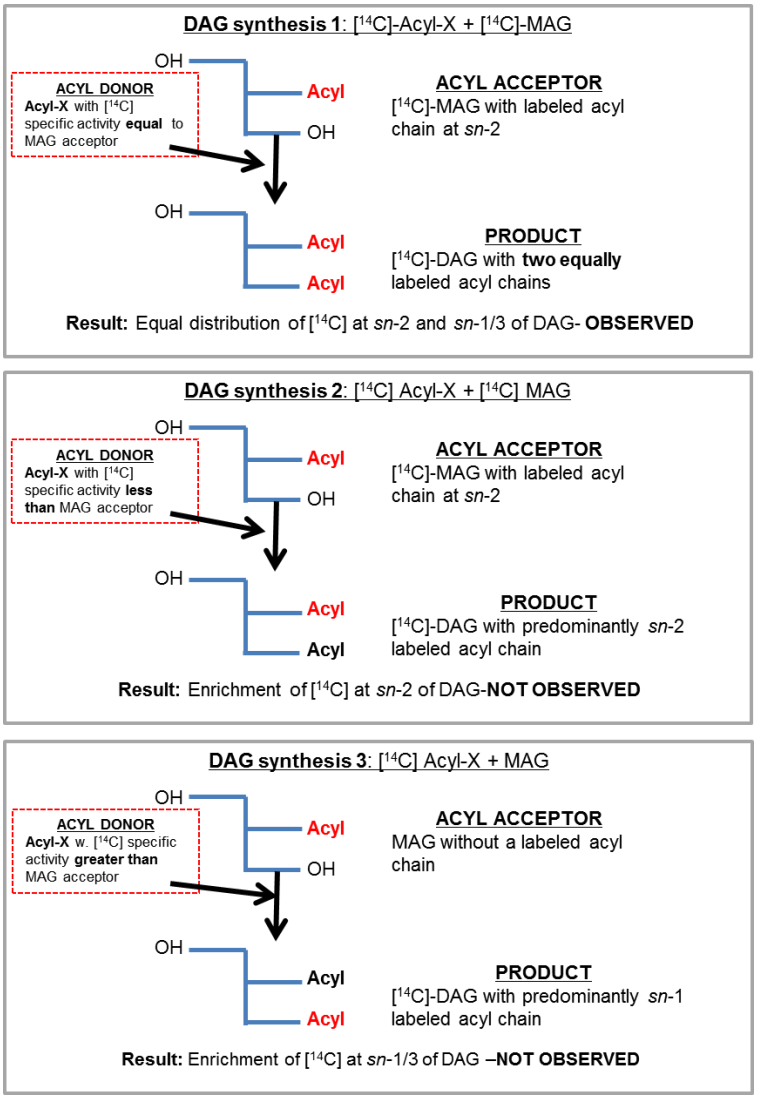

Figure 23: Alternative scenarios for DAG synthesis in Bayberry. For each scenario the relative specific activity ([^{14}C] per acyl chain) of potential acyl-donors and the *sn*-2 MAG acceptor were varied and the distribution of [^{14}C] acyl chain in the product, [^{14}C]-DAG, predicted. Only scenario 1 results in equal distribution of [^{14}C] between the *sn*-1/3 and *sn*-2 positions of DAG, as observed experimentally. Regiospecificity of the acyl chains on the *sn*-1 and *sn*-3 positions of DAG is not specified.

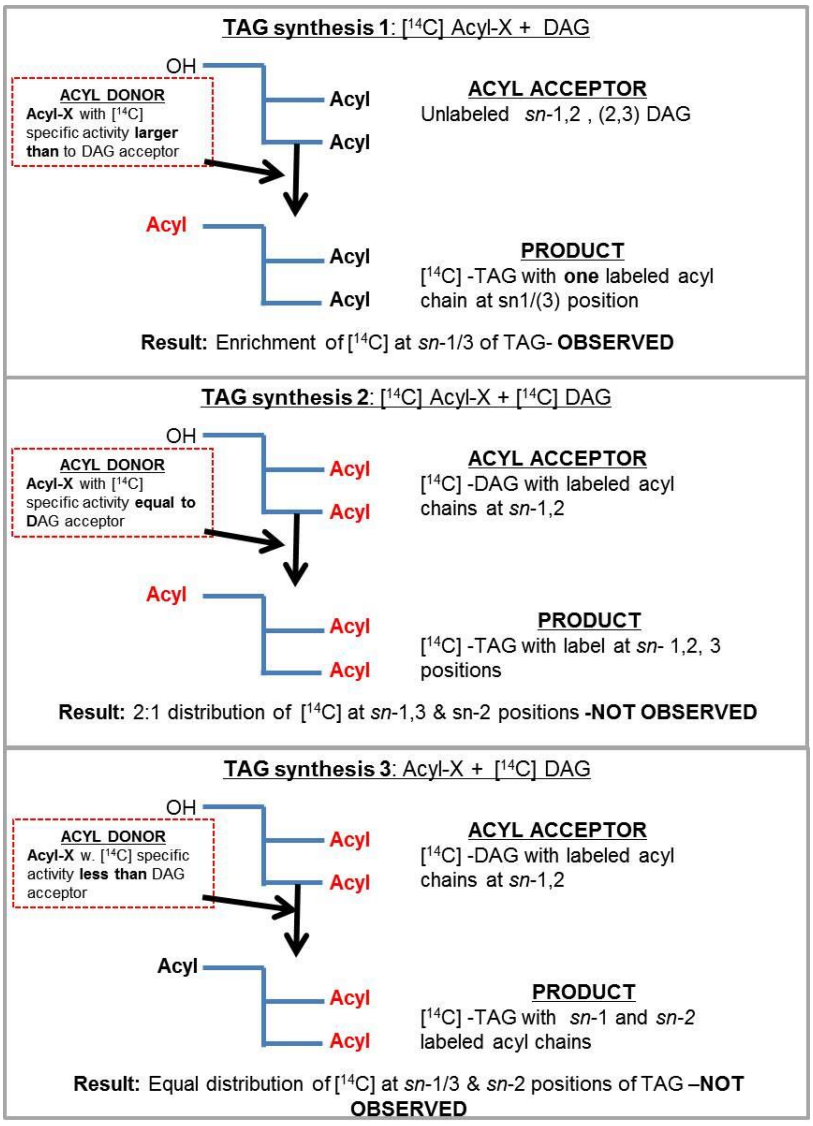

Figure 24: Alternative scenarios for TAG synthesis for Bayberry wax. For each scenario, the relative specific activity of acyl-donors and the *sn*-1,2 (2,3) DAG acceptor molecule were varied, and the distribution of the [^{14}C]-acyl chains in the product, [^{14}C]-TAG, predicted. Only scenario 1 results in enrichment of [^{14}C]-acyl chains in the *sn*-1/3 position of TAG observed experimentally. Regiospecificity of the acyl-chains on the *sn*-1 and *sn*-3 positions of DAG are not specified. Other scenarios, not pictured here (i.e. a DAG:DAG transacylase, or an enrichment of [^{14}C]- at one position in DAG) were considered, but were also not consistent with the experimental observations.

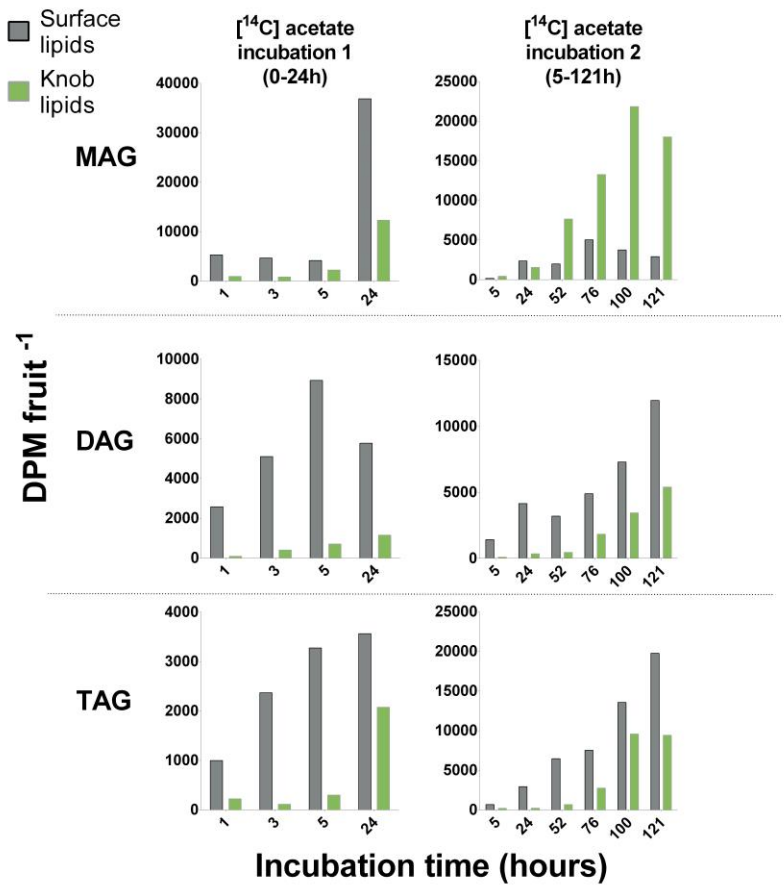

Figure 25: Distribution of [^{14}C]-glycerolipids recovered in the extracellular wax lipids, and the tissue after wax extraction (i.e. the cellular or knob lipids). Clusters of 5-10 fruits were submerged in labeling buffer containing 200 µCi [^{14}C]-acetate. The clusters were harvested at intervals from 1h-24h (incubation 1) or 5h - 5 days (incubation 2). At time points indicated, surface wax was removed by submerging the fruit clusters in chloroform for 30s, then lipids were extracted from the knobs with 3:2 hexane: isopropanol. The radiolabel incorporated into the surface wax or into the knob lipid fraction for each of MAG and DAG and TAG is presented. [1]

[1] The accumulation of labeled DAG and TAG in lipids that remained with the knobs following wax removal was contamination from secreted wax, and does not reflect cellular accumulation of DAG and TAG. This is based on the observation that the labeled TAG and DAG increased in the knob lipid through time, but were still detected immediately within the surface wax. This trend is the opposite of what would be expected if the wax is synthesized intracellularly followed by export.

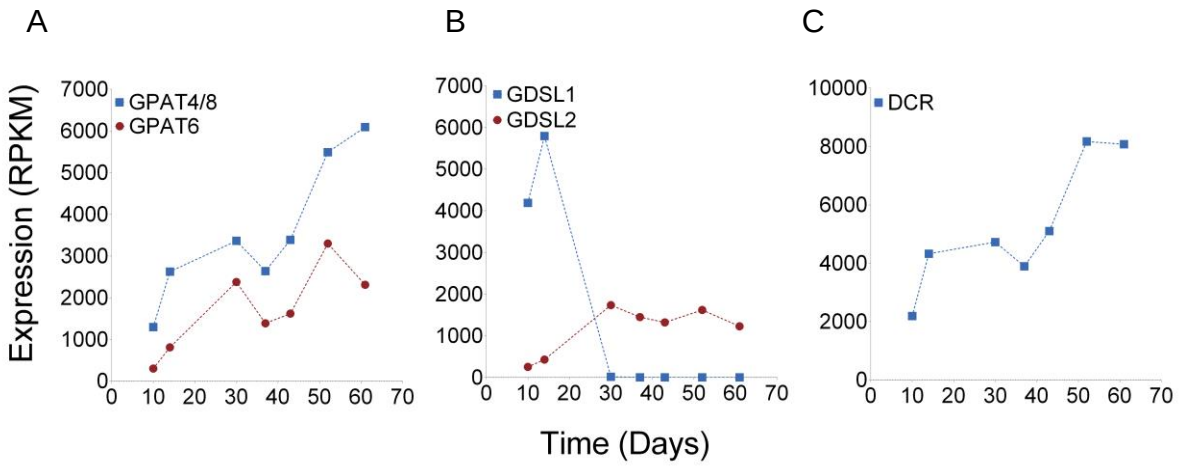

Figure 26: Time-course of expression of transcripts for the abundant cutin-associated acyltransferases /transacylases in Bayberry knobs. (A) Homologs to the sn-2 specific Arabidopsis GPATs. (B) The two most highly expressed GDSL-motif enzymes. GDSL1 is related to tomato CD1 (Yeats et al. 2012). (C) Homolog to Arabidopsis DCR. The days (x-axis) are the same as reported in the season-long compositional analysis. (x-axis in Figure 6 D).

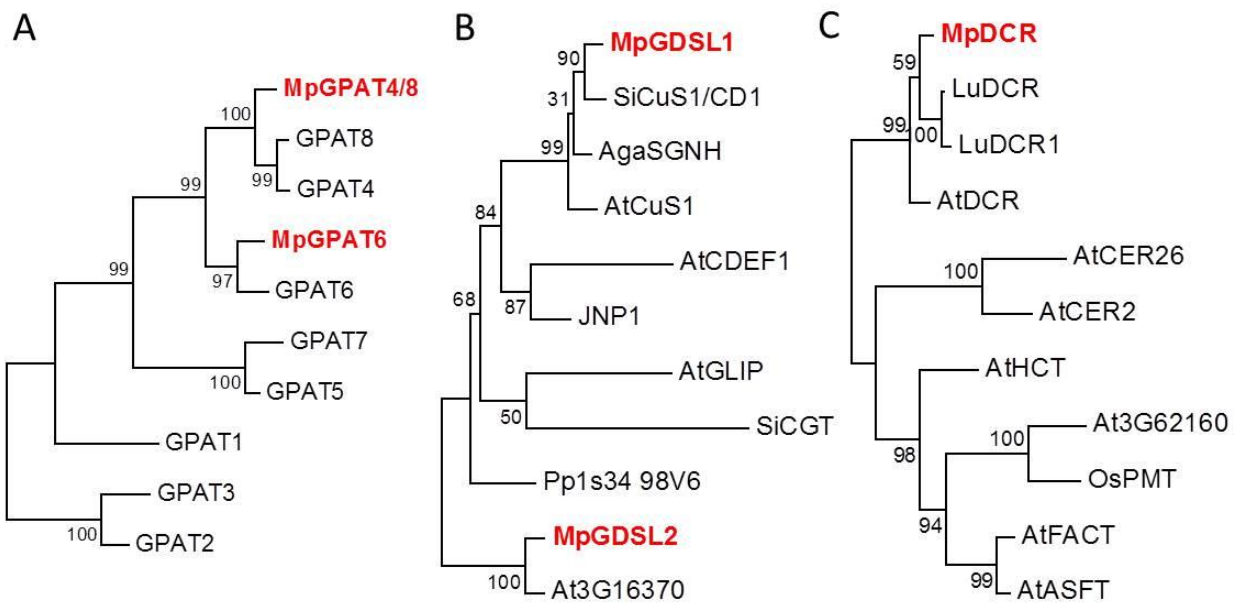

Figure 27: Phylogenetic relationships between highly expressed Bayberry acyltransferases/ transacylases and predicted or characterized genes in other plants. The highest expressed Bayberry homologs are bolded and highlighted in red. (A) *sn*-2 GPAT family. Bayberry GPATs were compared only to Arabidopsis *sn*-2 GPATs. (B) GDSL-motif superfamily. (C) Selected DCR-like HXXXD acyltransferases**.** The numbers on each branch designate bootstrap values. Gene identifiers are found in the materials and methods.

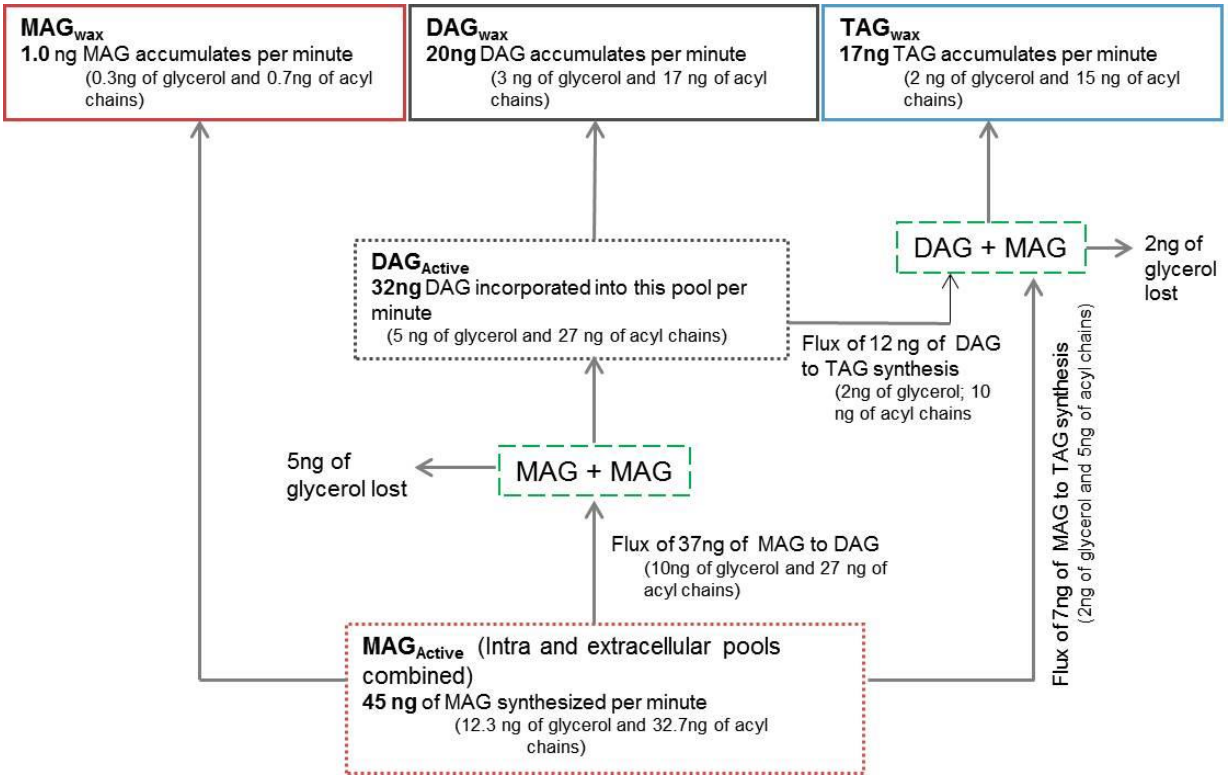

Figure 28: Flux of intact glycerolipids, glycerol backbone and acyl chains for Bayberry surface wax synthesis. Using the proposed reaction sequence - MAG + MAG → DAG, followed by DAG + MAG → TAG- the figure outlines required flux through active MAG and DAG pools to achieve a ratio of MAG:DAG:TAG accumulation of 2:45:53 in the surface wax at the stage of fruit development used for labelling (approximately days 38-45). Boxes with continuous borders designate the pools of glycerolipid in the wax, boxes with dotted borders indicate metabolically active pools. Green colored dashed boxes indicate putative reactions in the model (MAG + MAG and DAG + MAG). Sizes of boxes and arrows are not to scale. There is no distinction between intra and extracellular reactions in this scheme. In this model it is also assumed there is no breakdown of lipids, and that the active pools sizes are constant.

2.8. Supplemental tables for chapter 2

Table 3: Molar composition of acylglycerol species in surface wax through development. All of the acylglycerol species are saturated, and the order of the acyl chains in each species is not specified. SE from 3-4 replicates is indicated for the total mol percentage of TAG, DAG and MAG.

	Acylglycerol species	Day 14	19	24	30	38	45	53	60	67	74	85	90	108	128	159
TAGs	14,14,14	0.0	0.0	0.0	0.0	0.0	0.0	0.2	0.4	0.6	0.7	1.0	1.2	0.7	1.3	1.2
	14,14,16	0.0	0.0	0.0	0.0	0.2	1.3	1.7	2.3	3.0	3.3	3.7	4.5	4.2	4.7	4.9
	14,16,16	0.0	0.0	0.3	1.5	2.2	5.8	7.0	7.4	7.9	7.5	7.6	7.9	8.0	8.0	8.9
	16,16,16	100	85.6	66.3	69.1	60.5	46.1	37.0	28.6	23.5	19.5	17.4	14.9	16.1	13.8	16.1
	16,16,18	0.0	1.6	6.1	6.4	5.4	3.4	2.4	1.7	1.3	0.7	0.5	0.7	0.6	0.6	0.7
	Total TAG (mol%)	100 ± 0	87.2 ±7.1	72.7 ± 6.0	77.0 ± 5.2	68.3 ± 5.0	56.7 ± 3.3	48.2 ± 2.7	40.4 ± 3.0	36.3 ± 3.4	31.7 ± 2.8	30.3 ± 2.3	29.2 ± 1.9	29.6 ± 3.0	28.4 ± 1.6	31.9 ± 1.8
DAGs	14, 14	0.0	0.0	0.0	0.0	0.0	0.0	0.3	0.6	1.7	2.4	3.0	3.8	3.0	3.9	3.2
	14, 16	0.0	0.0	0.7	0.4	0.7	3.1	5.1	7.8	10.4	12.8	14.7	16.2	15.1	17.2	15.2
	16, 16	0.0	10.7	25.7	21.1	29.0	37.5	42.1	45.3	44.5	44.3	44.0	42.7	43.5	41.6	42.4
	16, 18	0.0	0.0	0.5	0.7	0.5	0.5	0.9	0.5	0.4	0.6	0.5	0.4	0.4	0.6	0.5
	Total DAG (mol%)	0.0	10.7 ± 5.7	26.9 ± 5.7	22.3 ± 5.0	30.2 ± 4.8	41.2 ± 3.4	48.4 ± 2.4	54.2 ± 2.5	57.0 ± 2.1	60.1 ± 1.3	62.2 ± 1.1	63.1 ± 1.2	62.0 ± 1.6	63.3 ± 0.7	61.2 ± 1.2
MAG	16 (mol%)	0.0	0.0	1.5 ± 0.4	1.1 ± 0.4	1.4 ± 0.2	2.2 ± 0.1	3.3 ± 0.4	5.3 ± 0.6	6.7 ± 1.4	8.2 ± 1.6	7.5 ± 1.3	7.7 ± 0.9	8.3 ± 1.5	8.3 ± 0.9	6.9 ± 0.7

Table 4: Distribution of radioactivity in different lipid classes after incubation of knobs with [^{14}C]-glycerol for the times indicated.

	Glycerolipid species (%)				
Time (min)	MAG	DAG	TAG	PC	Unknown
30	65.7	15.6	4.1	2.5	7.6
90	58.6	26.9	2.3	3.9	4.1
180	39.4	44.0	4.7	3.4	4.3
360	25.1	51.5	8.1	3.8	6.7
660	18.1	48.9	12.0	4.7	9.7

Table 5: Percentage of radiolabel in the glycerol backbones of MAG, DAG and TAG after incubation of knobs with [^{14}C]-glycerol.

	Proportion of label in glycerol backbone (%)			
Time (min)	MAG	DAG	TAG	MAG+DAG+TAG
30	90	84	---	88
90	88	87	---	86
180	82	79	63	80
360	71	67	60	68
660	59	61	53	59

Table 6: Percentage of [^{14}C]-acetate incorporation into glycerolipids and unknown compounds through time. The unknown area includes 7-9 compounds. Figure 10B and 10C presents this data normalized to DPM μg^{-1} lipids.

	Glycerolipid species (%)				
Time (min)	MAG	DAG	TAG	PC	Unknown
1h time course					
5	71.6	29.5	0	0	0
15	68.8	22.2	0.9	0.2	7.8
30	48.7	28.5	2.4	1.9	18.5
60	41.1	29.5	3.8	1.9	23.8
11h time course					
20	44.3	15.8	2.0	9.1	26.6
60	43.9	27.1	1.5	5.7	21.9
180	23.3	39.0	4.1	7.4	26.2
360	16.0	40	6.8	6.5	31.0
660	16.1	38.7	7.8	6.1	31.3

CHAPTER 3

HOW DID NATURE ENGINEER THE HIGHEST SURFACE LIPID ACCUMULATION AMONG PLANTS? EXAMINING THE EXPRESSION OF ACYL-LIPID ASSOCIATED GENES FOR THE ASSEMBLY OF EXTRACELLULAR TRIACYLGLYCEROL BY BAYBERRY FRUITS

To be submitted to BBA Molecular and Cell Biology of Lipids special issue on plant lipid biology (November, 2015).

Authors: Jeffrey P. Simpson, John B. Ohlrogge

3.1. Acknowledgements

We thank the MSU Center for Advanced Microscopy's Abby Vanderberg and Alicia Pastor for sample preparation and assistance with SEM and TEM, respectively. RNA sequencing was performed by the DOE Joint Genome Institute (JGI), with special assistance from Kerrie Barry, Erika Lindquist and Anna Lipzen. Transcriptome assembly and databases were provided by Nick Thrower (MSU) and Curtis Wilkerson (MSU). We also thank the MSU Grounds department for maintenance of the Bayberry shrubs. This work was supported by Department of Energy–Great Lakes Bioenergy Research Center Cooperative Agreement DE-FC02-07ER64494. J.P.S. received a National Science and Engineering Research Council of Canada (NSERC) post graduate fellowship (PGS-D3).

3.2. Abstract

Bayberry (Myrica pensylvanica) fruits are covered with a remarkably thick layer of crystalline wax that consists almost entirely of triacylglycerol (TAG) and diacylglycerol (DAG) with saturated fatty acids. This is the only documented example of a major accumulation of seed-like glycerolipids in a plant surface wax. Previously we demonstrated that the assembly of Bayberry surface wax is distinct from conventional TAG and surface waxes, and instead may proceed through a pathway related to synthesis of the polyester cutin. In this study, we identified developmental, transcript and metabolic changes in Bayberry associated with the evolution of its unique surface lipid biology. Microscopic examination revealed the origins of the multicellular tissue (Bayberry knobs) which produces and secretes the wax. There was no evidence of knobs rupturing during wax accumulation periods, indicating the wax is actively secreted to the surface, which is similar to most cuticular lipids. Comparison of transcript expression in Bayberry knobs through development, to genetically related tissues (Bayberry leaves, M. rubra fruits), epidermal tissue, and oil-rich tissues, revealed exceptionally high expression of transcripts for 5 enzymes and 3 proteins of acyl-lipid metabolism. The predicted activities of the putative proteins encoded by the most highly expressed transcripts are associated with production of saturated fatty acids, and assembly and secretion of surface glycerolipids. The protein sequences encoded by transcripts expressed in Bayberry knobs are 100% identical to the sequences expressed in Bayberry leaves, which do not produce surface TAG or DAG. Together, these results indicate TAG biosynthesis and secretion in Bayberry is remarkably similar to pathways for cuticular lipid synthesis and also imply that modifications in transcript expression, rather than evolution of new gene functions or enzyme specificity, was crucial for Bayberry to evolve an extraordinarily specialized lipid metabolism and cell biology.

3.3. Introduction

The external surfaces of all aerial plant tissues are covered with a hydrophobic barrier called the cuticle. The major constituents of the cuticle are acyl-lipid based and include the insoluble polyester cutin and the soluble waxes embedded within and on top of cutin. While the cuticle is essential for plant development and survival, the fatty acid composition and abundance of cuticular lipids differs between plant species (Jetter et al., 2006; Stark and Tian, 2006). One striking example are the fruits Bayberry (i.e. *Myrica or Morella pensylvanica*) which are covered with a layer of surface wax that constitutes over 30% of its dry weight; the highest reported accumulation of surface wax in plants (Simpson and Ohlrogge, 2015). In addition, the surface wax is composed primarily of glycerolipids, notably triacylglycerol (TAG) and diacylglycerol (DAG) with saturated fatty acids (Harlow et al., 1965; Hawthorne and Miller, 1987; Simpson and Ohlrogge, 2015). These are lipids typically found in plant seeds, pollen and some fruit mesocarps, and no other plant has been reported to contain TAG or DAG as the major constituents of its surface waxes. Bayberry surface TAGs are not used as an energy/carbon reserve for the plant during germination, as oil seed TAG is, but instead the wax may be an attractant for some species of birds which in turn disperse the seeds (Place and Stiles, 1992). The abundance and physical properties of Bayberry wax also make it a popular source of wax for candle making.

Previously, we used a combination of molecular species analysis, microscopy, and kinetic labeling with [^{14}C]-lipid precursors to demonstrate that Bayberry surface glycerolipids are synthesized by a pathway distinctly different from conventional membrane or storage glycerolipid synthesis (Simpson and Ohlrogge, 2015). Instead, the data points to glycerolipid synthesis for Bayberry wax being analogous to the assembly of the insoluble surface polyester

cutin. Notably, labeling revealed *sn*-2 MAG as an initial intermediate in the production of Bayberry wax. *sn*-2 MAG is also an intermediate in the production of cutin (Beisson et al., 2012) and *sn*-2 MAG can serve as an acyl donor for cutin polyester synthesis (Li et al., 2007a; Yeats et al., 2012). In Bayberry, analysis of the kinetics of radiolabeled DAG and TAG synthesis and the distribution of radiolabeled acyl chains on their glycerol backbones was consistent with acyl-CoA independent reactions for DAG and TAG synthesis, *sn*-2 MAG as their primary acyl donor, and the final assembly of TAG occurring extracellulary. The pathway we proposed for assembly for Bayberry wax was similar to proposed models for cutin polyester assembly (Beisson and Ohlrogge, 2012; Yeats et al., 2012; Yeats et al., 2014), however there are still many unknowns for both pathways for glycerolipid assembly

In this study we further examined Bayberry's unique surface lipid biology and metabolism by observing the development of the tissue that synthesizes the wax (i.e. Bayberry knobs), and also asking whether transcript expression and/or changes in the protein sequences of the predicted genes may have contributed to the development of Bayberry's unique surface wax. Transcript expression in Bayberry knobs was quantified by RNA-seq. Overall, the most highly expressed annotated genes are homologous to genes associated with the production of saturated fatty acids, the assembly cutin, and secretion of surface lipids (top 55 expressed genes or top 99.5% percentile). The expression levels of transcripts for these predicted genes in Bayberry knobs were analyzed during seven stages of wax development and also compared to related tissues: (1) cutin producing tissues tomato epidermis (Matas et al., 2011) and cherry exocarp (Alkio et al., 2014), (2) TAG producing tissues *Brassica naups* embryo (Troncoso-Ponce et al., 2011) and oil palm (Bourgis et al., 2011), and (3) genetically related non-wax producing tissues *Myrica rubra* fruits (Feng et al., 2012) and *M. pensylvanica* leaves. Together, these results

indicated that Bayberry is exceptional in the expression of a small subset of annotated cutin assembly genes, and that changes in their predicted protein sequences to evolve novel functionality or specificity may not have been required to define the composition, quantity and localization of Bayberry's glycerolipid surface wax. This analysis of the genetic features of Bayberry surface wax production may aid in understanding of genes and mechanisms that are available for glycerolipid assembly in non-seed tissue and glycerolipid secretion from cells and onto external plant surfaces.

3.4. Results and discussion

3.4.1. The largest reported accumulation of surface lipids in plants is by Bayberry fruits

The surfaces of Bayberry fruits are coated with an extremely thick and unusual layer of crystalline wax (Figure 29). At maturity, the wax coverage is 8700µg cm $^{-2}$ (Simpson and Ohlrogge, 2015) which is 100 to 1000-fold higher than most other plant species, and is at least 8-fold higher than Carnauba leaves (Figure 36) (Kolattukudy, 1976; Jetter et al., 2006). We previously demonstrated that the pathway for Bayberry wax synthesis is related to the assembly of the insoluble plant surface glycerolipid polyester cutin (Simpson and Ohlrogge, 2015). However, in contrast to cutin, the estimated rate of fatty acid incorporation into Bayberry surface wax glycerolipids is 714 µg FA cm^{-2} day^{-1}, which is ~ 45-fold higher than cutin synthesis for tomato and cherry fruits (Isaacson et al., 2009; Alkio et al., 2014). This results in an surface lipid load for Bayberry wax over 10-fold higher than those fruit tissues, and also over 100-fold higher compared to Arabidopsis stems (Baker, 1982; Stark and Tian, 2006). Thus, Bayberry fruits are the highest documented accumulator of surface lipids among plants.

The composition of Bayberry surface wax differs from any other previously characterized plant surface lipid. Bayberry wax does not contain any detectable amounts of common cutin-like fatty acids or wax constituents, such as alkanes, wax esters and alcohols. Instead, it is composed almost exclusively of glycerolipids triacylglycerol (TAG), diacylglycerol (DAG) and monoacylglycerol (MAG) with unmodified and completely saturated fatty acids. The accumulation of TAG makes Bayberry wax more similar to oil seed lipids, than any plant surface lipid. The glycerolipids in Bayberry wax represent approximately 30% of the dry weight of the entire fruit, and 56% of the mass of the knobs which produce the wax (i.e. knobs). The accumulation of Bayberry surface wax is quantitatively comparable to *Brassica naups* seeds

(~35% oil), but less than the oil-accumulating mesocarp of oil palm (~90% oil). However, the estimated the rate of fatty acid incorporation into Bayberry wax glycerolipids is 0.4 µg FA gFW^{-1} $hour^{-1}$ (Simpson and Ohlrogge, 2015) which is 4-fold lower than *B. napus* embryos and oil palm (Bourgis et al., 2011). The composition of Bayberry wax is also generally quite different from oil crops due to the large amounts (>99%) of saturated fatty acids, significant DAG and MAG accumulation (65% and 4% , respectively), and Bayberry glycerolipids are assembled by a completely different pathway compared to oil seeds(Simpson and Ohlrogge, 2015). The saturated fatty acids in Bayberry wax gives it a very high melting point (~ 45°C), and thus the surface wax is a solid at room temperature and can be referred to as a "vegetable tallow".

As a comparison we note that the production of a secreted soluble glycerolipid by Bayberry is somewhat analogous to the glycerolipid estolides that accumulate on the stigmas of some plant species, notably in *Solanaceae*. These estolides consist of C18:1 and C18:2- ω-hydroxylated fatty acids that are esterified to two or three positions a glycerol backbone and to each other to form oligomers with an average of 8 acyl chains per glycerol (Koiwai and Matsuzaki, 1988). The biosynthetic pathway for these glycerol polyesters has not been determined, however in petunia stigmas a P450 fatty acid hydroxylase, similar to types used in cutin fatty acid production, was identified as important for the synthesis of estolides (Han et al., 2010). One study reported that the estolides can accumulate to 10-20% of the fresh weight of tobacco stigma buds (Matsuzaki et al., 1983). While the total accumulation of estolides is comparable to Bayberry wax, unlike Bayberry, the stigma glycerolipids appear to accumulate on the surface via rupture of underling cells (Konar and Linskens, 1966), and we could not detect any similar ω-hydroxylated fatty acids in Bayberry wax glycerolipids.

3.4.2. Bayberry fruit development and initiation and secretion of the wax layer

To understand the biology underlying the unique lipid metabolism of Bayberry, we further documented aspects of fruit development from pollination to lipid secretion that have not previously been published. Bayberry fruit deposits its unique surface wax continuously over approximately 8-weeks, and the surface wax persists on the fruits through the fall and winter months. The wax does not accumulate on the surfaces of the drupe fruit-proper, but instead is produced by and accumulate on unusual multicellular structures (called knobs) that protrude from the fruit surface (Figure 29). Each ~5mm diameter fruit is completely covered with 200 to 250 of the ~500µm (diameter) knobs. Other *Myricaceae* fruits that do not produce the same abundant wax also appear to have knobs, thus these structures may not be specific for the synthesis of large quantities of surface wax. We could not find any reports describing the development and morphology of knobs or similar large protrusions from fruit surfaces.

Bayberry fruits were clearly visible throughout the female shrubs 2 to 3 weeks after pollen production was observed on the male plants. Between 5 and 15 fruits developed per 1-3 cm long branch (Figure 29 F). The knobs were detected very early in fruit development, when the fruit was still inside the flower tissue. Thus, the knobs form concurrently with the fruit-proper, rather than later in development as an outgrowth from more developed tissue (Figure 29 E). By early June, most of the green fruits had expanded past their subtending flower bracts and were fully visible throughout the shrub; however the glycerolipid surface wax was not detectable at that stage (Figure 29 G, H).

At early stages of wax accumulation (mid to late June), wax crystals were scattered across the surfaces of numerous cells on each single knob (Figure 29 I). Two to three weeks after initial detection of the wax, knob surfaces were completely covered with wax (Figure 29 J).

Significantly, during that period, we did not observe any fracturing of the knob surfaces. Furthermore, chemically removing the wax later in the season revealed an intact knob surface, and fruits stained with Sudan Red 7B revealed a contiguous cutin layer (Figure 29 K, L). Those observations, coupled with the prolonged period of wax accumulation (~8 weeks) and lack of detection of lipids within the cells by confocal microscopy (Simpson and Ohlrogge, 2015) indicates that the wax is actively secreted from the knobs, rather than released via disintegration of knob cells that have filled with lipids. This process is analogous to cutin/suberin, surface wax and sporopollenin polymer secretion (Samuels et al., 2008; Quilichini et al., 2015). However, it differs from the cell rupturing observed in stigma estolides (Konar and Linskens, 1966) and pollen coat lipids (Helsop-Harrison, 1968).

The ultrastructure of the knobs was also examined by light and transmission electron (TEM) microscopy. Knob epidermal cells were rectangular with a diameter of 20-30µm and tightly packed around the circumference of the tissue (Figure 30 A). Internal cells were more spherical in shape, with a diameter of 40-70µm, and loosely arranged within the knobs. TEM of the epidermal cells identified chloroplasts, mitochondria and ER, but no clearly defined lipid storage structures (i.e. lipid droplets). A close association of the ER with the plasma membrane was observed, which may be contact sites important for lipid secretion (Samuels and McFarlane, 2012) (Figure 30 B,C). In contrast, the internal cells were organelle poor and many were filled with electron dense globules. Similarly stained globules were evident in some epidermal cells, but none appeared to fill the entire cell (Figure 30 D). Those globules likely did not contain lipids, since osmium-tetroxide (used in TEM preparation) does not stain saturated lipids. Furthermore, confocal microscopy after staining with neutral lipid dyes (Simpson and Ohlrogge, 2015) indicated that lipid droplets are not present within the knobs. Instead, the electron dense

globules may represent vacuoles filled with phenolic compounds, such as anthocyanin's and/or tannins, which are abundant in *Myrica* fruits (Feng et al., 2012) and are stained by-osmium tetroxide through complexes with their O-dihydroxy groups (Nielson and Griffith, 1978).

The subcellular morphology of the epidermal cells, compared to the internal knob cells, also suggested that the epidermis is the only cell layer directly involved in wax production and secretion. This observation was also consistent with the fact that staining did not reveal any wax in the interstitial spaces below the epidermis (Simpson and Ohlrogge, 2015); however we cannot yet rule out the possibility that some underlying cells may be involved in wax production.

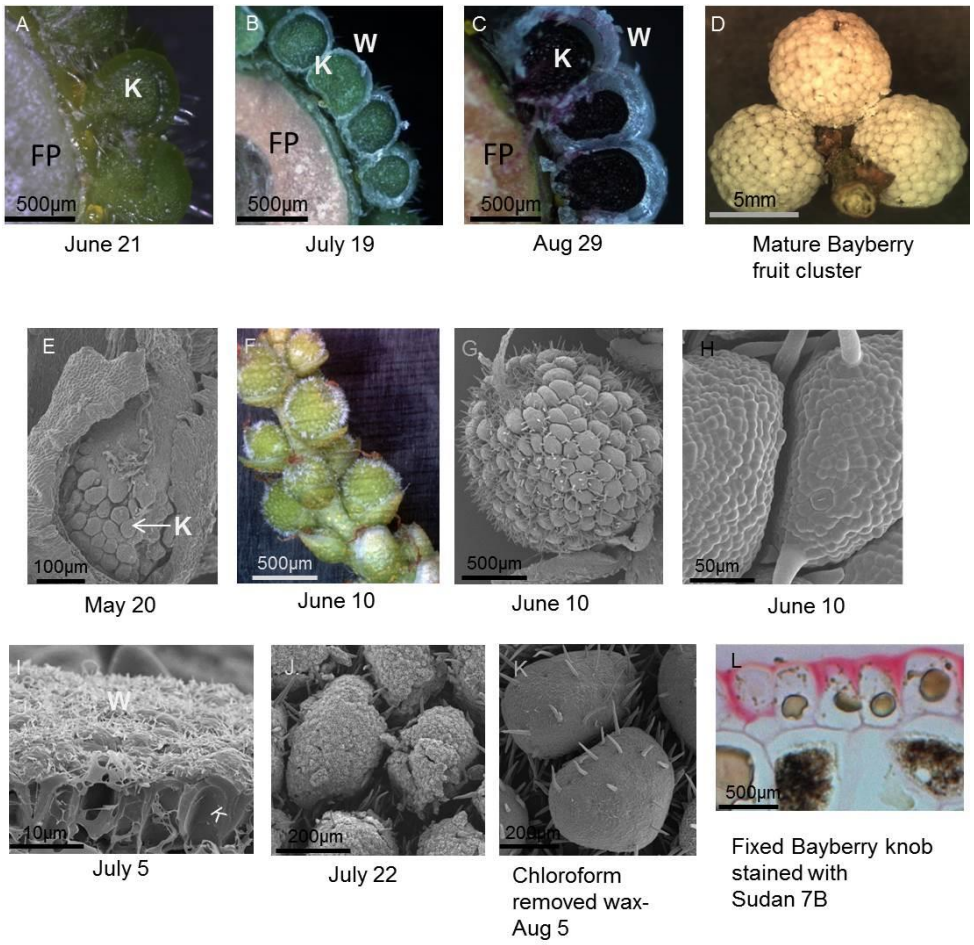

Figure 29: Wax accumulation on the surfaces of Bayberry fruits/knobs through development. (A-D) Cross sections of Bayberry fruits. Sections were made on freshly harvested fruits and immediately photographed with a dissecting microscope. Wax was detected by GC-FID in June 21 fruits, but was not abundant enough to be visible. (E) SEM image of a dissected flower exposing a developing fruit with knobs. The fruit is within the subtending bracts and the raised tissue on the fruit are the knobs. (F) Light photograph of a developing fruit cluster. (G) SEM image of a whole fruit early in its development. (H) Magnification of the knob surface in G. (I) SEM cross-section of a single knob illustrating wax coverage at < 10% of final production. (J) SEM of the surface of knobs with wax coverage at ~50% of final production. (K) SEM of the surfaces of knobs after wax was chemically removed by chloroform. (L) A chemically fixed Bayberry knob stained for cutin with Sudan red 7B. Surface wax was removed by the chemical fixation of the tissue. The symbols 'K' represents knobs, 'FP 'refers to fruit proper (i.e. fruit not including the knobs) and 'W' refers to wax.

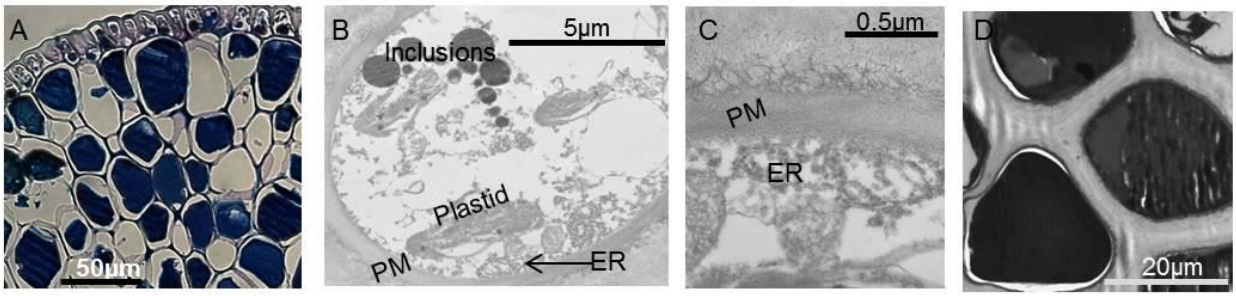

Figure 30: Ultrastructure of Bayberry knobs.(A) Toluidine- blue stained section of a knob prior to imaging under TEM. (B) TEM of a knob epidermal cell. (C) Magnification of ER region in B. (D) TEM image of an internal knob cell. Cells were filled with an unknown substance that was extremely electron dense.

3.4.3. Features of transcript expression in Bayberry knobs may contribute to a specialized lipid metabolism

RNA-seq was used to identify highly expressed gene transcripts that may be associated with the massive accumulation of glycerolipid wax on the surfaces of Bayberry fruits. Knob cDNA was sequenced at seven intervals through development, encompassing a time when the wax layer was undetectable (day 10 and 15), to 50% of the final wax yield (day 61) (Figure 37). We previously reported that 13 of the 55 most highly expressed transcripts in the knobs encode genes associated with pathways involved in plant acyl-lipid metabolism (Simpson and Ohlrogge, 2015). An additional feature was that 8 of the 13 predicted genes are annotated as biosynthetic enzymes that together can define a pathway from the production of saturated fatty acids to the assembly of Bayberry surface wax. For comparison, even for oil crops that produce more TAG and at a higher rate than Bayberry knobs, within their top 55 most highly expressed transcripts there are not more than four genes that encode enzymes involved in acyl-lipid metabolism (Table 7).

During wax synthesis, the most highly expressed transcript that is associated with fatty acid synthesis (FAS) is annotated as fatty acid thioesterase B (FATB). FATB specifically releases C16:0 fatty acids from FAS. Five other highly expressed transcripts in Bayberry knobs are annotated as acyltransferases required for assembly of the extracellular glycerolipid cutin. They included, two isoforms of *sn*-2 GPATs (Li et al., 2007b; Li-Beisson et al., 2009), defective in cuticular ridges (DCR) (Panikashvili et al., 2009) and two GDSL-motif lipases/transacylases (Girard et al., 2012; Yeats et al., 2012). Moreover, transcripts encoding other glycerolipid acyltransferases, (i.e. Kennedy Pathway enzymes) were expressed at levels at least 50-fold lower. The secretion of the wax to the surface may be facilitated by the ABCG transporters and

also lipid transfer proteins (LTPs) (Samuels et al., 2008). Indeed, Bayberry knobs contain highly expressed transcripts for one ABCG transporter and three LTPs. Based on homology to Arabidopsis, those putative proteins may be involved in the active secretion of wax to the Bayberry fruit surfaces.

We acknowledge that transcript levels does not reflect protein levels or enzyme activity, and it is likely that less abundant transcripts (i.e. not in the top 55 most highly expressed) in Bayberry knobs, are also important for the assembly and secretion of its surface wax. However, for abundant mRNA's, expression level and protein amount were reported to be well correlated (Ponnala et al., 2014; Weber, 2015), and there are many examples of highly expressed transcripts being associated with specialized metabolism (van de Loo et al., 1995; Tissier, 2012). In the sections below, we describe how high expression of specific acyl-lipid genes, may have contributed to the evolution of Bayberry wax.

3.4.4. High expression of FATB gene in Bayberry knobs may be responsible for completely saturated MAG, DAG and TAG species and C14:0 production for its surface wax

The fatty acid composition of Bayberry surface wax is unusual for any surface wax or glycerolipid in plants. As previously reported, the fatty acids of mature Bayberry wax are C14:0, C16:0 with trace amounts of C18:0. Not even minor amounts (< 1%) of unsaturated fatty acids or fatty acids with a chain length less than C14:0 or greater than C18:0 were detected in the wax at any point though development (Simpson and Ohlrogge, 2015). Glycerolipids with such a simple and entirely saturated fatty acid composition are not found in plant membranes or storage lipids (Gunstone et al., 2007). Although some plants, such as *Cuphea*, accumulate greater than 95 mol percent saturated fatty acids in their seed oil, the fatty acids in *Cuphea* TAG are short or medium

chain (C8:0-C12:0) giving its glycerolipids a lower melting point compared to the di- and tri-C16:0 glycerolipids in Bayberry wax (Banerji et al., 1984; Gunstone et al., 2007; Kim et al., 2015; Simpson and Ohlrogge, 2015).

During the 51-day RNA sampling period of Bayberry knobs, the amount of unsaturated fatty acids in the knobs, which approximates the quantity of polar lipids, ranged between 15 to 20 µg fruit knobs^{-1}. During the same period, wax accumulated from undetectable levels to 4000-5000 µg fruit knobs $^{-1}$ (Figure 38). Most of the unsaturated fatty acids accumulated early in fruit development, and the amount of unsaturated fatty acids in the knobs did not change as the surface wax layer grew. This means that when surface wax is most actively deposited, over 99% of the fatty acids synthesized by knob cells are saturated and are used almost exclusively for surface wax synthesis.

How did Bayberry knobs evolve the capacity to specifically synthesize and incorporate only saturated fatty acids into glycerolipids destined for its surface wax? A primary mechanism is likely related to the very high expression of transcripts for an annotated fatty acid thioesterase B (FATB) gene and its expression relative to an annotated fatty acid thioesterase A (FATA). Previously characterized FATB proteins were shown to catalyze the release of C16:0 and shorter acyl chains from acyl-carrier protein (ACP) of FAS. In contrast, FATA is most active with C18:0 ACP and C18:1-ACP, formed via C18:0 by the plastid stearoyl-ACP desaturase (SAD). (Salas and Ohlrogge, 2002; Bonaventure et al., 2003). In Bayberry knobs, beginning from when surface wax was barely detectable (day 10) to when knobs produced detectable levels of wax (day 30), the expression of its putative FATB gene increased over 5-fold, from ~170 RPKM to 1000 RPKM. That level of expression resulted in FATB being the highest expressed transcript involved in FAS, and the FATB transcript was consistently within the top 40-50 most highly

expressed annotated genes in the knobs when wax was accumulating. Significant to the production of entirely saturated fatty acids for the surface wax, Bayberry FATB gene expression was also 20 to 40-fold higher than the expression of a putative FATA gene (Figure 31 A). In contrast, for the other plant tissues analyzed here, the expression ratio of genes annotated as FATB and FATA ranged between 1 to 5 (Figure 31 A), including tomato epidermis which must produce greater than 85 mol % C16:0 derived fatty acids for its cutin. Thus, Bayberry is exceptional both in its very high expression of FATB and the ratio of expression of FATB:FATA transcripts.

Another notable feature of Bayberry wax composition, which may be related to the expression of FATB, is the incorporation of "medium-chain" C14:0 fatty acids into DAG and TAG. While at maturity DAG and TAG contained 20-25% C14:0 fatty acids and 75-80% C16:0 fatty acids, their relative abundance was not constant through the season (Figure 32 A). Figure 32 B also illustrates the rate of C14:0 fatty acid accumulation increasing through the season, while the incorporation of C16:0 fatty acids into glycerolipids slowed after day 60. In fact, during the final 5 days of wax synthesis, C14:0 was incorporated into TAG and DAG at a similar rate to C16:0.

Other plant species which accumulates large amounts of medium and short chain fatty acids express multiple isoforms of FATB proteins (Voelker, 1996; Kim et al., 2015). However, only one transcript was annotated as FATB in both Bayberry knobs and leaves. Instead, we considered that the synthesis of C14:0 fatty acids was related to flux through FAS, as the highest rates of C14:0 accumulation coincided with an overall reduction in surface wax synthesis (evidenced by the decrease in accumulation of the dominant C16:0 fatty acid in the surface wax).

Increased production of C14:0 fatty acids, relative to C16:0, has been observed in some plants which are perturbed in different reactions of FAS (Harwood, 1988). For example, increased C14:0 is observed when FAS substrates malonyl-CoA and reductant (NADPH) are lowered, but also when the levels of ACP and acetyl-CoA are increased. The first two examples may directly affect the extension of C14:0 to C16:0, while the latter two examples may cause a saturation of FAS enzymes which favors premature termination of acyl-ACPs by thioesterases (Harwood et al 1988). A third contributing factor to C14:0 production, and which may be specific to Bayberry knobs, could be that FATB is so abundant that it occasionally out-competes ketoacyl-ACP 1 enzyme (KASI), which extends the fatty acid from C14:0 to C16:0, resulting in increased release of C14:0 fatty acids by the more abundant FATB protein

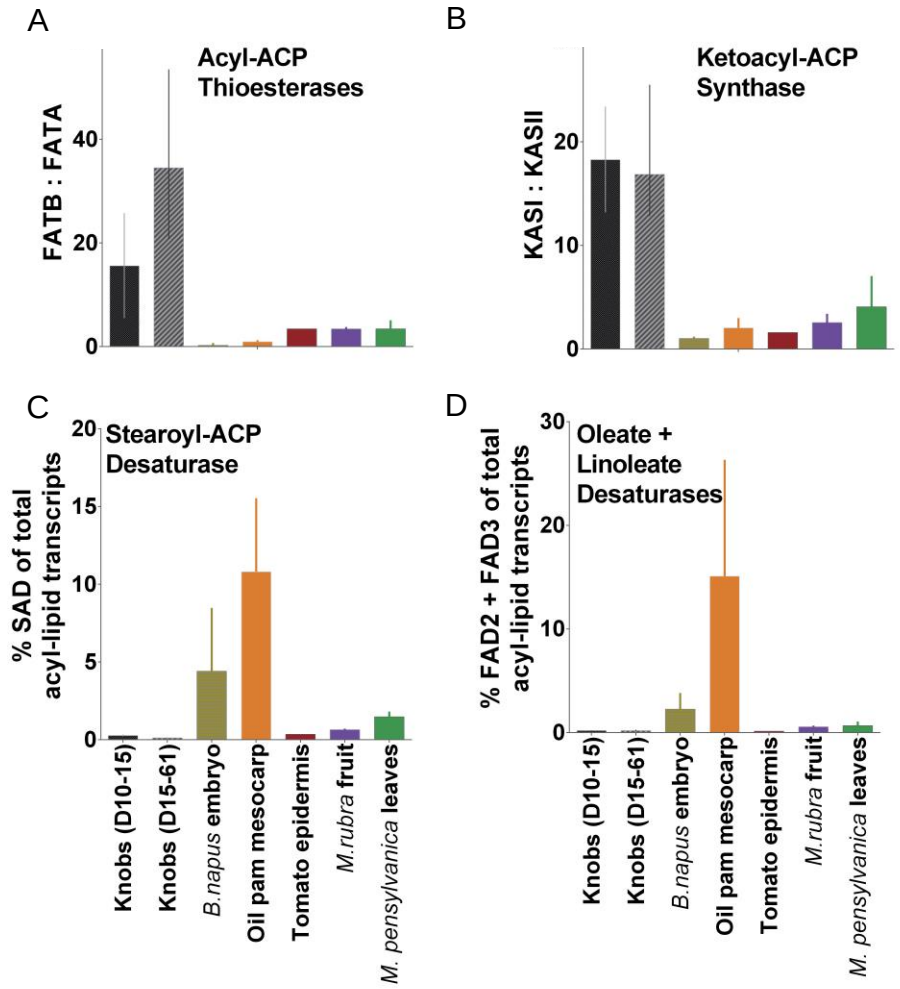

Figure 31: Specialized expression of genes which may contribute to fatty acid quality in Bayberry knobs. For Bayberry knobs, average expression (RPKM) was calculated for stages when wax was not visible (days 10-15 and black bars), and when wax was activity being synthesized (days 30-61 and grey bars). Other species in the graphs are separated by color. For each species, except tomato, the average expression of the respective annotated gene across a time-course was computed and the range of expression is represented by the error bars. (A) Presents the ratio of expression of transcripts for fatty acid thioesterase (FAT) B and FATA thioesterase. (B) Presents the ratio of transcripts for keto acyl-ACP synthase (KAS) I and KAS II expression. (C), (D) The expression of desaturases SAD (C) and FAD2 and FAD3 (D), relative to the total number of normalized transcripts associated with acyl-lipid metabolism.

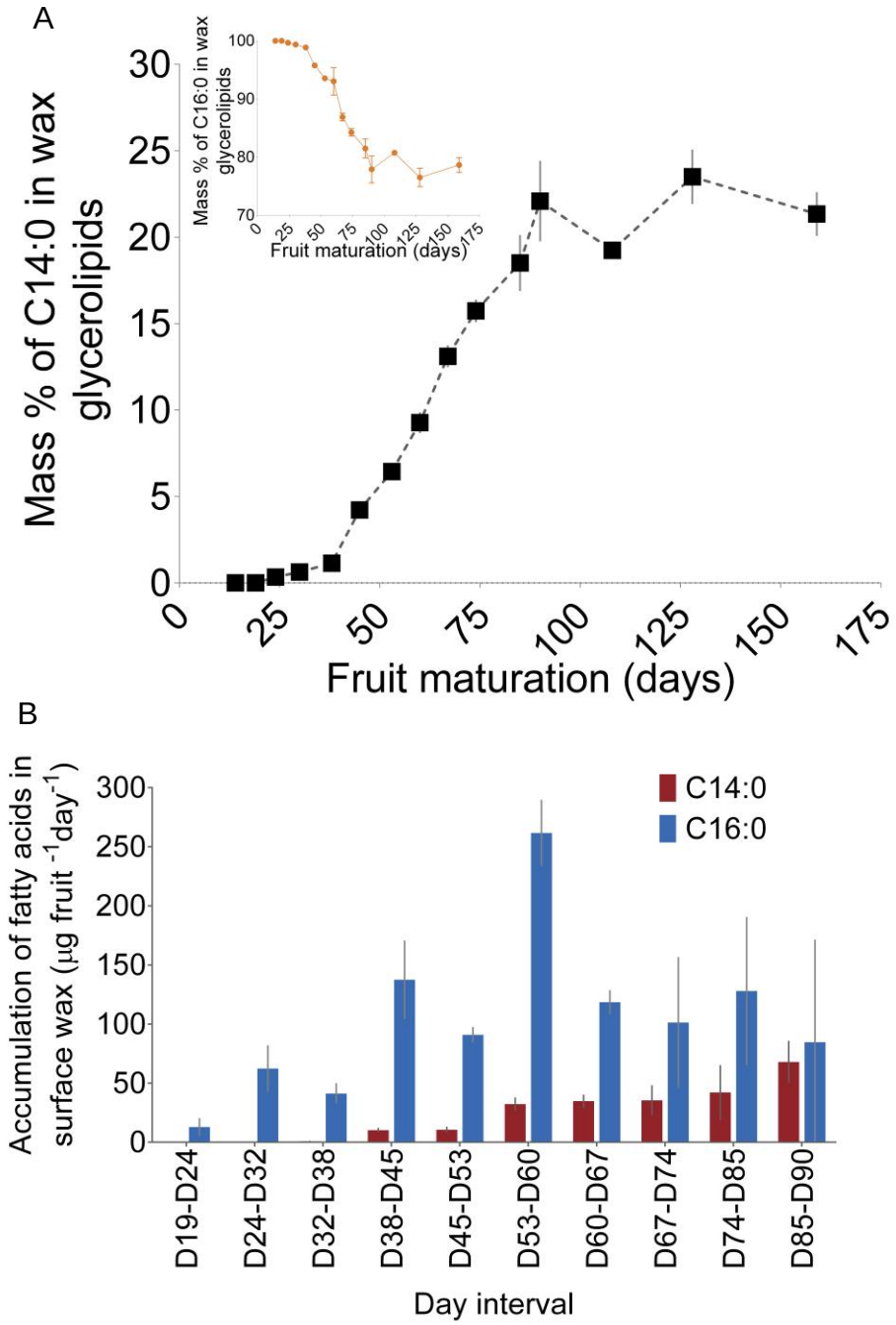

Figure 32: 14:0 fatty acid accumulation in Bayberry wax.(A) The mass percentage of 14:0 and 16:0 (insert) fatty acids in Bayberry wax glycerolipids through development. (B) Rate of production of each fatty acid in Bayberry wax glycerolipids through sampling intervals. Each point represents the average of 3-4 replicates ± SE.

3.4.5. Reduced expression of transcripts for ketoacyl-ACP synthases and fatty acid desaturases may also have contributed to the high saturated fatty acid content in Bayberry wax

Also consistent with the production of almost exclusively saturated fatty acids, Bayberry knobs expressed transcripts for putative ketoacyl-ACP synthases (KAS) II and fatty acid desaturases differently and at lower levels compared to other plant species (Figure 33 B, C, D). KASII proteins catalyzes the condensation of malonyl-ACP to acyl-ACP primarily for the elongation of C16:0 to C18:0 (Li-Beisson et al., 2010) while KASI is the condensing enzyme for C4:0 to C16:0 elongation. In agreement with the low (1%) C18:0 and lack of unsaturated fatty acids in Bayberry wax, KASII transcripts were expressed several fold lower than KASI transcripts. In contrast, oil crops, *M. pensylvanica* leaves and *M. rubra* fruits, which all contain C18 fatty acids for membranes, express transcripts for KASII and KASI at approximately equal levels (Figure 33 B).

Transcripts for the plastid localized fatty acid desaturase (SAD), and the ER localized desaturases fatty acid desaturases (FAD) 2 and 3 were low in Bayberry knobs, relative to other acyl-lipid genes (< 2%). In contrast, other plants were all more represented in transcripts encoding desaturase enzymes (Figure 33 C, D), specifically SAD. Thus, in addition to favoring the production of C16:0 fatty acids, Bayberry knobs also downregulate transcripts for several enzymes which produce and modify C18:0 fatty acids.

While Bayberry knobs appear unique in its massive expression of FATB and reduced expression of desaturases, the relative abundance of transcripts for other genes associated FAS was similar between Bayberry knobs and the other plant species analyzed here (Figure 39). Similar consistent relative expression levels among FAS genes was previously noted among multiple different oil crops (Troncoso-Ponce et al., 2011).

3.4.6. The initiation of Bayberry surface wax synthesis is associated with high expression of transcripts for specific cutin assembly genes

In contrast to the *sn*-1 acylation of glycerol-3-phosphate (G3P) in conventional intracellular glycerolipid synthesis,[^{14}C] labeling studies demonstrated that the first reaction for Bayberry wax assembly is the production of*sn*-2 MAG (Simpson and Ohlrogge, 2015). In Arabidopsis, this reaction is catalyzed by the bifunctional, cutin-specific *sn*-2 GPATs (Yang et al., 2010). It is hypothesized that in cutin production, the *sn*-2 MAG participates in intracellular reactions, act as a shuttle of oxygenated fatty acids from epidermal cells to the apoplast for cutin assembly or a component of the cuticle (Beisson et al., 2012; Beisson and Ohlrogge, 2012) . Specifically in Arabidopsis, *sn*-2 MAGs are secreted into aerial surface waxes (Li et al., 2007a), and *in vitro* assays demonstrated that an extracellular localized and cutin-associated GDSL motif lipase/transacylase enzyme can catalyze the exchange of acyl-chains from *sn*-2 MAG to free ω-OH on other *sn*-2 MAGs to synthesize a cutin-like polyester (Yeats et al., 2012; Yeats et al., 2014). We proposed a model for Bayberry wax assembly that is analogous to current models for cutin assembly (Beisson et al., 2012; Beisson and Ohlrogge, 2012).In particular, kinetic labeling of Bayberry knobs indicated (1) that *sn*-2 MAG is the first detected intermediate in TAG synthesis and may serve as the acyl-donor for DAG and TAG synthesis, and (2) that TAG is assembled extracellulary from extracellular biosynthetically active pools of DAG and *sn*-2 MAG (Simpson and Ohlrogge, 2015).

The model for Bayberry surface wax assembly was proposed in part based on the very high expression of cutin-associated acyltransferase transcripts (*sn*-2 GPATs, DCR GDSL-motif lipases) (Simpson and Ohlrogge, 2015). However, it was unclear whether Bayberry knobs are unique in their high expression of transcripts for cutin associated acyltransferases compared to

other plant tissues actively accumulating cutin. We therefore compared the expression of the putative cutin assembly genes in Bayberry knobs to homologous genes identified in the transcriptomes of tomato epidermis (Matas et al., 2011) and cherry fruits enriched in exocarp (i.e. epidermis of fruits) tissue (Alkio et al., 2014). The cutins of tomato and cherry are composed of C16:0 hydroxylated fatty acids, but their rates of synthesis are over 10-fold less than the rate of wax deposition on Bayberry fruits. Consistent with the large difference in rate of surface lipid deposition, the expression of putative *sn*-2 GPATs and a homolog of Arabidopsis DCR was approximately 10-fold higher in Bayberry knobs compared to tomato and cherry epidermal tissues (Figure 34 A, B). Of the transcripts encoding for putative GDSL-motif enzymes in Bayberry knobs, only MpGDSL2, was highly expressed during the period of active wax deposition (days 30-51). However, tomato or cherry do not express genes similar to MpGDSL2 at very high levels (Figure 34 C, D). While the uniquely high expression of MpGDSL2 in Bayberry knobs is suggestive of a specific role in its wax assembly, functional characterization of MpGDSL2 and closely related GDSL-motif proteins from other plant species have not been done.

This comparison demonstrates that transcript expression in Bayberry knobs is uniquely represented in known or suspected (based on homology) cutin assembly enzymes. Based on available evidence, we hypothesize that those specific highly expressed transcripts in Bayberry knobs encode for proteins that are important for the synthesis of its abundant and unusual surface wax. We speculate that Bayberry knobs express those transcripts at a high level because the tissue requires an increased amount of the enzyme to accommodate the massive production of surface lipids and/or because the putative Bayberry enzymes may not be yet adapted to assemble glycerolipids with non-cutin (i.e. no hydroxy groups) fatty acyl groups.

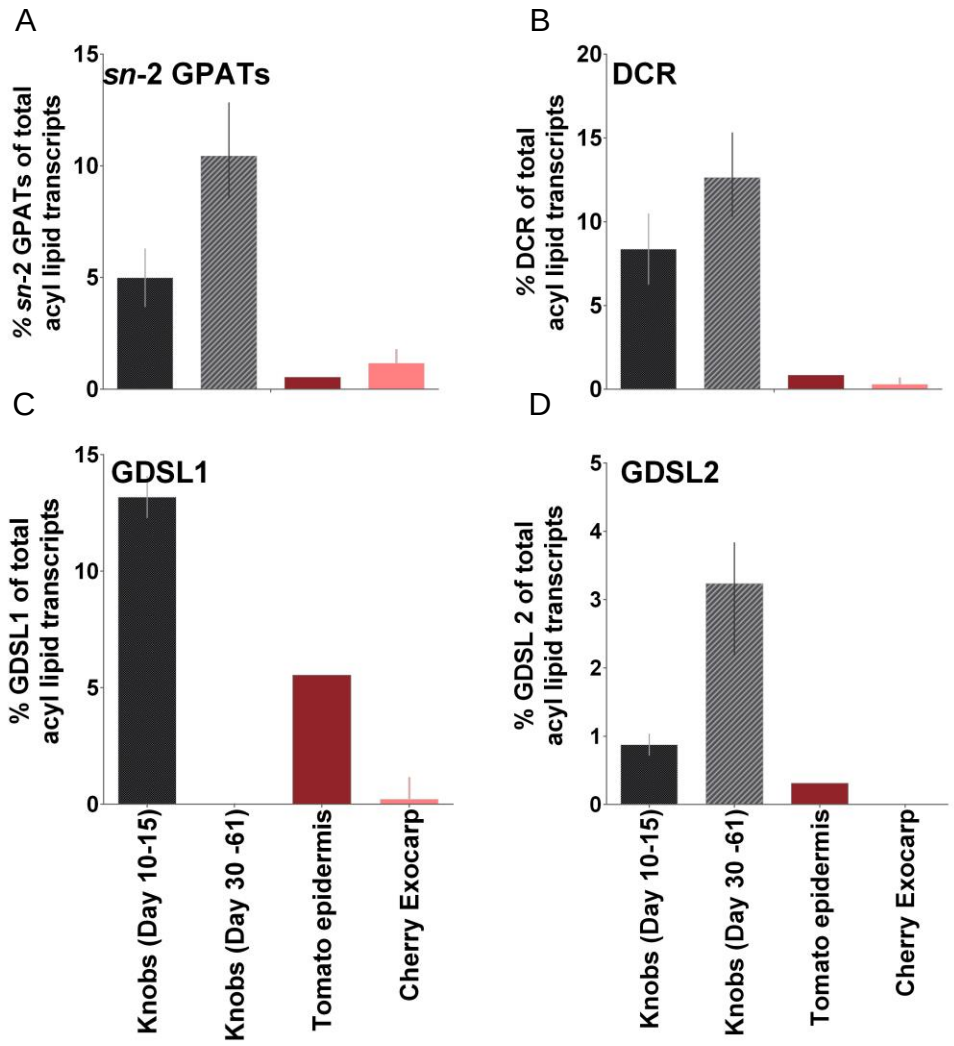

Figure 33: Expression of cutin-associated transcripts in Bayberry knobs (black and gray bars) and their homologs in tomato (red) and cherry epidermis (pink) enriched tissue. Each bar in each graph reports the percentage of (A) *sn*-2 GPATs, (B) DCR, (C,D) GDSL lipases to the total number of normalized transcripts associated with acyl-lipid metabolism identified in each library. For Bayberry knobs, average expression (RPKM) was calculated for stages when wax was not visible (days 10-15 and black bars), and when wax was activity being synthesized (days 30-61 and grey bars). The error bars denote the range of expression. For cherry, expression of the respective gene was averaged across a time-course, with the range of expression is also represented by the error bars.

3.4.7. Downregulation of key cutin-genes in Bayberry knobs may prevent cutin synthesis and favor the synthesis of the soluble glycerolipid wax

Bayberry knobs produce a cutin layer containing primarily dihydroxypalmitate (DHP) fatty acids (Figure 40), which is derived from C16:0 fatty acids. However, although C16:0 fatty acids are precursors for both cutin and Bayberry surface wax, both end-products share the same assembly enzymes, and both glycerolipids accumulate in the same location, we could not detect any overlap in the acyl chain composition of the two glycerolipids (i.e. no TAG estolides in Bayberry or hydroxy fatty acids in soluble glycerolipids). This implied that Bayberry knobs have significantly down-regulated the flux of C16:0 fatty acids towards enzymes which contribute to the synthesis of cutin, and instead diverted saturated fatty acids towards DAG and TAG synthesis. While the very high expression of transcripts encoding *sn*-2 GPAT, DCR and MpGDSL2 is clearly associated with the synthesis of Bayberry wax, we also examined whether any lipid related genes were specifically down regulated, which may indicate a strategy to prevent the continued synthesis of the insoluble polyester cutin.

Cutin is deposited early in the development of a plant tissue (Suh et al., 2005) and the first two sampling stages for RNA-seq were from very young fruits when surface wax was barely detectable. In Bayberry knobs, some transcripts which were annotated as being associated with cutin synthesis or acyl-lipid metabolism exhibited differential expression between the first two sampling stages (i.e. no wax accumulation) and the final sampling stages (i.e. wax production) (Figure 34, Table 8). The expression of MpGDSL1 was the most striking case, as it was one of the highest expressed transcripts during the first two sampling dates, but was one of the lowest expressed from days 30-51, when surface wax accumulation was greatest (Figure 34 B). MpGDSL1 is closely related to cutin deficient 1 (CD1) in tomato (Simpson and Ohlrogge, 2015).

CD1 is one of the highest expressed enzymes in tomato fruit epidermis and was demonstrated through mutant studies and *in vitro* assays to likely catalyze the extracellular assembly of cutin with *sn*-2 MAG as the acyl-donor (Yeats et al., 2012; Yeats et al., 2014). In contrast to MpGDSL1, MpGDSL2 increased in expression (to within the top 20 most highly expressed genes) when wax was accumulating. As discussed above, the disparate expression patterns of the two putative GDSL-motif enzymes in Bayberry knobs is suggestive of MpGDSL2 having a specific role for the assembly of DAG and TAG, while MpGDSL1 may contribute to cutin synthesis. However, because GDSL-motif enzymes are extracellular, and are thermostable (Yeats et al., 2014),-it is possible that MpGDSL1 continues to be active in extracellular wax synthesis, despite the decrease in transcript levels.

Analogous to the expression of MpGDSL1, the expression of homologs to three cutin-associated P450 hydroxylases were at their highest levels at the first two sampling times, and then decreased in expression over 100-fold through the remaining sampling times (Figure 34 E). The Arabidopsis homologs for these putative Bayberry p450's are, HOTHEAD (Kurdyukov et al., 2006), CYP86A4 and CYP77A6/A4 (Li-Beisson et al., 2009). In cutin synthesis, these enzymes modify newly synthesized fatty acids with hydroxy or acid functional groups (Beisson et al., 2012) which facilitate ester linkages to other fatty acids creating the cutin polyester. It was unclear why a P450 hydroxylase annotated as CYP86A8 (Wellesen et al., 2001) increased in transcript abundance during the wax accumulation phase in Bayberry; however, no hydroxy-fatty acids were ever detected in Bayberry MAG, DAG or TAG.

Together, the reduction in expression in Bayberry knobs for transcripts encoding a putative CD1 enzyme (i.e. MpGDSL1) and putative P450 hydroxylases contrasts sharply with elevated expression for MpGDSL2,*sn*-2 GPATs and DCR (Figure 34 A, B). Transcripts for

putative Bayberry *sn*-2 GPATs and DCR were also highly expressed at the first two sampling stages suggesting that they together may be involved in the synthesis of cutin for the knobs. Thus, we hypothesize that for Bayberry knobs to initiate glycerolipid wax synthesis, the cells may uncouple the temporal regulation of cutin genes by downregulating only a subset of genes involved in the synthesis of cutin (i.e. p450s, MpGDSL1), while maintaining a high expression of genes such as *sn*-2 GPATs and DCR. This change, compared to tissues actively synthesizing cutin, may allow Bayberry knobs to produce and secrete soluble glycerolipids without hydroxy fatty acids after cutin is deposited on the young fruits.

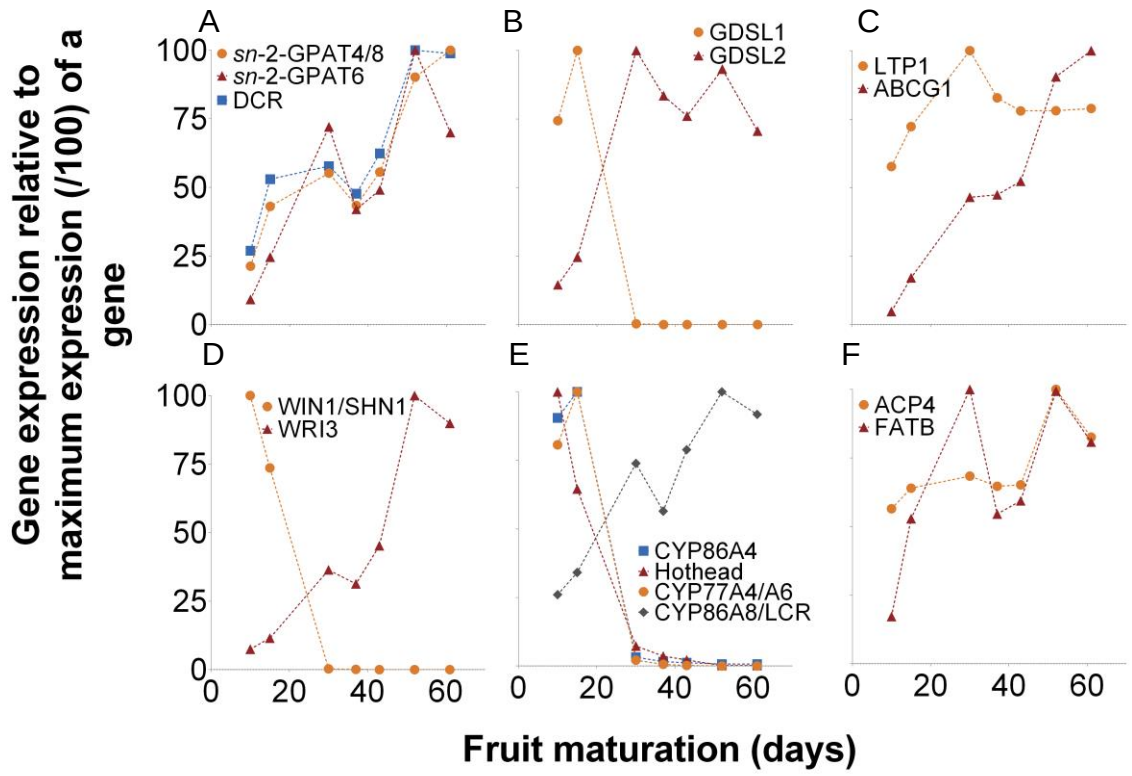

Figure 34: Relative expression of transcripts for selected putative Bayberry acyl-lipid genes in the knobs through development. Expression was calculated relative to the highest expression value during development (set to 100). (A) Cutin assembly genes. (B) GDSL-motif enzymes. (C)Transporter proteins. (D) Transcription factors. (E) P450's that modify cutin fatty acids. (F) Abundant FAS genes.

3.4.8. ABCG transporter and lipid transfer proteins may contribute to the secretion of Bayberry wax

Transcripts encoding annotated ABCG transporters and lipid transfer proteins (LTP's) were within the top 50 most highly expressed transcripts in Bayberry knobs. ABCG transporters (Beisson et al., 2012; Landgraf et al., 2014; Yadav et al., 2014) and LTPs (Debono et al., 2009; Lee et al., 2009) are thought to contribute to the transport cuticular waxes and cutin precursors through the cell membrane and cell wall onto plant surfaces, respectively. While, direct evidence is not yet available and their affinity for specific lipids has not been established (Kunst et al., 2006), the example of Bayberry glycerolipid wax secretion may provide additional insights into lipid export and possible substrate/functional flexibility of the transporters.

The most abundant ABCG transporter gene in Bayberry knobs was related to Arabidopsis ABCG1 (Figure 41). The expression of Bayberry ABGG1 increased 20-fold through development (Figure 34 C) and was expressed 3 to 5 fold higher than the next highest expressed ABCG transporter gene, suggesting in Bayberry ABCG1 functions as a homodimer. In other plants, ABCG1 proteins have been implicated in the production of suberin for potato tubers (Landgraf et al., 2014) Arabidopsis roots, seed coat and pollen wall (Yadav et al., 2014), and in tobacco stigmas may be involved in triacylglycerol estolide accumulation (Otsu et al., 2004).

The most highly expressed transcripts in Bayberry knobs were annotated as LTP1 (Figure 42). LTPs are small (~9 kDA), soluble proteins, that have extracellular secretory domains and can bind lipids (Pyee et al., 1994; Thoma et al., 1994; Kader, 1996). LTP1 genes are highly expressed in epidermal cells, and the proteins are very abundant on plant surfaces. LTPs are believed to function in the secretion of hydrophobic substances from cells and a role for the gene was established in stigmas, trichomes, and roots that form symbiotic relationships with

microorganisms; however functional assays with the protein have not been done. (Thoma et al., 1994; Choi et al., 2012; Lei et al., 2014). Unlike ABCG transporters and most cutin assembly genes discussed above, LTPs are very abundant in tomato epidermis and cherry exocarp tissue. Thus, Bayberry knobs are not exceptional in very high expression of LTPs.

3.4.9. Comparison of gene expression and predicted proteins sequences between Bayberry knobs and leaves and *M. rubra* fruits that do not produce glycerolipid wax

Bayberry wax is different in overall structure to conventional cuticular lipids and intracellular lipids. Thus, we next examined whether the predicted protein sequences for those highly expressed transcripts in Bayberry knobs may have changed, relative to their respective homolog in other *Myricaceae* tissues (Bayberry leaves and *M.rubra* fruits). The most commonly cited mechanisms for the evolution of new pathways in plants, specifically in specialized metabolism, involve; (1) gene duplication followed by neo-or sub functionalization (Weng, 2014), or (2) broadening /altering enzyme specificity to allow for additional metabolic reactions (Xu et al., 2007). For example, hypothetically, a duplication of a *sn*-2 GPAT gene may have allowed for one protein to evolve the ability to prefer C16:0 fatty acids over hydroxy fatty acids.

To examine the extent to which the ability to produce Bayberry wax required gene duplications and evolved protein sequences, we compared the predicted protein sequences for the highly expressed acyl-lipid related transcripts derived from leaves and knobs collected from the same plants. Bayberry leaf wax does not accumulate MAG, DAG or TAG, and its cutin layer is predominantly C16:0 based. However, the predicted protein sequences for 12 out of the 13 highly expressed-annotated lipid genes in Bayberry knobs were 100% identical to sequences assembled from reads derived only from the leaves (a putative ABCG1 protein was truncated in

the knobs) This suggested that changes in protein sequences did contribute to the evolution of soluble surface wax synthesis by Bayberry knobs. Because only transcribed sequences were analyzed, we cannot rule out the possibility that there may have been modifications in non-coding DNA sequences that may have affected expression or RNA stability; however it is unlikely that each of the highly expressed genes experienced a separate modification in their regulatory regions. In addition, we compared predicted protein sequences to Chinese Bayberry (*Myrica rubra*), which diverged approximately 30 million years ago from *Myrica pensylvanica* (Liu et al., 2015). *M. rubra* fruits do not appear to produce an abundant layer of wax similar to *M. pensylvanica* (Feng et al. 2011) yet the predicted proteins for the highly expressed transcripts in the knobs share 90%- 95% identity.

3.4.10. Transcription factors which may contribute to the expression of cutin assembly genes

We also searched for putative transcription factors that may have contributed to the high expression of the cutin-specific gene transcripts in Bayberry knobs. From approximately 700 putative transcription factors identified in Bayberry, we searched for transcription factors that were; (1) abundantly expressed (i.e. within top 10% of transcription factors) during the wax accumulation period (i.e. day 30-51), (2) exhibited differential expression between knobs and *M. pensylvanica* leaves and *M. rubra* fruits, and (3) were annotated as being associated with acyl-lipid metabolism. Applying these criteria identified genes homologous to Arabidopsis Wrinkled 3 (WRI3) (At1g16060) and MYB30 (At3g28910).

The 25th most highly expressed putative transcription factor in knobs was homologous to Arabidopsis WRI3. The number of transcripts for Bayberry putative WRI3 increased during wax accumulation period (Figure 34 D) and the gene was expressed 44-fold more highly in the knobs

than in leaves, and 9-fold higher than a homologous sequence identified in *M. rubra* fruits. Arabidopsis WRI3 is closely related to Wrinkled 1 (WRI1), which regulates seed oil-biosynthesis by controlling the expression of genes involved in glycolysis and fatty acid synthesis (Cernac et al., 2006; Baud and Lepiniec, 2009). Indicative of a role in surface wax synthesis, an Arabidopsis knockout in *wri3* did not affect seed oil content, but instead caused a severe reduction in floral cutin and wax load (To et al., 2012). Thus, its specific expression in Bayberry knobs, relative to leaves or *M. rubra* fruits, suggests a WRI3 transcription factor may contributes to high fatty acid synthesis to support the massive wax production by Bayberry knobs

MYB30 was the 15th highest expressed putative transcription factor in knobs, was expressed 3-fold higher than Bayberry leaves and 9-fold higher than *M. rubra* fruits. MYB30 was reported to be a positive regulator of hypersensitive cell death (Vailleau et al., 2002), but is a candidate for influencing Bayberry wax production because it was shown to upregulate genes associated with cutin and very long chain fatty acid synthesis (Raffaele et al., 2008).

One transcription factor that was not highly expressed in the knobs and did not show differential expression between the knobs and the leaves and *M. rubra* were transcripts homologous to the WIN/SHINE transcription factor family. WIN/SHINE transcription factors in Arabidopsis and tomato bind directly to cutin-associated genes and overexpression and knockout of the transcription factor disrupted cutin accumulation (Aharoni et al., 2004; Kannangara et al., 2007). Interestingly, much like MpGDSL1 and the cutin-associated hydroxylases, expression of WIN/SHINE was highest at the 1st two sampling stages, but its expression dropped significantly at all stages after (Figure 34 D, Table 8). That this transcription factor was not expressed in the knobs suggests that WIN/SHINE is not directly involved in the synthesis of Bayberry surface wax.

3.5. Conclusions

Bayberry surface wax is an extraordinarily example of specialized acyl-lipid metabolism in both quantity and quality of its products. Bayberry fruits secrete the largest known amount of surface lipids in plants, and a surface wax composition of DAG, TAG and MAG has never been described in other plant species. The biosynthesis of DAG and TAG for Bayberry wax is different from conventional intracellular glycerolipid synthesis in plants. Instead, the data clearly indicate that Bayberry knobs have evolved a novel pathway for TAG synthesis and that this was achieved in large part by "re-purposing" genes of cutin synthesis to instead synthesize DAG and TAG in its soluble surface waxes.

In this study we also compared the development of the lipid secreting tissue (i.e. knobs) and transcript expression levels to related species in terms of lipid quantity and quality (i.e. oil crops, epidermal tissues, other *Myrica* species). Overall, this analysis demonstrated exceptionally high expression of transcripts encoding putative enzymes which are known to contribute to the synthesis of saturated fatty acids, and are associated with the assembly of cutin. Furthermore, indicative of a diversion of saturated fatty acids directly to acylation by *sn*-2 GPATs, the expression of transcripts encoding putative enzymes for the synthesis of cutin-like fatty acids (i.e. P450 hydroxylases) were strongly downregulated in the knobs during the period of most active wax synthesis. Finally, a comparison between knobs and leaves and *M. rubra* fruits of the predicted protein sequence for those highly expressed gene transcripts indicated no significant differences which would suggest altered specificity or expression. Thus, we make the perhaps surprising conclusion that the synthesis of surface DAG and TAG in Bayberry wax was achieved without any changes in the protein sequences of the likely key enzymes,. Together, this comparative analysis demonstrates how the extent of gene expression in Bayberry knobs are

involved in the synthesis of surface DAG and TAG, and identifies a suite of genes that when upregulated may have been sufficient to establish the trait.

Figure 35 presents a model for Bayberry wax biosynthesis which extends the model proposed in Simpson and Ohlrogge (2015). The model assigns functions to the highly expressed gene transcripts in knobs based on the known or putative activities of characterized homologs and also the radiolabeling of Bayberry knobs presented in Simpson and Ohlrogge (2015): (1) A putative Bayberry FATB gene may favor the release of C14:0 and C16:0 fatty acids from FAS and contribute to the lack of 18:0 and desaturated fatty acids in the wax. (2) For Bayberry wax synthesis, C16:0 (and C14:0) acyl-CoAs are transferred to G3P to form *sn*-2 MAG. Transcripts for *sn*-2 GPATs are highly represented in the knobs and likely contribute to the synthesis of *sn*-2 MAG. (3) Radiolabeling data was consistent with *sn*-2 MAG assembly into DAG by an intracellular MAG:MAG transacylase. Because transcripts annotated as Arabidopsis DCR was the most highly expressed gene encoding an intercellular enzyme in the knobs, Bayberry DCR may contribute to intracellular DAG assembly. (4) DAG and MAG may be exported to the surface by a combination of ABCG transporters and LTPs. (5) TAG may be assembled outside of the cell by proposed extracellular GDSL-motif enzymes. However, because the pathway for cutin synthesis has not been entirely determined, and the localizations and activities of the highly expressed Bayberry enzymes could not be directly tested, the proposed model is hypothetical and there may be additional unknown reactions not shown in the figure.

The function of Bayberry wax is most likely not as an energy/carbon store for the plant, but instead the wax could act as an attractant to some species of birds for seed dispersal (Fordham, 1983; Place and Stiles, 1992). In that regard, Bayberry wax is analogous to the large accumulations of lipids seen in the fleshy mesocarps of oil palm, olive, and avocado. However,

in contrast to Bayberry, those tissues upregulated conventional fatty acid and TAG synthesis genes to produce large quantities of TAG and store it within the cells (Bourgis et al., 2011; Kilaru et al., 2015). While Bayberry and oil-accumulating mesocarps may have experienced similar selection pressures for increased seed dispersal, Bayberry knobs have instead re-purposed enzymes associated with the synthesis of the glycerolipid cutin to accumulate extracellular TAG and DAG. This evolution apparently required overexpression, and did not require new enzymes.

From a biotechnology perspective, could other plants be engineered to accumulate large amounts of DAG and TAG in extracellular waxes like Bayberry? Evidence here suggests that this may be achieved by altering the timing and expression levels of genes associated with the biosynthesis of cutin, which are expressed in all plants. It has already been demonstrated that overexpressing suberin associated GPAT5 and also a suberin associated transcription factor induces the synthesis of suberin like fatty acids in leaf waxes and leaf cutin (Li et al., 2007a; Kosma et al., 2014). This indicates that epidermal lipid metabolism in plants can be remodeled to produce and secrete unnatural lipids by simply overexpression of single metabolic genes or a transcription factor. Furthermore, results from Bayberry and those previous studies demonstrate the plasticity in ABCG proteins to transport different types of lipids out of cells. This research on Bayberry surface DAG and TAG synthesis may prove useful in understanding alternative pathways to produce glycerolipids in plants and engineering plants for secretion of high value lipids that have toxic or negative consequences when accumulated in cells.

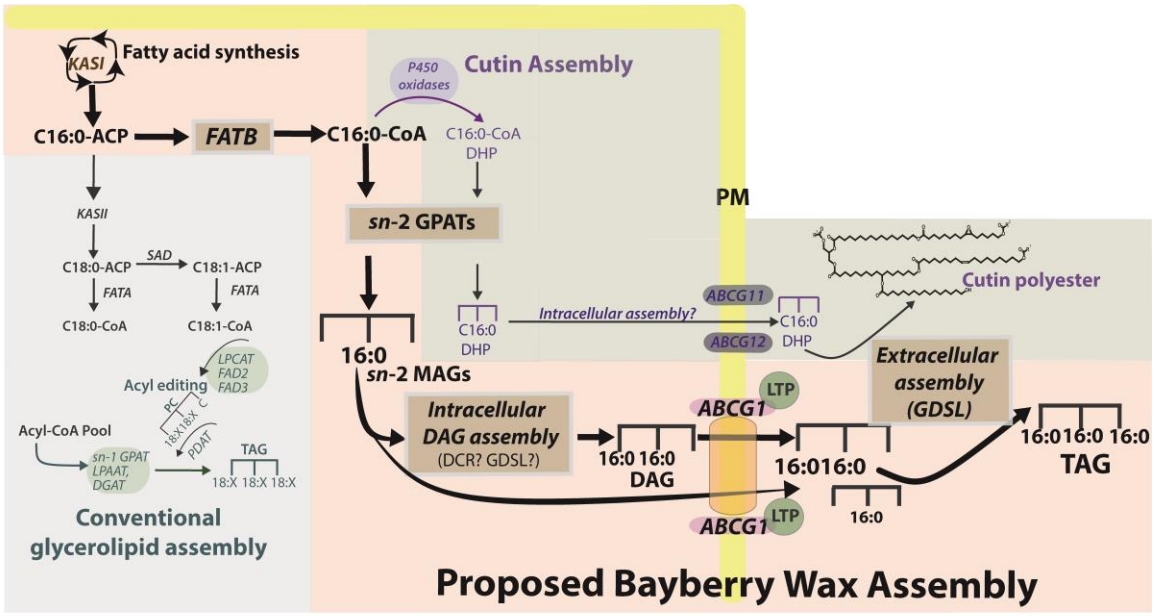

Figure 35: Proposed Bayberry wax assembly pathway with predicted enzymatic steps . The cell boundary is denoted by the yellow strip, representing the plasma membrane (PM). Intracellular reactions are to the left of the PM, and extracellular reactions are to the right of the PM. We do not distinguish any organelles in this diagram and not all reactions are shown. Bayberry wax assembly is highlighted in pink. For comparison, conventional intracellular glycerolipid synthesis (gray) and cutin assembly (purple/green) are also drawn. We note that some aspects of the pathways are hypothetical, and have not been demonstrated by direct assays with purified enzymes. All pathways begin with the synthesis of fatty acids (top left of diagram). For most intracellular glycerolipids, C18:0 fatty acids are produced, then desaturated, and assembled into TAG. For Bayberry wax, C16:0 is released from FAS by FATB and then is diverted to *sn*-2 MAG synthesis by *sn*-2 GPATs. In cutin synthesis, most C16:0 fatty acids are hydroxylated by P450 enzymes to produce dihydroxypalmitate (DHP), which are then utilized by *sn*-2 GPATs to produce *sn*-2 MAG. For Bayberry wax, labeling data predicted that DAG assembly occurs intracellularly and that DCR may be involved in that step. It is not clear if there are any intracellular assembly steps in cutin synthesis. In this model, glycerolipids are secreted from the cell by ABCG transporters and LTPs, and then assembled into TAG or cutin by extracellular localized GDSL-motif enzymes.

3.6. Materials and methods

3.6.1. Plant material

Myrica pensylvanica fruits were collected from plants on the campus of Michigan State University (42°43N, 84°23W). Experiments were done on tissue harvested from 2011- 2015. Fruits were used fresh (i.e. within minutes after collection from plants) or were immediately frozen in liquid nitrogen and stored at -80°C for later analysis.

3.6.2. Wax and lipid extraction and analysis

Surface waxes were extracted from Bayberry fruits by immersing fruits for up to 30 seconds in chloroform. Extraction of knob lipids were done according to (Hara and Radin, 1978) Intact wax was analyzed by high temperature gas chromatography using an DB5-HT column according to Simpson and Ohlrogge (2015). Fatty acid methyl esters were prepared from intact lipids and analyzed according to procedures in Li-Beisson et al. (2010). Also, Bayberry knob cutin was analyzed according to protocols described in Li-Beisson et al. (2010)

3.6.3. Microscopy of Bayberry fruits

Here, standard light microcopy, and scanning and transmission electron microcopy were used to visualize Bayberry knobs. Details for light microscopy and SEM are described in Simpson and Ohlrogge (2015). For transmission electron microcopy (TEM), we used both chemical fixation and high pressure freezing followed by chemical fixation. For chemical fixation Bayberry fruits were placed immediately in fixation buffer containing 4% formaldehyde and 2.5% glyceraldehyde in 0.1 M sodium cacodylate buffer. Samples were post-fixed in 1%

osmium tetroxide and then subjected to an ethanol dehydration series. Samples were slowly imbedded in 14310 Ultra BED resin (Electron Microscopy Sciences) and polymerized at 60°C for 5 days. High pressure freezing and freeze substitution was on done on some samples and performed as described in McFarlane et al. (2008).

Ultrathin sections for TEM examination were prepared with a diamond knife on a Power Tome_XL microtome (Brockeler Instruments), and then placed of Formvar coated copper grids. Post-staining was done with 2% uralyl acetate and Reynolds lead citrate. Samples were viewed under a JEOL 100CX TEM.

3.6.4. RNA-seq of Bayberry knob tissue

Details for RNA extraction and sequencing are for Bayberry knobs and leaves are described in Simpson and Ohlrogge (2015). Gene expression data for *B. napus* (Troncoso-Ponce et al., 2011), oil palm (Bourgis et al., 2011), tomato (Matas et al., 2011) and cherry (Alkio et al., 2014) were obtained from the supplemental files of the respective manuscripts. Transcriptome for *M. rubra* fruits was downloaded from NCBI and re-assembled according to the parameters described in Simpson and Ohlrogge (2015). To compare between species, we associated each contig(s) from the respective libraries to its most significant (e value) Arabidopsis homolog.

APPENDIX

3.7. Supplemental figures for chapter 3

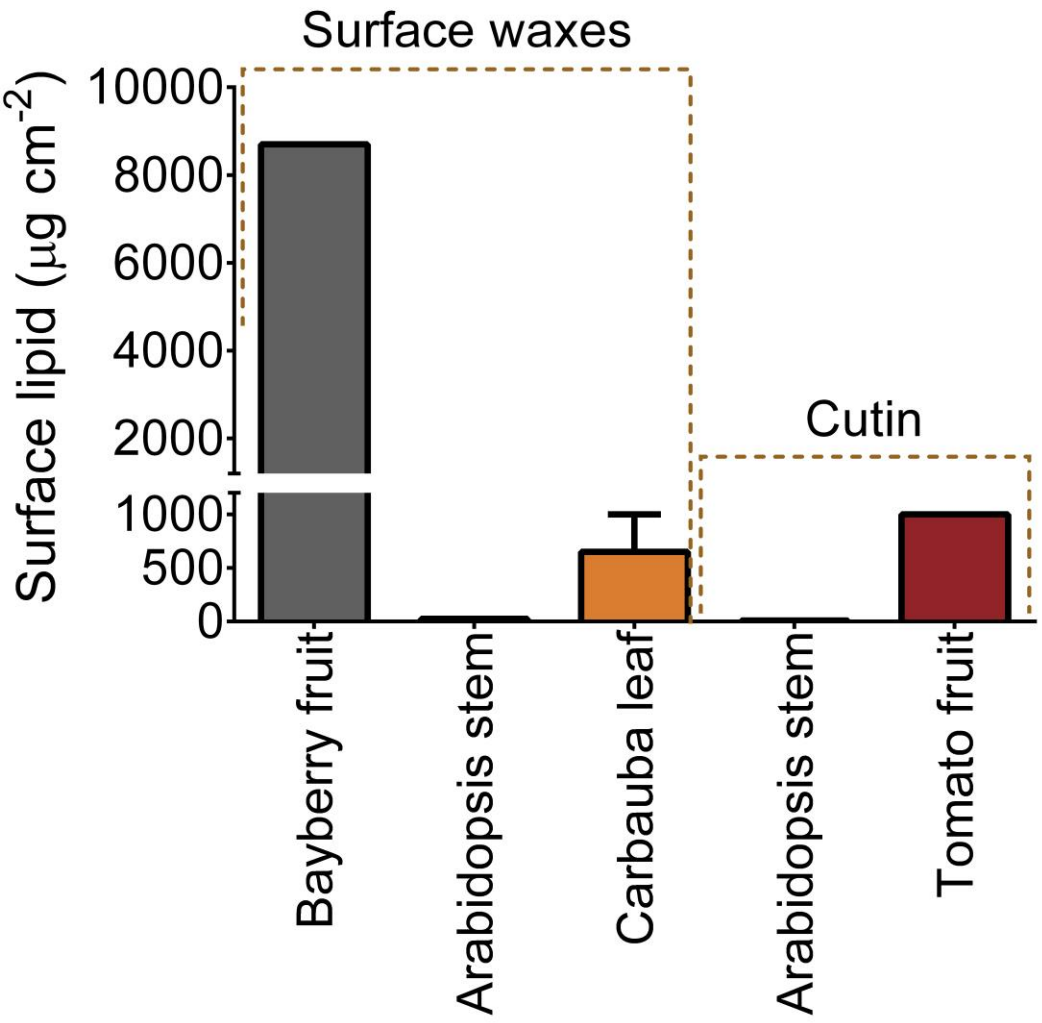

Figure 36: Comparison of surface wax accumulation by Bayberry fruits relative other plant surface lipids. The values for Bayberry wax are from Simpson and Ohlrogge (2015). Arabidopsis wax and cutin values, and tomato cutin values are from Suh et al. (2005) and Yeats et al (2012), respectively. The wax load for Carnauba palm is reported in Kolattukudy (1980) and Jetter et al. (2006).

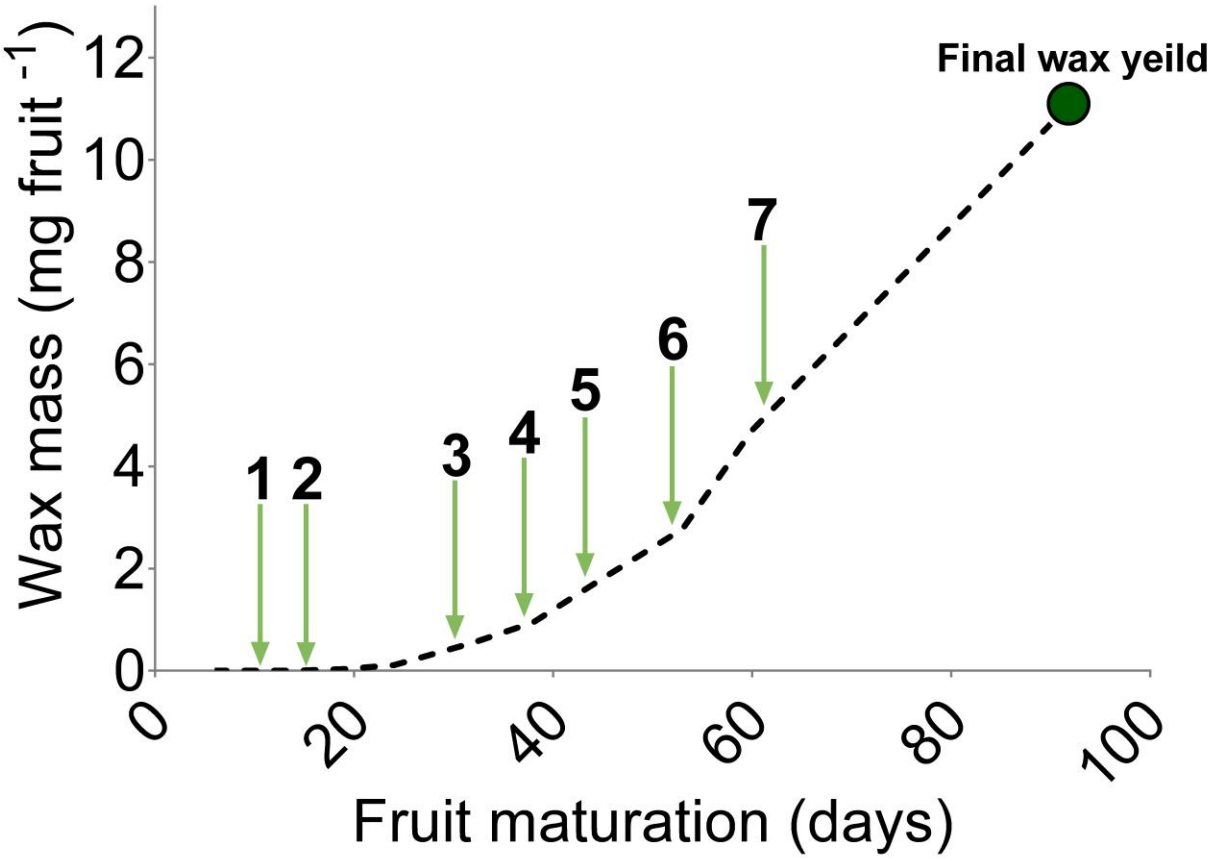

Figure 37: The wax content on Bayberry fruits at each mRNA sampling time. Sampling times are designated by the green arrows and are numbered 1-7.

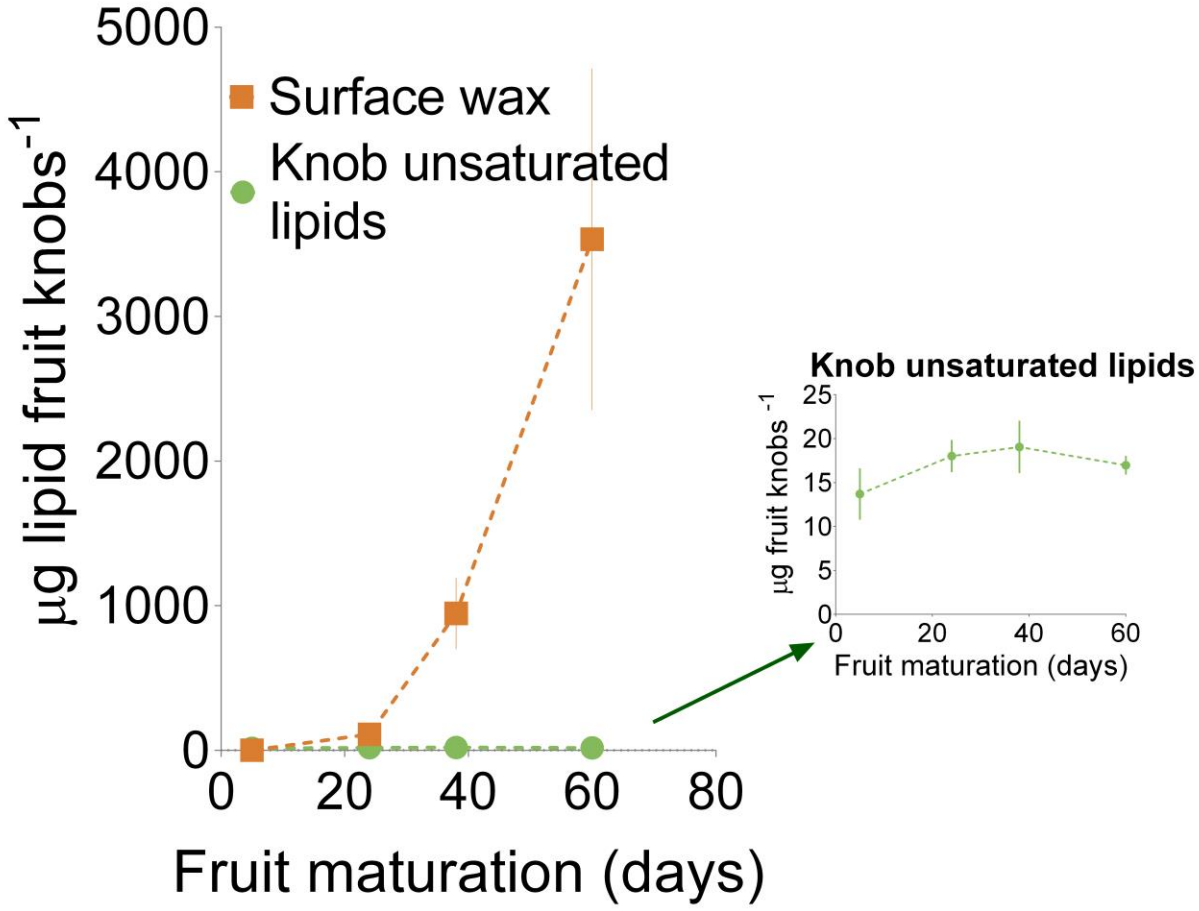

Figure 38: Amount of saturated lipids in Bayberry surface wax and unsaturated lipids in the knob cells. Each point reports the mean of 3 replicates ± SD.

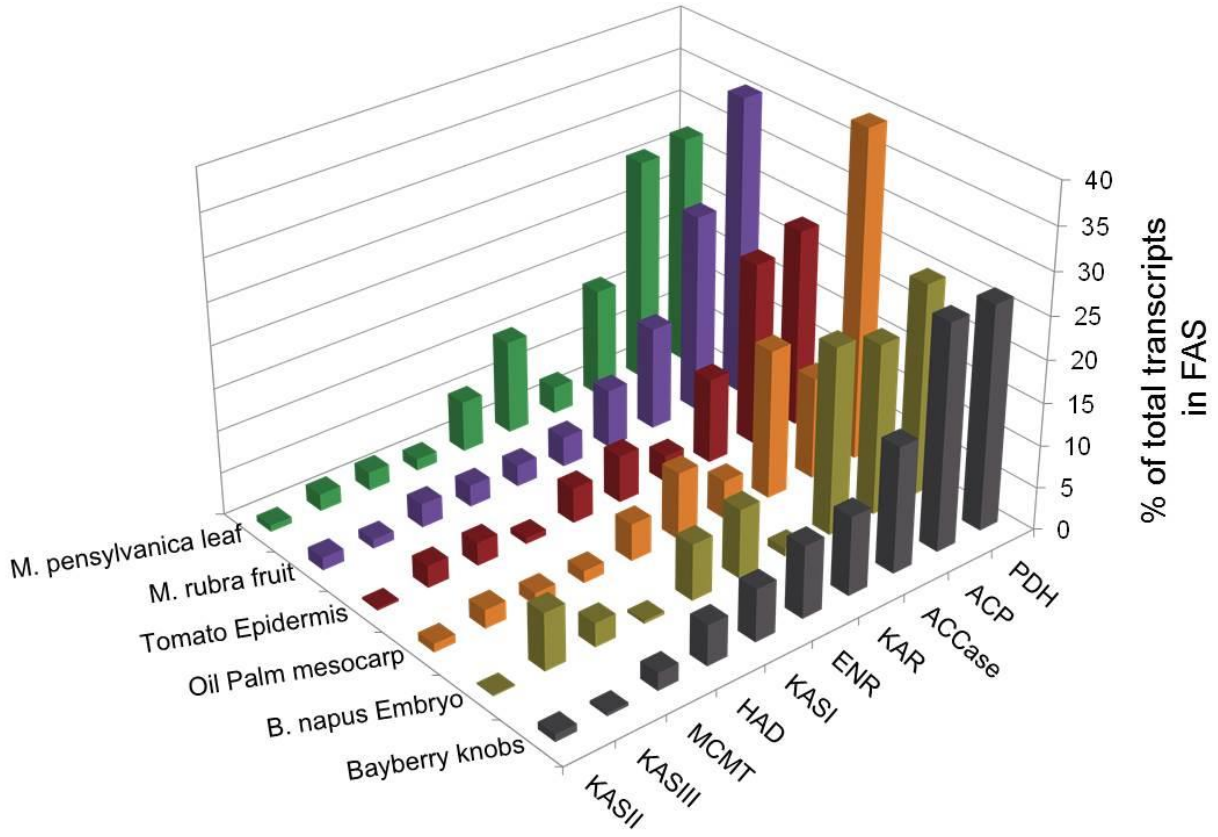

Figure 39: Relative expression levels of transcripts for plastid fatty acid synthesis genes in Bayberry knobs, oil-crops, tomato epidermal tissue and related Bayberry species and tissues. Abbreviations: PDH, pyruvate dehydrogenase complex; ACP, acyl carrier protein; ACCase, acetyl-CoA carboxylase complex; KAR, ketoacyl-ACP reductase; ENR, enoyl-ACP reductase; KAS, ketoacyl-ACP synthase; HAD, hydroxyacyl-ACP dehydrase; MCMT, malonyl-CoA: ACP manonyltransferase.

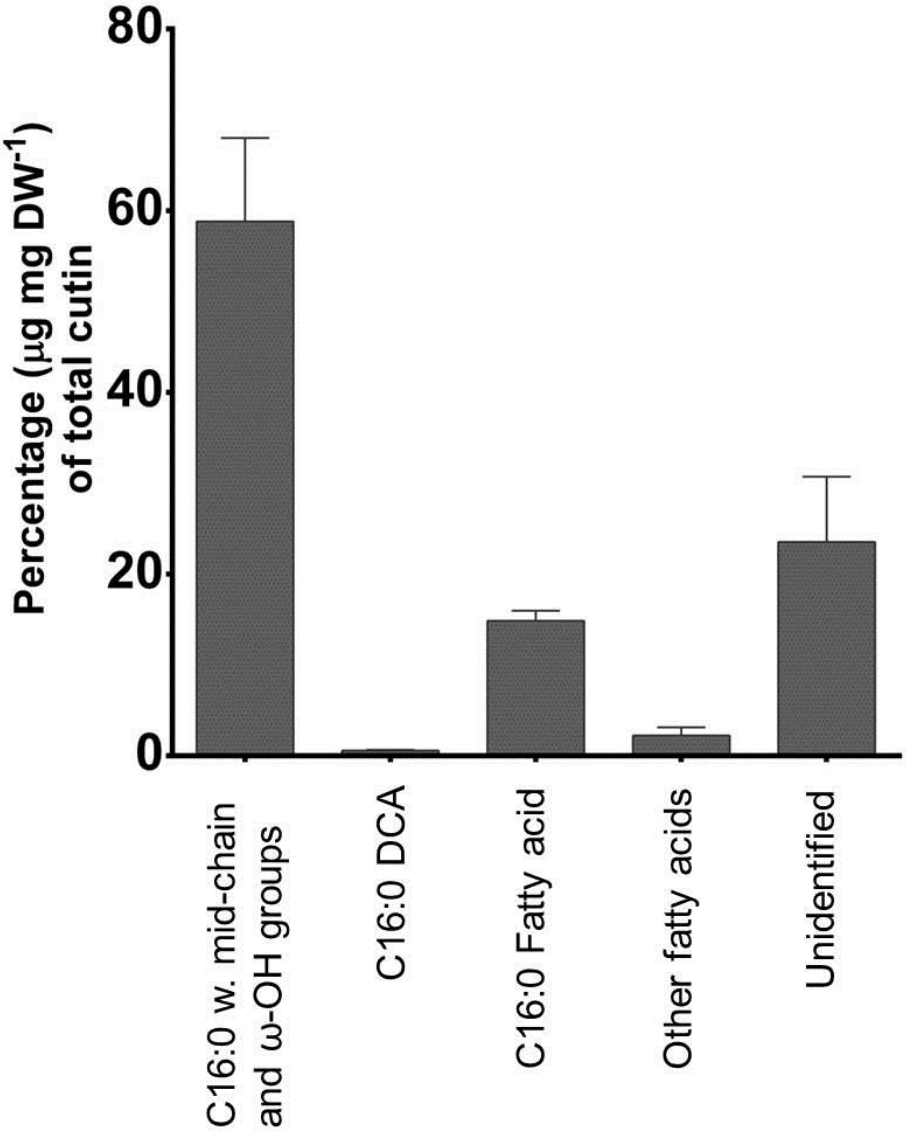

Figure 40: Cutin monomer composition of Bayberry knobs averaged over 3 stages of development. Monomers were released by base-catalyzed transmethylation with sodium methoxide and analyzed as trimethylsilyl ether derivatives. (OH = hydroxy, DCAs = dicarboxylates). Each bar is average ± range.

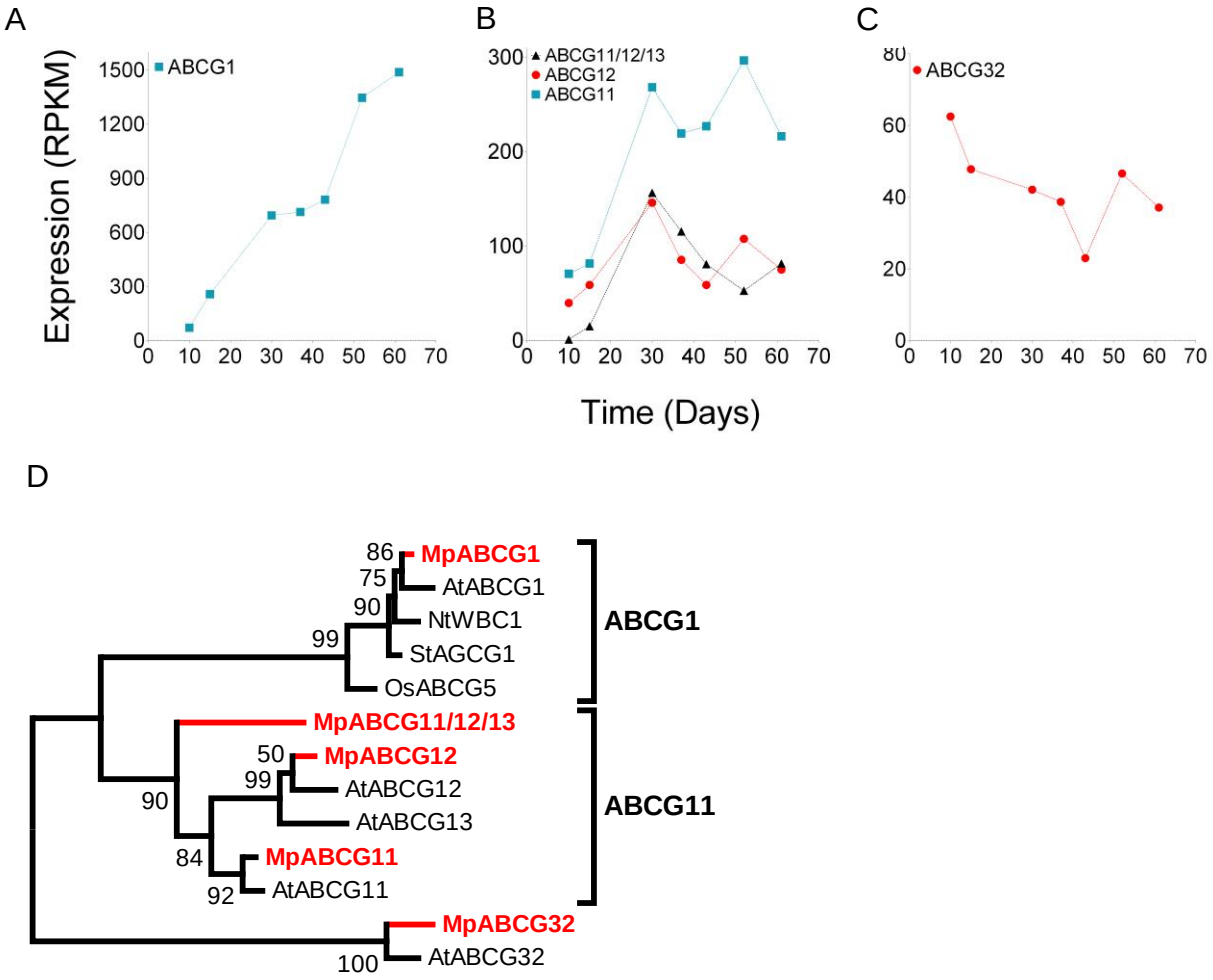

Figure 41: Time-course of expression of the abundant ABCG transporters in Bayberry (A, B, C) and their phylogenetic relationships to predicted or characterized ABCG genes in other plants (D). The highest expressed Bayberry homologs are bolded and colored red. Bayberry genes are named based on their closest Arabidopsis homologs. The sequence ID for Bayberry homologs are: ABCG1 (Mp2107273), ABCG11/12/13 (Mp2097660), ABCG11 (Mp2089466), ABCG12 (Mp2111678), ABCG11/12/13 (Mp2236196), ABCG32 (Mp2141357) The species and sequence ID's for the non-Bayberry sequences are: Arabidopsis: AtABCG1 (At2G39350), AtABCG12 (At1G51500), AtABCG13(At1G51460), AtABCG11 (At1G17840), AtABCG32 (At2G26910). *Nicotiana tabacum* NtWBC1 (Q5MY56). *Solanum tuberosum* (XP_006345915). Phylogenetic trees were constructed according to Simpson and Ohlrogge (2015).

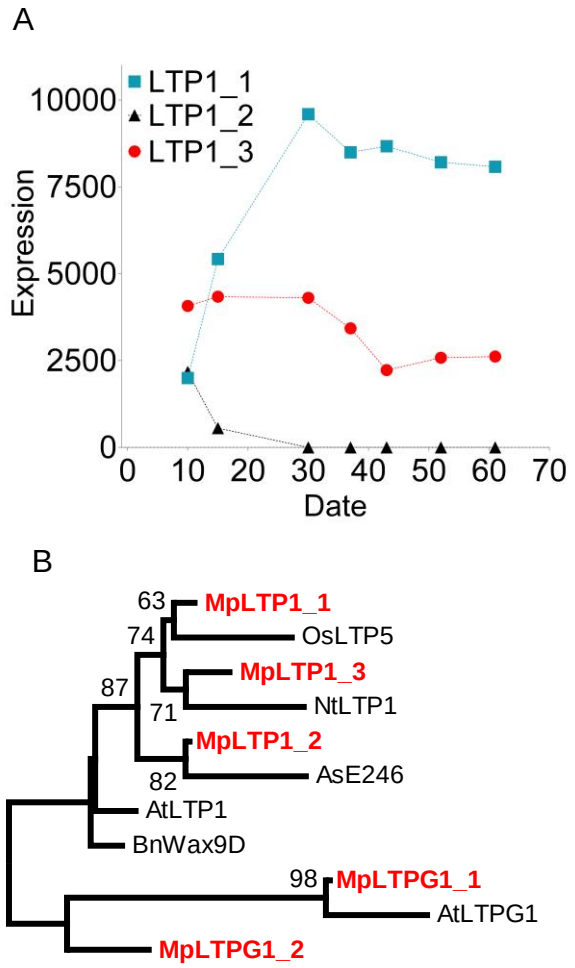

Figure 42: Time-course of expression of the abundant lipid transfer proteins (LTPs) homologs in Bayberry (A) and their phylogenetic relationships to predicted or characterized LTPs in other plants (B). The highest expressed Bayberry homologs are bolded and colored red. Bayberry genes are named based on their closest Arabidopsis homolog. The sequence ID for Bayberry homologs are: LTP1 (Mp2044016), LTP1_2 (Mp2097660), LTP1_3(Mp2069206), LTPG1_1 (Mp2092270), LTPG1_2 (Mp2138205). The species and sequence ID's for the non-Bayberry sequences are: OsLTP5- *Oryza sativa* (Os11g02389); NtLTP1 – *Nicotiana tabacum* (Q42952); ASE246- *Astragalus sinicus* (Q07A25); BnWax9D- *Brassica oleracea* (Q43304), AtLTP1- Arabidopsis (At2G38540), AtLTPG1- Arabidopsis (At1G27950). Phylogenetic trees were constructed according to Simpson and Ohlrogge (2015).

3.8. Supplemental tables for chapter 3

Table 7: The highest expressed acyl-lipid related proteins in *B. napus* seeds, oil palm mesocarp and tomato epidermal tissue and their ranks (out of total annotated contigs) in the respective transcriptomes.

Species/tissue	Rank in tissue	Top Arabidopsis homolog	Acyl lipid pathway
B. napus embryo	7,8,9,17,49	Oleosins	Lipid storage
	19	Caleosin	Lipid Storage
	33,71	Soluble ACP desaturase	Fatty acid synthesis
	36	Steroloesin	Lipid storage
	74	Lineolate desaturase (FAD3)	Lipid synthesis
	80	Acyl carrier protein 1	Fatty acid synthesis
Oil palm mesocarp	7	Oleate desaturase (FAD2)	Lipid synthesis
	13	Soluble ACP desaturase	Fatty acid synthesis
	25,51	PDH subunits	Fatty acid synthesis
	41	Acyl carrier protein 4	Fatty acid synthesis
	49	Keto-acyl ACP reductase	Fatty acid synthesis
	68,92	ACCase subunits	Fatty acid synthesis
	76	Enoyl-ACP reductase	Fatty acid synthesis
Tomato epidermis	1,6,14,36	Lipid transfer proteins	Lipid secretion
	18	GDSL lipase (CUS2)	Cutin synthesis

Table 8: Genes associated with cuticular lipid synthesis and their average expression rank (out of total annotated contigs) and change in expression, from the first two sampling stages (when wax was not evident), to the final sampling stage when the fruits accumulated 50% of its total wax.

		RANK IN EXPRESSION LEVEL		Fold decrease or increase in expression (RPKM)
	Gene	Days 10-15 (no wax)	DAYS 30-61 (wax)	
Cutin assembly	GPAT4/8	16	8	2
	GPAT6	88	11	4
	DCR	9	3	2
	GDSL2	195	18	4
	GDSL1	3	8931	-1250
Lipid secretion	Lipid transfer protein (LTP1)	1	1	6
	ABCG transporter 1 (WBC1)	498	34	6
Transcription factors	WIN/SHINE	3463	10175	-1092
	Wrinkled 3	2780	361	6
Fatty acid modification	CYP77A4/A6	477	9998	-149
	CYP86A4	326	9200	-63
	Hothead	837	9338	-30
	CYP86A8/LCR	881	259	3
Other genes	KCS10	208	24	4
	KCS19	209	25	4
	FATB	162	40	2
	ACP4	68	46	1.2

CHAPTER 4

CONCLUSIONS AND FUTURE RESEARCH PERSPECTIVES

4.1. Research questions

The decision to investigate Bayberry wax biosynthesis for my dissertation research was motivated by three major goals: (1) Study the biology of the plant cuticle. (2) Understand how lipids are secreted from plant cells. (3) Investigate alternative pathways for triacylglycerol synthesis in plants. The surface wax of Bayberry fruits have been used for hundreds of years to make candles. However, despite the knowledge of its abundant surface wax layer, Bayberry fruits are rarely cited as such and there has been almost no research on the biochemistry of Bayberry wax. In fact, the most recent chemical characterization on the plant was done 50 years ago by Harlow et al. (1965), where it was reported that the surface wax represents up to 25% of the mass of the fruit, and that a major component of the wax is TAG with saturated fatty acids. These properties are striking for both a surface lipid and a TAG accumulating plant tissue and raised interesting questions about cuticular lipid and TAG synthesis in plants.

The cuticle is the largest biological interface in nature and has diverse and important roles in the development, growth and survival of the plant. The use of forward and reverse genetics over the past decade has identified many genes critical to the development and function of the cuticle. These include transcription factors (i.e. SHN/WIN), cutin assembly enzymes (i.e. *sn*-2 GPATs, p450 hydroxylases, lipases as "cutin synthases", HXXXD acyltransferases) and proteins important for cuticular lipid secretion (i.e. ABCG transporters, LTPs) (Beisson et al., 2012). However, despite these discoveries, there is still limited knowledge on how surface lipids are synthesized intracellularly, how monomers or oligomers are secreted to the surface, extracellular cutin assembly, and the overall structure of cutin. While Bayberry does not produce a conventional surface lipid, it does have some important characteristics that could make it a model to study some aspects of cuticular lipid biology. Firstly, Bayberry knobs produce at least

ten-fold more surface lipids than any other plant species and over a longer period of time, making the tissue more amenable to *in vivo* biochemical studies and visualization. Second, biochemical studies may be simplified using Bayberry because the wax is soluble and accumulates continuously on a fully grown plant tissue. Thirdly, because the fatty acids in Bayberry wax are unmodified and highly abundant, it may offer better insights about how epidermal cells separate the massive flux of fatty acids destined for the cuticle from fatty acids needed for intracellular membrane polar lipids. However, the fact that little is known about the genetics of Bayberry, and that I could not get Bayberry to flower and produce fruits under controlled conditions (i.e. in a greenhouse) are limitations to using Bayberry as a model system.

In addition to furthering understanding of basic cuticle biology, research on Bayberry may have biotechnological applications. Accumulation of TAG or other hydrocarbons in vegetative tissues may enhance the energy density and value of plant biomass if the lipids are extracted for biodiesel or burned in a biomass power plant (Ohlrogge et al., 2009). Furthermore, plant surface lipids represent high-energy compounds that remain intact during the plant's life cycle, mostly because they are not easily accessed or degraded (Yang and Ohlrogge, 2009). Thus, engineering plants to secrete lipids, in the form of TAG, from vegetative tissues to their surface could represent one way to produce biofuels and other types of economically important glycerolipids (i.e. butters) with greater stability and thereby increase the total value of a crop. Bayberry could be an attractive model to study because it has a never previously described pathway to produce TAG, and deposits the TAG outside of its cell. However, there are limitations to this proposal, notably that transcripts highly expressed in Bayberry knobs are difficult to assay in heterologous systems, and that there may be other unidentified factors

specific to Bayberry, and not conventional cuticular lipid synthesis, which contributes to the synthesis of its surface wax.

4.2. Summary of findings on Bayberry surface wax synthesis and secretion

My initial research questions were: (1) Is Bayberry wax composed entirely of TAG or does it contain any other components, such as conventional plant surface waxes (i.e. alkanes) and intermediates to TAG? (2) Is the glycerolipid wax released from degradation of cells that have filled with lipids (as in Chinese Tallow, stigma estolides, pollen lipids), or is it actively secreted like cuticular lipids? (3) How is TAG, synthesized? Does Bayberry use reactions similar to TAG synthesis in oil seeds, or has it evolved a new pathway to synthesize TAG? Fortunately, Bayberry plants are located by the front doors of the Plant Biology Building at Michigan State University, giving me an abundant supply of plant material to study.

The initial experiments involved qualitatively and quantitatively documenting the accumulation of surface wax on Bayberry fruits. These experiments were critical to formulate hypotheses on possible biosynthetic pathways for the wax, which were subsequently tested by the radiolabeling experiments. Photographs of the plant and the fruits were taken through an entire growing season (April to September) to demonstrate the timing and location of the surface wax. Surface wax was also extracted at weekly intervals throughout the growing season, and the amount and composition of the wax was determined. The observation that the surface wax accumulated continuously through approximately 8-weeks, and that the wax layer grew uniformly on the fruit surface indicated that the glycerolipids are not released by degradation of the knobs tissue, but instead are actively secreted from the knob cells. Furthermore, the compositional analysis revealed that the wax contains essentially only DAGs, TAGs and MAGs

with saturated fatty acids and no conventional surface waxes (i.e. alkanes) could be identified. Most intriguingly, *sn*-2-MAG was discovered as a significant component of the wax. *sn*-2 MAG is a glycerolipid previously shown to be an early intermediate in the biosynthesis of the surface lipid polyesters cutin and suberin (Li et al., 2007a) and its identification provided preliminary evidence that the synthesis of Bayberry wax glycerolipids may use a mechanism related to cutin synthesis, and not conventional TAG synthesis. Furthermore, the fact that DAG, and not TAG, is the most abundant lipid component in mature Bayberry wax provided additional evidence that TAG is probably not synthesized by a pathway similar to oil-seeds.

The following season, wax assembly pathways were examined by labeling Bayberry fruits with two precursors to glycerolipids, [^{14}C]-glycerol and [^{14}C]-acetate. While those labels have been used extensively to study membrane and oil seed lipid synthesis in plants, similar experiments have not been done to examine the biosynthesis of surface lipids. The kinetics of [^{14}C] incorporation into Bayberry surface wax provided direct biochemical support that Bayberry synthesizes DAG and TAG differently from conventional glycerolipid synthesis in seeds and leaves. Instead, the results indicated that Bayberry synthesizes intermediates and assembles the glycerolipids in a manner similar to the synthesis of the surface glycerolipid cutin. Specifically, *sn*-2 MAG was the first glycerolipid labeled by [^{14}C]-glycerol and there was a precursor-product relationship between *sn*-2 MAG and DAG and TAG. Unexpectedly, identical initial labeling kinetics were observed with [^{14}C]-acetate. This pattern of labeling was not predicted if the same acyl-donors acted at the *sn*-2 and *sn*-1/3 positions of MAG to produce DAG and TAG and instead suggested that all newly synthesized acyl-groups flux through a pool of *sn*-2 MAG before they are incorporated into DAG and TAG. Thus, these data point towards DAG and TAG synthesis by acyl-CoA independent transacylase reactions, which would represent a new

pathway to synthesize DAG and TAG in plants. To gather further information about how DAG and TAG may be assembled, regiospecific analysis of [^{14}C]-acyl chains were examined. Overall, the distribution of labeled acyl chains in DAG and TAG produced from [^{14}C]-acetate labeling coupled with the kinetics of [^{14}C]-*sn*-2 MAG synthesis supported the hypothesis that DAG is formed intracellularly by a MAG:MAG transacylase, while TAG is synthesized extracellularly from secreted MAG and DAG by a MAG:DAG transacylase. This mechanism of acyl-chain incorporation is similar to an extracellular MAG:MAG transacylase enzyme reported for cutin assembly (Yeats et al., 2012).

In addition, cDNA sequencing by Illumina was performed on Bayberry's wax producing tissue (i.e. knobs) to identify genes that may be involved in this specialized lipid metabolism. Strikingly, thirteen out of the top fifty-five most highly expressed transcripts in Bayberry knobs were associated with fatty acid production and surface lipid synthesis. Bayberry is the most dramatic example yet identified of transcriptional specialization towards lipid production. Significantly, the known and putative activities of the most highly expressed transcripts supported the biochemical data indicating that TAG and DAG in Bayberry wax may be synthesized and secreted by mechanisms related to cutin. Specifically, the most highly expressed transcripts in the tissue were related to genes associated with the production and secretion of surface lipids. These genes included genes annotated as; (1) fatty acid thioesterase (FAT) B involved in the production of saturated fatty acids, (2) *sn*-2 glycerol-3-phosphate acyltransferase (GPAT) to synthesize *sn*-2 MAG, (3) GDSL-motif enzymes previously shown to have extracellular glycerolipid transacylase activity, (4) BAHD (HXXXD) acyltransferase defective in cuticular ridges (DCR) which may be involved in intracellular lipid assembly, and (5) ABCG transporters and lipid transfer proteins (LTPs) which are involved in surface lipid secretion. I

propose that the massive expression of these specific putative genes allowed Bayberry to evolve its unique production of saturated glycerolipids on its fruit surface.

4.3. Unknowns and future experiments to further characterize Bayberry wax synthesis

4.3.1. Direct biochemical evidence for proposed reactions by enzyme assays

Together, the data presented in this dissertation provides compelling evidence that a novel pathway for triacylglycerol synthesis in plants is responsible for massive wax accumulation on the surfaces of Bayberry fruits. The model was developed based on labeling kinetics and the putative or known activities of the highly expressed transcripts in Bayberry knobs in the synthesis of Arabidopsis or Tomato cutin. Thus, some details regarding the reactions proposed are hypothetical because they are based on indirect evidence. However, it is important to note that before the use of biochemical genomics, plant metabolic pathways were elucidated by the use of radioactive tracers. Nevertheless, a number of questions remain regarding how these highly expressed putative enzymes in Bayberry knobs may interact to synthesize surface DAG and TAG. In particular, it is unclear how the activity and substrate specificity's of *sn*-2 GPATs and GDSL-motif enzymes for Bayberry surface wax synthesis may differ from reactions to synthesize cutin (i.e. using normal unsubstituted fatty acids as opposed to dihydroxy fatty acids) and an *in vivo* function of the HXXXD acyltransferase DCR in cutin assembly and in Bayberry wax production is not yet clear.

Direct evidence of this pathway could be provided by expression and enzyme assays with the highly expressed enzymes (i.e. *sn*-2 GPATs, DCR, GDSL-motif enzymes). Unfortunately, despite multiple attempts, no activity for DCR and GDSL-motif enzymes was detected when heterologouly expressed in *E. coli*, yeast, or transiently in tobacco. I did detect a soluble protein

product when DCR was expressed in *E coli*, and GDSL-lipases expressed in *E. coli* killed the cells (not shown).Some reasons for the lack of activity for the proteins include, errors in the gene sequence, poor expression, improper substrates, unknown enzymatic partners or cofactors, enzyme stability or inhibition. Future work should be aimed at addressing these issues and studying alternative approaches to both express and test the activity of those important acyltransferases. Here, proteins were predicted from transcripts derived from RNA sequencing, and were synthesized. It is possible that RNA-seq did not predict the correct proteins, which could be remedied by producing cDNA's for those genes directly from Bayberry RNA. In addition to heterologous expression, activity could also be tested by complementation of Arabidopsis or tomato mutants that are knocked out in homologs to those Bayberry genes. For example, it would be important to determine if Bayberry homologs could restore the cutin phenotypes in Arabidopsis mutants disrupted in *dcr*, *abcg* and *gpat* knockout mutants. If functions can be established, then a challenging, but particularly attractive future investigation, would be to see if it is possible to induce soluble glycerolipid synthesis in other plants. This could involve introducing different combinations of the highly expressed Bayberry genes into wildtype and mutants of cutin genes that were downregulated in Bayberry knobs (i.e. P450 hydroxylases knockouts).

4.3.2. Localization of wax synthesis in Bayberry knobs

Bayberry wax is primarily detected surrounding the epidermis of the knobs, and not in the apoplast surrounding interior cells. Furthermore, many of the genes highly expressed in Bayberry knobs are surface lipid genes, which are primarily expressed in epidermal cell layers (Suh et al., 2005; Matas et al., 2011). Therefore, epidermal cells may be the only cell layer in the

knobs involved in wax synthesis. However, the tissue used for RNA sequencing was the entire knob, and not epidermal peals from knobs. Thus, it is surprising that surface lipid genes represented the highest expressed genes in the knobs, considering that the majority of the tissue harvested contained internal cells. *In situ* hybridization could be used to determine where in the knobs genes associated with surface lipid metabolism are expressed (i.e. in the epidermal cell layer or internal cells).

4.3.3. [^{14}C]-labeling experiments to determine intra- vs extra- cellular localization of wax synthesis

A [^{14}C] labeling experiment was performed to demonstrate the localization of wax synthesis (i.e. intra- versus extracellular) and to determine whether *sn*-2 MAG is secreted into the extracellular lipids and could act as an acyl-donor for TAG synthesis (Chapter 2). In those experiments, whole fruits (as opposed to dissected knobs) were labeled with [^{14}C]-acetate for up to 5 days, and at various time points, extracellular lipids and internal lipids were extracted separately. The kinetics of MAG accumulation in both lipid extracts and over time provided evidence for two independent pools of MAG; one inside of the knob cells and a pool outside of the knob cells. That finding was consistent with the hypothesis that DAG synthesis occurs inside the cells from an intracellular MAG pool, and TAG is synthesized outside of the cells with an extracellular MAG pool as the acyl-donor. While that experiment was repeated multiple times with similar results, there were inefficiencies in the incorporation of the labeled acetate into the fruits and it was not possible to extract all of the surface wax at each harvesting time. Furthermore, parallel incubations with [^{14}C]-glycerol was difficult to interpret because of poor incorporation of the label over time. Both issues complicated a more thorough analysis on the

kinetics of extracellular lipid assembly. For example, the timing of *sn*-2 MAG and DAG secretion could not be determined and the proportion of the DAG that was shunted to crystalline wax versus used as a substrate for TAG synthesis could not be estimated.

The aforementioned issues may be resolved by performing labeling experiments that better mimic natural conditions. To continuously supply the labeled substrates, fruits had to be submerged in a buffer and such conditions may have contributed to the inconsistent results by negatively affecting lipid synthesis and secretion of the lipids to the surface. Instead, labeling fruits with [^{14}C]-CO_2 would maintain a more natural state and may eliminate some problems associated with long-term submergence. Furthermore, a chase (i.e. remove labeled substrate) could be implemented to determine the proportion of labeled DAG that is incorporated into TAG versus the proportion of labeled DAG that remains in DAG over time. However, labelling fruits with [^{14}C]-CO_2 may be complicated because of lags introduced by filling a large number of intermediate pools to produce acetyl-CoA, and it is currently unknown how much the knobs contribute to CO_2 assimilation.

4.3.4. Additional microscopy of the wax producing tissue to demonstrate mechanism of secretion

The mechanism proposed for Bayberry wax secretion from the cells is based on current models for cuticular lipid secretion (Samuels et al., 2008). Briefly, cutin precursors (i.e. *sn*-2 MAG or oligomers) must migrate from their site of synthesis within the cell to the cell membrane. The mechanism of secretion is largely unknown, but may involve PM-ER contact sites (Samuels and McFarlane, 2012). Next, assembled lipids or neutral lipid precursors must move through the cell membrane and cell wall. Movement of cuticular lipids through the cell membrane is thought to be catalyzed by ABCG transporters, and movement of lipids through the

cell may be aided by lipid transfer proteins (LTPs); however, there has been no direct evidence illustrating such a function for either protein.

Transmission electron microscopy (TEM) was used here to document changes in the morphology of the knob cells as they secrete lipids and to identify cellular structures which may contribute to wax secretion. However, clear images of knobs showing subcellular structures through the entirety of wax layer development could not be obtained. The tissues tended to break apart during sectioning and when in the microscope, which was particularly problematic in older tissue. Multiple different preparation techniques were tried (i.e. high pressure freezing, low viscosity resins) with some improvement, but images were not up to the caliber of images from other plants, such as Arabidopsis. It is possible that Bayberry knobs are very recalcitrant to incorporation of resins, or that there are substances within the knobs that disrupt fixation. In addition to troubleshooting TEM preparation techniques, improved visualization of wax secretion could be obtained by freeze-fracture SEM, two-photo confocal microcopy and *in vivo* microcopy techniques. Images of this unique tissue may prove valuable to better understand how cells secrete lipids to their surfaces.

4.4. Future work to understand the evolution of Bayberry wax

Bayberry wax is an extraordinary example of specialized fatty acid metabolism, both in the quantity and quality of its products. As introduced above, the initial motivations of this work were to better understand the biology of surface lipid metabolism and to determine how plants might in the future be engineered to produce and secrete more surface lipids for biotechnical applications. While the fatty acid composition and gross structure of the soluble glycerolipids in Bayberry fruits is very different from cuticular lipids, many aspects of their synthesis and

secretion are shared. For example; (1) the production of *sn*-2 MAGs by GPATs, (2) secretion of *sn*-2 MAG, (3) extracellular glycerolipid assembly, (4) lack of cuticular lipid-accumulation within plant cells, and, (5) the possible involvement of ABCG transporters in cuticular lipid secretion. This work expands on previous work by also proposing a function for *defective in cuticular ridges* (DCR) in the intracellular assembly of secreted glycerolipids and demonstrating applicability of [^{14}C]-acetate and [^{14}C]-glycerol labeling to study cuticular lipid assembly reactions and identify intermediates. The observations of Bayberry surface wax synthesis may also enhance understanding of the biology of other extracellular lipids, such as stigma estolides.

Transcriptomic analysis of Bayberry knobs identified several extremely highly expressed lipid-related genes which implied that they are involved in the synthesis and secretion of Bayberry glycerolipid wax. The amino acid sequences of those predicted proteins were identical between Bayberry knobs and Bayberry leaf. Therefore, it was concluded that their high expression, rather than evolution of new sequences, was the major factor that allowed Bayberry to develop the trait of massive wax secretion. The evolutionary pressures that selected for this trait are very likely seed dispersal. Specifically, the wax may function to provide birds with a high-energy calorie source, and the birds disperse the seeds as they consume the wax (Place and Stiles, 1992). This function is consistent with the proposed seed dispersal function of oil-accumulating mesocarps (i.e. oil palm, olive, avocado) and arils (Howe and Smallwood, 1982; Lorts et al., 2008). However, in contrast to Bayberry, these tissues use conventional TAG synthesis genes to produce their large quantities TAG and they also store the lipids within cells (Bourgis et al., 2011; Troncoso-Ponce et al., 2011; Kilaru et al., 2015). In Bayberry, while the end product TAG is shared, Bayberry overexpressed genes involved in surface lipid metabolism and TAG is produced on the tissue surface. What is perhaps unique about Bayberry is that it also

needed to evolve a mechanism to differentiate between lipids for cutin synthesis from soluble glycerolipid waxes. It is unclear whether *Myricaceae* species are the only plants to have evolved this mechanism for TAG synthesis, and future research could search for TAG in the surface waxes of other plants.

4.5. Future applications of research described in this dissertation

From a biotechnological perspective, could other plants be engineered to accumulate large amounts of DAG and TAG in soluble waxes? Evidence from Bayberry suggests that simply altering the timing and expression of specific genes associated with the biosynthesis of cutin may allow for the synthesis of soluble extracellular glycerolipids. Indeed, it has already been demonstrated that epidermal lipid metabolism can be co-opted to produce and secrete "un-natural" lipids. Specifically, ectopically overexpressing suberin associated GPAT5 caused suberin-like fatty acids to accumulate in leaf waxes and leaf cutin (Li et al., 2007b; Li et al., 2007a), and overexpressing a suberin-associated transcription factor in leaves induced the synthesis of suberin- like fatty acids in waxes and cutin (Kosma et al., 2014).While those studies indicate that epidermal cells have the capacity to divert fatty acids into different types of glycerolipids and also secrete them from the cells, future research with Bayberry may be required to identify other unknown factors. Nevertheless, this knowledge may prove useful in engineering alternative pathways to produce glycerolipids in plants and engineering plants for secretion of high value lipids that have toxic or negative consequences when accumulated in cells.

As mentioned earlier, surface lipids are more resistant to degradation and may be less harmful to cellular metabolism, particularly if producing them in vegetative tissues. All plants

have the capacity to produce and secrete lipids from their epidermal cells, and some surface lipids are valuable and accumulate to large enough levels were it is economical to extract and sell them. The most prominent examples are from Carnauba palms, Candelilla stems, and the Ouricouri tree, which all produce surface waxes (i.e. alkanes, wax esters) with properties excellent for cosmetics, food coatings and polishes. Specifically, Carnauba wax accumulates to 5-10% of the mass of a leaf and is extracted from leaves by boiling them in water or scraping (Kitzke and Wilder, 1961). In 2014, approximately 16 million kilograms of Carnauba wax was exported from Brazil at approximately $8 per kilogram, making to total value of the wax at over 128 million dollars (source: http://carnaubadobrasil.com/1/en/beneficiamento.asp). While the composition of Bayberry wax, and genes involved in Bayberry wax synthesis, are very different from Carnauba, the economics of Carnauba raises the possibility that Bayberry genes could be introduced into crop plants to produce triacylglycerols in surface waxes of similar value. For example, cocoa butter currently sells for $4 per kilogram and the TAG compositions in cocoa butter are ; (1)C16:0, C18:1, C16:0 (2) C16:0, C18:1, C18:0, and (3) C18:0, C18:1, C18:0 (Gunstone et al., 2007), which is very similar to Bayberry's saturated surface TAG. Thus, it is possible that engineering a crop plant to express an optimal ratio of FAS thioesterases FATB and FATA, and cutin-acyltransferases that Bayberry uses to synthesize its surface TAG could result in surface TAG with a cocoa butter fatty acid composition. If the cocoa butter like-TAGs accumulated as a surface wax to 10% of the leaf dry weight, assuming that leaf dry weight is approximately 20 tonnes ha $^{-1}$, then 2000kg of TAG could be produced per hectare. If all of Michigan's corn plants (~2700ha) had this property, then the added value to the crop would be 21 million dollars.

REFERENCES

REFERENCES

Aharoni, A., Dixit, S., Jetter, R., Thoenes, E., van Arkel, G., and Pereira, A. (2004). The SHINE clase of AP2 domain transcription factors activates wax biosynthesis, alters cuticle properties, and confers drought tolerance when overexpressed in Arabidopsis. Plant Cell 16, 2463-2480.

Akoh, C.C., Lee, G.C., Liaw, Y.C., Huang, T.H., and Shaw, J.F. (2004). GDSL family of serine esterases/lipases. Prog. Lipid. Res. 43, 534-552.

Alkio, M., Jonas, U., Declercq, M., Van Nocker, S., and Knoche, M. (2014). Transcriptional dynamics of the developing sweet cherry (*Prunus avium* L.) fruit: Sequencing, annotation and expression profiling of exocarp-associated genes. Hort. Res. 1, 11.

Allen, D.K., Bates, P.D., and Tjellstrom, H. (2015). Tracking the metabolic pulse of plant lipid production with isotopic labeling and flux analyses: Past, present and future. Prog. Lipid. Res. 58, 97-120.

Arondel, V., and Kader, J.C. (1990). Lipid transfer in plants. Experientia 46, 579-858.

Badami, R.C., and Patil, K.B. (1981). Structure and occurrence of unusual fatty acids in minor seed oils. Prog. Lipid. Res. 19, 119-153.

Bafor, M., Jonsson, L., Stobart, A.K., and Stymne, S. (1990). Regulation of triacylglycerol biosynthesis in embryos and microsomal preparations from the developoing seeds of *Cuphea lanceolata*. Biochem. J. 272, 31-38.

Bago, B., Zipfel, W., Williams, R.M., Jun, J., Arreola, R., Lammers, P.J., Pfeffer, P.E., and Shachar-Hill, Y. (2002). Translocation and Utilization of Fungal Storage Lipid in the Arbuscular Mycorrhizal Symbiosis. Plant Physiol. 128, 108-124.

Bakan, B., Hamberg, M., Perrocheau, L., Maume, D., Rogniaux, H., Tranquet, O., Rondeau, C., Blein, J.P., Ponchet, M., and Marion, D. (2006). Specific adduction of plant lipid transfer protein by an allene oxide generated by 9-lipoxygenase and allene oxide synthase. J. Biol. Chem. 281, 38981-38988.

Baker, E.A. (1982). Chemistry and morphology of plant epicuticular waxes. In The Plant Cuticle, D.J. Culter, K.L. Alvin, and C.E. Price, eds (London: Academic Press), pp. 139-165.

Banerji, R., Chowdhury, A.R., Misra, G., and Nigam, S.K. (1984). Butter from plants. Fett. Wiss. Technol. 86, 279-284.

Barthlott, W., Neinhuis, C., Cutler, D., Ditsch, F., Meusel, I., Theisen, I., and Wilhelmi, H. (1998). Classification and terminology of plant epicuticular waxes. Bot. J. Linn. Soc. 126, 237-260.

Bates, P.D., and Browse, J. (2011). The pathway of triacylglycerol synthesis through phosphatidylcholine in Arabidopsis produces a bottleneck for the accumulation of unusual fatty acids in transgenic seeds. Plant J. 68, 387-399.

Bates, P.D., and Browse, J. (2012). The significance of different diacylglycerol synthesis pathways on plant oil composition and bioengineering. Front. Plant Sci. 3, 147.

Bates, P.D., Ohlrogge, J.B., and Pollard, M. (2007). Incorporation of newly synthesized fatty acids into cytosolic glycerolipids in pea leaves occurs via acyl editing. J. Biol. Chem. 282, 31206-31216.

Bates, P.D., Stymne, S., and Ohlrogge, J. (2013). Biochemical pathways in seed oil synthesis. Curr. Opin. Plant Biol. 16, 358-364.

Bates, P.D., Durrett, T.P., Ohlrogge, J.B., and Pollard, M. (2009). Analysis of acyl fluxes through multiple pathways of triacylglycerol synthesis in developing soybean embryos. Plant Physiol. 150, 55-72.

Baud, S., and Lepiniec, L. (2009). Regulation of *de novo* fatty acid synthesis in maturing oilseeds of Arabidopsis. Plant Physiology and Biochemistry 47, 448-455.

Beisson, F., and Ohlrogge, J. (2012). Plants: Knitting a polyester skin. Nat. Chem. Biol. 8, 603-604.

Beisson, F., Li-Beisson, Y., and Pollard, M. (2012). Solving the puzzles of cutin and suberin polymer biosynthesis. Curr. Opin. Plant Biol. 15, 329-337.

Beisson, F., Li, Y., Bonaventure, G., Pollard, M., and Ohlrogge, J.B. (2007). The acyltransferase GPAT5 is required for the synthesis of suberin in seed coat and root of Arabidopsis. Plant Cell 19, 351-368.

Bessire, M., Borel, S., Fabre, G., Carraca, L., Efremova, N., Yephremov, A., Cao, Y., Jetter, R., Jacquat, A.C., Metraux, J.P., and Nawrath, C. (2011). A member of the PLEIOTROPIC DRUG RESISTANCE family of ATP binding cassette transporters is required for the formation of a functional cuticle in Arabidopsis. Plant Cell 23, 1958-1970.

Bird, D., Beisson, F., Brigham, A., Shin, J., Greer, S., Jetter, R., Kunst, L., Wu, X., Yephremov, A., and Samuels, L. (2007). Characterization of Arabidopsis ABCG11/WBC11, an ATP binding cassette (ABC) transporter that is required for cuticular lipid secretion. Plant J. 52, 485-498.

Bonaventure, G., Salas, J.J., Pollard, M.R., and Ohlrogge, J.B. (2003). Disruption of the FATB gene in Arabidopsis demonstrates an essential role of saturated fatty acids in plant growth. Plant Cell 15, 1020-1033.

Bourgis, F., Kilaru, A., Cao, X., Ngando-Ebongue, G.F., Drira, N., Ohlrogge, J.B., and Arondel, V. (2011). Comparative transcriptome and metabolite analysis of oil palm and date palm mesocarp that differ dramatically in carbon partitioning. Proc. Natl. Acad. Sci. USA 108, 12527-12532.

Brautigam, A., Schliesky, S., Kulahoglu, C., Osborne, C.P., and Weber, A.P. (2014). Towards an integrative model of C4 photosynthetic subtypes: insights from comparative transcriptome analysis of NAD-ME, NADP-ME, and PEP-CK C4 species. J. Exp. Bot. 65, 3579-3593.

Brockerhoff, H. (1965). Sterospecific analysis of triglycerides: An analysis of human depot fat. Arch. Biochem. Biophys. 110, 586-592.

Brundrett, M.C., Kendrick, B., and Peterson, C.A. (1991). Efficient lipid staining in plant material with Sudan Red 7B or Fluoral Yellow 088 in polyethylene glycol -gIycerol. Biotech Histochem 91, 111-116.

Cahoon, E.B., Shockey, J.M., Dietrich, C.R., Gidda, S.K., Mullen, R.T., and Dyer, J.M. (2007). Engineering oilseeds for sustainable production of industrial and nutritional feedstocks: solving bottlenecks in fatty acid flux. Curr. Opin. Plant Biol. 10, 236-244.

Cameron, K.D., Teece, M.A., and Smart, L.B. (2006). Increased accumulation of cuticular wax and expression of lipid transfer protein in response to periodic drying events in leaves of tree tobacco. Plant Physiol. 140, 176-183.

Cao, J., Li, J.L., Li, D., Tobin, J.F., and Gimeno, R.E. (2006). Molecular identification of microsomal acyl-CoA:glycerol-3-phosphate acyltransferase, a key enzyme in *de novo* triacylglycerol synthesis. Proc. Natl. Acad. Sci. USA 103, 19695-19700.

Carlsson, A.S., Yilmaz, J.L., Green, A.G., Stymne, S., and Hofvander, P. (2011). Replacing fossil oil with fresh oil - With what and for what? Eur. J. Lipid Sci. Tech. 113, 812-831.

Cernac, A., Andre, C., Hoffmann-Benning, S., and Benning, C. (2006). WRI1 is required for seed germination and seedling establishment. Plant Physiol. 141, 745-757.

Chapman, K.D., Dyer, J.M., and Mullen, R.T. (2012). Biogenesis and functions of lipid droplets in plants: Thematic Review Series: Lipid Droplet Synthesis and Metabolism from yeast to Man. J. Lipid Res. 53, 215-226.

Chen, G., Woodfield, H.K., Pan, X., Harwood, J.L., and Weselake, R.J. (2015). Acyl-Trafficking During Plant Oil Accumulation. Lipids 50, 1057-1068.

Chen, G., Komatsuda, T., Ma, J.F., Nawrath, C., Pourkheirandish, M., Tagiri, A., Hu, Y.G., Sameri, M., Li, X., Zhao, X., Liu, Y., Li, C., Ma, X., Wang, A., Nair, S., Wang, N., Miyao, A., Sakuma, S., Yamaji, N., Zheng, X., and Nevo, E. (2011). An ATP-binding cassette subfamily G full transporter is essential for the retention of leaf water in both wild barley and rice. Proc. Natl. Acad. Sci. USA 108, 12354-12359.

Choi, Y.E., Lim, S., Kim, H.J., Han, J.Y., Lee, M.H., Yang, Y., Kim, J.A., and Kim, Y.S. (2012). Tobacco NtLTP1, a glandular-specific lipid transfer protein, is required for lipid secretion from glandular trichomes. Plant J. 70, 480-491.

Christie, W.W. (2011). The Analysis of Lipids other than Fatty Acids. Sections A and B. Introduction and High-Temperature Gas Chromatography of Triacylglycerols.

Christie, W.W., and Han, X. (2010). Lipid Analysis: Isolation Separation and Lipodomic Analysis. (England: The Oily Press).

Cresti, M., Keijzer, C.T., Tiezzi, A., Ciampolini, F., and Focardi, S. (1986). Stigma of *Nicotiana*: Ultrastructural and biochemical studies. Am. J. Bot. 73, 1713-1722.

Dahlqvist, A., Stahl, U., Lenman, M., Banas, A., Lee, M., Sandager, L., Ronne, H., and Stymne, S. (2000). Phospholipid:diacylglycerol acyltransferase: An enzyme that catalyzes the acyl-CoA-independent formation of triacylglycerol in yeast and plants. Proc. Natl. Acad. Sci. USA 97, 6487-6492.

Davidson, A.L., Dassa, E., Orelle, C., and Chen, J. (2008). Structure, function, and evolution of bacterial ATP-binding cassette systems. Microbiol. Mol. Biol. Rev. 72, 317-364, table of contents.

Debono, A., Yeats, T.H., Rose, J.K., Bird, D., Jetter, R., Kunst, L., and Samuels, L. (2009). Arabidopsis LTPG is a glycosylphosphatidylinositol-anchored lipid transfer protein required for export of lipids to the plant surface. Plant Cell 21, 1230-1238.

Deeley, R.G., Westlake, C., and Cole, S.P.C. (2006). Transmembrane transport of endo- and xenobiotics by mammalian ATP-binding cassette multidrug resistance proteins. Physiol. Rev. 86, 849-899.

Dominguez, E., Heredia-Guerrero, J.A., and Heredia, A. (2015). Plant cutin genesis: Unanswered questions. Trends Plant Sci 20, 551-558.

Durrett, T.P., Benning, C., and Ohlrogge, J. (2008). Plant triacylglycerols as feedstocks for the production of biofuels. Plant J. 54, 593-607.

Durrett, T.P., McClosky, D.D., Tumaney, A.W., Elzinga, D.A., Ohlrogge, J., and Pollard, M. (2010). A distinct DGAT with *sn*-3 acetyltransferase activity that synthesizes unusual, reduced-viscosity oils in Euonymus and transgenic seeds. Proc. Natl. Acad. Sci. USA 107, 9464-9469.

Feng, C., Chen, M., Xu, C.J., Bai, L., Yin, X.R., Li, X., Allan, A.C., Ferguson, I.B., and Chen, K.S. (2012). Transcriptomic analysis of Chinese bayberry (*Myrica rubra*) fruit development and ripening using RNA-Seq. BMC Genomics 13, 19.

Fordham, A.J. (1983). Of birds and bayberries: Seed dispersal and propagation of three *Myrica* species. Arnoldia 43, 20-23.

Gao, J., and Simon, M. (2005). Identification of a novel keratinocyte retinyl ester hydrolase as a transacylase and lipase. J. Invest. Dermatol. 124, 1259-1266.

Ge, W., Song, Y., Zhang, C., Zhang, Y., Burlingame, A.L., and Guo, Y. (2011). Proteomic analyses of apoplastic proteins from germinating Arabidopsis thaliana pollen. Biochim. Biophys. Acta. 1814, 1964-1973.

Girard, A.L., Mounet, F., Lemaire-Chamley, M., Gaillard, C., Elmorjani, K., Vivancos, J., Runavot, J.L., Quemener, B., Petit, J., Germain, V., Rothan, C., Marion, D., and Bakan, B. (2012). Tomato GDSL1 is required for cutin deposition in the fruit cuticle. Plant Cell 24, 3119-3134.

Gongora-Castillo, E., Childs, K.L., Fedewa, G., Hamilton, J.P., Liscombe, D.K., Magallanes-Lundback, M., Mandadi, K.K., Nims, E., Runguphan, W., Vaillancourt, B., Varbanova-Herde, M., Dellapenna, D., McKnight, T.D., O'Connor, S., and Buell, C.R. (2012). Development of transcriptomic resources for interrogating the biosynthesis of monoterpene indole alkaloids in medicinal plant species. PLoS One 7, e52506.

Goni, F.M., and Alonso, A. (1999). Structure and functional properties of diacylglycerols in membranes. Prog. Lipid. Res. 38, 1-48.

Grabherr, M.G. (2011). Full-length transcriptome assembly from RNA-Seq data without a reference genome. Nat. Biotechnol. 29, 644-652.

Griffiths, G., and Harwood, J.L. (1991). The regulation of triacylglycerol biosynthesis in cocoa (*Theobroma cacao*). Planta 184, 279-284.

Griffiths, G., Stymne, S., and Stobart, A.K. (1988). Phosphatidylcholine and its relationship to triacylglycerol biosynthesis in oil-tissues. Phytochemistry 27, 2089-2093.

Gunstone, F.D., Harwood, J.L., and Dijkstra, A.J. (2007). The Lipid Handbook. (Boca Raton: CRC Press).

Hall, I.V. (1975). The Biology of Canadian Weeds 7. *Myrica pensylvanica* Loisel. Can. J. Plant Sci. 55, 163-169.

Hamilton, J.A., Johnson, R.A., Corkey, B., and Kamp, F. (2001). Fatty acid transport. J. Mol. Neurosci. 16, 99-108.

Han, J., Clement, J.M., Li, J., King, A., Ng, S., and Jaworski, J.G. (2010). The cytochrome P450 CYP86A22 is a fatty acyl-CoA omega-hydroxylase essential for estolide synthesis in the stigma of *Petunia hybrida*. J. Biol. Chem. 285, 3986-3996.

Hara, A., and Radin, N. (1978). Lipid extraction of tissues with a low-toxicity solvent. Anal. Biochem. 90, 420-426.

Harlow, R.D., Litchfie.C, Fu, H.C., and Reiser, R. (1965). Triglyceride composition of *Myrica Carolinenis* fruit coat fat (Bayberry Tallow). J. Am. Oil Chem. Soc. 42, 4.

Harwood, J.L. (1988). Fatty acid metabolism. Annu. Rev. Plant Phys. 39, 37.

Hawthorne, S.B., and Miller, D.J. (1987). Analysis of commercial waxes using capillary supercritical fluid chromatography-mass spectrometry. J. Chromatogr. 388, 397-409.

Heid, H.W., and Keenan, T.W. (2005). Intracellular origin and secretion of milk fat globules. Eur. J. Cell Biol. 84, 245-258.

Helsop-Harrison, J. (1968). Tapetal origin of pollen-coat substances in *Lilium*. New Phytol. 67, 779-786.

Hoffmann-Benning, S., and Kende, H. (1994). Cuticle biosynthesis in rapidly growin internodes of deep-water rice. Plant Physiol. 104, 719-723.

Howe, H.F., and Smallwood, J. (1982). Ecology of seed dispersal. Ann. Rev. Ecol. Syst. 13, 201-228.

Huang, M.D., Chen, T.L., and Huang, A.H. (2013). Abundant type III lipid transfer proteins in Arabidopsis tapetum are secreted to the locule and become a constituent of the pollen exine. Plant Physiol. 163, 1218-1229.

Huguet, V., Gouy, M., Normand, P., Zimpfer, J.F., and Fernandez, M.P. (2005). Molecular phylogeny of *Myricaceae*: A reexamination of host-symbiont specificity. Mol. Phylogenet. Evol. 34, 557-568.

Isaacson, T., Kosma, D.K., Matas, A.J., Buda, G.J., He, Y., Yu, B., Pravitasari, A., Batteas, J.D., Stark, R.E., Jenks, M.A., and Rose, J.K. (2009). Cutin deficiency in the tomato fruit cuticle consistently affects resistance to microbial infection and biomechanical properties, but not transpirational water loss. Plant J. 60, 363-377.

Jaworski, J., and Cahoon, E.B. (2003). Industrial oils from transgenic plants. Curr. Opin. Plant Biol. 6, 178-184.

Jenkins, C.M., Mancuso, D.J., Yan, W., Sims, H.F., Gibson, B., and Gross, R.W. (2004). Identification, cloning, expression, and purification of three novel human calcium-independent phospholipase A2 family members possessing triacylglycerol lipase and acylglycerol transacylase activities. J. Biol. Chem. 279, 48968-48975.

Jensen, J.K., Schultink, A., Keegstra, K., Wilkerson, C.G., and Pauly, M. (2012). RNA-Seq analysis of developing nasturtium seeds (*Tropaeolum majus*): Identification and characterization of an additional galactosyltransferase involved in xyloglucan biosynthesis. Mol. Plant 5, 984-992.

Jetter, R., Kunst, L., and Samuels, L. (2006). Composition of plant cuticular waxes. In Biology of the Plant Cuticle, M. Riederer and C. Muller, eds (Blackwell Publishers), pp. 145-181.

Kader, J.C. (1996). Lipid-transfer proteins in plants. Annu. Rev. Plant Phys. 47, 627-654.

Kang, J., Park, J., Choi, H., Burla, B., Kretzschmar, T., Lee, Y., and Martinoia, E. (2011). Plant ABC Transporters. In The Arabidopsis Book, pp. e0153.

Kannangara, R., Branigan, C., Liu, Y., Penfield, T., Rao, V., Mouille, G., Hofte, H., Pauly, M., Riechmann, J.L., and Broun, P. (2007). The transcription factor WIN1/SHN1 regulates cutin biosynthesis in Arabidopsis thaliana. Plant Cell 19, 1278-1294.

Karlgren, A., Carlsson, J., Gyllenstrand, N., Lagercrantz, U., and Sundstrom, J.F. (2009). Non-radioactive *in situ* hybridization protocol applicable for Norway spruce and a range of plant species. J. Vis. Exp.

Kellogg, R.B., and Patton, J.S. (1983). Lipid droplets, medium of energy exchange in the symbiotic anemone *Condylactis gigantea*- A model coral polyp. Mar. Biol. 75, 137-149.

Kikuta, Y., Ueda, H., Takahashi, M., Mitsumori, T., Yamada, G., Sakamori, K., Takeda, K., Furutani, S., Nakayama, K., Katsuda, Y., Hatanaka, A., and Matsuda, K. (2012). Identification and characterization of a GDSL lipase-like protein that catalyzes the ester-forming reaction for pyrethrin biosynthesis in Tanacetum cinerariifolium- a new target for plant protection. Plant J. 71, 183-193.

Kilaru, A., Cao, X., Dabbs, P.B., Sung, H.J., Rahman, M.M., Thrower, N., Zynda, G., Podicheti, R., Ibarra-Laclette, E., Herrera-Estrella, L., Mockaitis, K., and Ohlrogge, J.B. (2015). Oil biosynthesis in a basal angiosperm: Transcriptome analysis of *Persea americana* mesocarp. BMC Plant Biol. 15, 203.

Kim, H.J., Silva, J.E., Vu, H.S., Mockaitis, K., Nam, J.W., and Cahoon, E.B. (2015). Toward production of jet fuel functionality in oilseeds: identification of FatB acyl-acyl carrier protein thioesterases and evaluation of combinatorial expression strategies in *Camelina* seeds. J. Exp. Bot. 66, 4251-4265.

Kitzke, E.D., and Wilder, E.A. (1961). The cuticle wax of the Cuban Palm *Copernicia hospita*. J. Am. Oil Chem. Soc. 38, 699-700.

Koenig, D., Jimenez-Gomez, J.M., Kimura, S., Fulop, D., Chitwood, D.H., Headland, L.R., Kumar, R., Covington, M.F., Devisetty, U.K., Tat, A.V., Tohge, T., Bolger, A., Schneeberger, K., Ossowski, S., Lanz, C., Xiong, G., Taylor-Teeples, M., Brady, S.M., Pauly, M., Weigel, D., Usadel, B., Fernie, A.R., Peng, J., Sinha, N.R., and Maloof, J.N. (2013). Comparative transcriptomics reveals patterns of selection in domesticated and wild tomato. Proc. Natl. Acad. Sci. USA 110, E2655-2662.

Koiwai, A., and Matsuzaki, T. (1988). Hydroxy and normal fatty acid distrubution in stigmas of *Nicotiana* and other plants. Phytochemistry 27, 2827-2830.

Kolattukudy, P.E. (1965). Biosynthesis of wax in *Brassica oleracea*. Biochemistry 4, 1844-1855.

Kolattukudy, P.E. (1970). Biosyntheisis of a lipid polymer, cutin: The structural component of the plant cuticle. Biochem. Biophys. Res. Commun. 41, 299-305.

Kolattukudy, P.E. (1976). Chemistry and Biochemistry of Natural Waxes. (New York: Elseiver).

Kolattukudy, P.E. (2001). Polyesters in higher plants. Adv. Biochem. Eng. Biotechnol. 71, 1-49.

Kolattukudy, P.E., and Walton, T.J. (1972). Structure and biosynthesis of the hydroxy fatty acids of cutin in *Vicia faba* leaves. Biochemistry 11, 1897-1907.

Konar, R.N., and Linskens, H.F. (1966). The morphology and anatomy of the stigma of *Petunia hybrida*. Planta 71, 365-371.

Kosma, D.K., Murmu, J., Razeq, F.M., Santos, P., Bourgault, R., Molina, I., and Rowland, O. (2014). AtMYB41 activates ectopic suberin synthesis and assembly in multiple plant species and cell types. Plant J. 80, 216-229.

Kunst, L., Browse, J., and Somerville, C. (1988). Altered regulation of lipid biosynthesis in a mutant of Arabidopsis deficient in chloroplast glycerol-3-phosphate acyltransferase activity Proc. Natl. Acad. Sci. USA 85, 4143-4147.

Kunst, L., Jetter, R., and Samuels, A.L. (2006). Biosynthesis and transport of plant cuticular waxes. In Biology of the Plant Cuticle, M. Riederer and C. Muller, eds (USA: Blackwell Publishers.

Kurdyukov, S., Faust, A., Trenkamp, S., Bar, S., Franke, R., Efremova, N., Tietjen, K., Schreiber, L., Saedler, H., and Yephremov, A. (2006). Genetic and biochemical evidence for involvement of HOTHEAD in the biosynthesis of long-chain alpha-,omega-dicarboxylic fatty acids and formation of extracellular matrix. Planta 224, 315-329.

Landgraf, R., Smolka, U., Altmann, S., Eschen-Lippold, L., Senning, M., Sonnewald, S., Weigel, B., Frolova, N., Strehmel, N., Hause, G., Scheel, D., Bottcher, C., and Rosahl, S. (2014). The ABC transporter ABCG1 is required for suberin formation in potato tuber periderm. Plant Cell 26, 3403-3415.

Lee, S.B., Go, Y.S., Bae, H.J., Park, J.H., Cho, S.H., Cho, H.J., Lee, D.S., Park, O.K., Hwang, I., and Suh, M.C. (2009). Disruption of glycosylphosphatidylinositol-anchored lipid transfer protein gene altered cuticular lipid composition, increased plastoglobules, and enhanced susceptibility to infection by the fungal pathogen *Alternaria brassicicola*. Plant Physiol. 150, 42-54.

Lehner, R., and Kuksis, A. (1993). Triacylglycerol synthesis by an *sn*-1,2 (2,3)- diacylglycerol transacylase from rat intestinal microsomes. J. Biol. Chem. 268, 8783-8796.

Lei, L., Chen, L., Shi, X., Li, Y., Wang, J., Chen, D., and Xie, F. (2014). A nodule-specific lipid transfer protein AsE246 participates in transport of plant-synthesized lipids to symbiosome membrane and is essential for nodule organogenesis in Chinese milk vetch. Plant Physiol. 164, 1045-1058.

Li-Beisson, Y., Pollard, M., Sauveplane, V., Pinot, F., Ohlrogge, J., and Beisson, F. (2009). Nanoridges that characterize the surface morphology of flowers require the synthesis of cutin polyester. Proc. Natl. Acad. Sci. USA 106, 22008-22013.

Li-Beisson, Y., Shaorrosh, B., Beisson, F., Andersson, M.X., Arondel, V., Bates, P.D., Baud, S., Bird, D., DeBono, A., Durrett, T.P., Franke, R.B., Graham, I., Katayama, K., A.A., K., Larson, T., Markham, J.E., Miguel, M., Molina, I., Nishida, I., Rowland, O., Samuels, L., Schmid, K.M., Wada, H., Welti, R., Xu, C., Zallot, R., and Ohlrogge, J. (2010). Acyl-lipid metabolism. In The Arabidopsis Book.

Li, H., Pinot, F., Sauveplane, V., Werck-Reichhart, D., Diehl, P., Schreiber, L., Franke, R., Zhang, P., Chen, L., Gao, Y., Liang, W., and Zhang, D. (2010). Cytochrome P450 family member CYP704B2 catalyzes the {omega}-hydroxylation of fatty acids and is required for anther cutin biosynthesis and pollen exine formation in rice. Plant Cell 22, 173-190.

Li, Y., Beisson, F., Ohlrogge, J., and Pollard, M. (2007a). Monoacylglycerols are components of root waxes and can be produced in the aerial cuticle by ectopic expression of a suberin-associated acyltransferase. Plant Physiol. 144, 1267-1277.

Li, Y., Beisson, F., Koo, A.J., Molina, I., Pollard, M., and Ohlrogge, J. (2007b). Identification of acyltransferases required for cutin biosynthesis and production of cutin with suberin-like monomers. Proc. Natl. Acad. Sci. USA 104, 18339-18344.

Lindorff-Larsen, K., Lerche, M.H., Poulsen, F.M., Roepstorff, P., and Winther, J.R. (2001). Barley lipid transfer protein, LTP1, contains a new type of lipid-like post-translational modification. J. Biol. Chem. 276, 33547-33553.

Liu, L., Jin, X., Chen, N., Li, X., Li, P., and Fu, C. (2015). Phylogeny of *Morella rubra* and its relatives (*Myricaceae*) and genetic resources of Chinese Bayberry using RAD sequencing. PLoS One, 1-16.

Lorts, C.M., Briggeman, T., and Sang, T. (2008). Evolution of fruit types and seed dispersal: A phylogenetic and ecological snapshot. J. Syst. Evol. 46, 396-404.

Lu, C., Xin, Z., Ren, Z., Miquel, M., and Browse, J. (2009). An enzyme regulating triacylglycerol composition is encoded by the ROD1 gene of Arabidopsis. Proc. Natl. Acad. Sci. USA 106, 18837-18842.

Mackenzie, C.J., Yoo, B.Y., and Seabrook, J.E.A. (1990). Stigam of *Solanum tubersoum* c.v. Shepody: Morphology, ultrastructure and secretion Am. J. Bot. 77, 1111-1124.

Matas, A.J., Agusti, J., Tadeo, F.R., Talon, M., and Rose, J.K. (2010). Tissue-specific transcriptome profiling of the citrus fruit epidermis and subepidermis using laser capture microdissection. J. Exp. Bot. 61, 3321-3330.

Matas, A.J., Yeats, T.H., Buda, G.J., Zheng, Y., Chatterjee, S., Tohge, T., Ponnala, L., Adato, A., Aharoni, A., Stark, R., Fernie, A.R., Fei, Z., Giovannoni, J.J., and Rose, J.K. (2011). Tissue- and cell-type specific transcriptome profiling of expanding tomato fruit provides

insights into metabolic and regulatory specialization and cuticle formation. Plant Cell 23, 3893-3910.

Matsuzaki, T., Koiwai, A., and Kawashima, N. (1983). Changes in stigma-specific lipids of tobacco plant during flower development. Plant Cell Physiol. 24, 207-213.

McFarlane, H.E., Young, R.E., Wasteneys, G.O., and Samuels, A.L. (2008). Cortical microtubules mark the mucilage secretion domain of the plasma membrane in Arabidopsis seed coat cells. Planta 227, 1363-1375.

McFarlane, H.E., Shin, J.J., Bird, D.A., and Samuels, A.L. (2010). Arabidopsis ABCG transporters, which are required for export of diverse cuticular lipids, dimerize in different combinations. Plant Cell 22, 3066-3075.

McFarlane, H.E., Watanabe, Y., Yang, W., Huang, Y., Ohlrogge, J., and Samuels, A.L. (2014). Golgi- and trans-Golgi network-mediated vesicle trafficking is required for wax secretion from epidermal cells. Plant Physiol. 164, 1250-1260.

McKay, A.F. (1948). Occurrence of stearic acid in Bayberry tallow (wax). J. Org. Chem. 13, 86-88.

Meisel, L., Fonseca, B., Gonzalez, S., Baeza-Yates, R., Cambiazo, V., Campos, R., Gonzalez, M., Orellana, A., Retamales, J., and Silva, H. (2005). A rapid and efficient method for purifying high quality total RNA from peaches (*Prunus persica*) for functional genomics analysis. Biol. Res. 38, 83-88.

Mekhedov, S., Martinez de Ilarduya, O., and Ohlrogge, J. (2000). Toward a functional catalog of the plant genome. A survery of genes for lipid biosynthesis. Plant Physiol. 122, 389-401.

Mintz-Oron, S., Mandel, T., Rogachev, I., Feldberg, L., Lotan, O., Yativ, M., Wang, Z., Jetter, R., Venger, I., Adato, A., and Aharoni, A. (2008). Gene expression and metabolism in tomato fruit surface tissues. Plant Physiol. 147, 823-851.

Molina, I., and Kosma, D. (2015). Role of HXXXD-motif/BAHD acyltransferases in the biosynthesis of extracellular lipids. Plant Cell Rep. 34, 587-601.

Molina, I., Ohlrogge, J.B., and Pollard, M. (2008). Deposition and localization of lipid polyester in developing seeds of *Brassica napus* and *Arabidopsis thaliana*. Plant J. 53, 437-449.

Murphy, D.J. (1993). Structure, function and biogenesis of storage lipid bodies and oleosins in plants. Prog. Lipid. Res. 32, 247-280.

Murphy, D.J. (2001). The biogenesis and functions of lipid bodies in animals, plants and microorganisms. Prog. Lipid. Res. 40, 325-438.

Murphy, D.J. (2012). The dynamic roles of intracellular lipid droplets: from archaea to mammals. Protoplasma 249, 541-585.

Nielson, A.J., and Griffith, W.P. (1978). Tissue fixation and staining with osmium tetroxide: the role of phenolic compounds. J. Histochem. Cytochem. 26, 138-140.

Nieuwland, J., Feron, R., Huisman, B.A., Fasolino, A., Hilbers, C.W., Derksen, J., and Mariani, C. (2005). Lipid transfer proteins enhance cell wall extension in tobacco. Plant Cell 17, 2009-2019.

Ohlrogge, J., and Browse, J. (1995). Lipid biosynthesis. Plant Cell 7, 957-970.

Ohlrogge, J., and Benning, C. (2000). Unraveling plant metabolism by EST analysis. Curr. Opin. Plant Biol. 3, 224-228.

Ohlrogge, J., Allen, D., Berguson, B., DellaPenna, D., Shachar-Hill, Y., and Stymne, S. (2009). Driving on biomass. Science 324, 1019-1020.

Otsu, C.T., daSilva, I., de Molfetta, J.B., da Silva, L.R., de Almeida-Engler, J., Engler, G., Torraca, P.C., Goldman, G.H., and Goldman, M.H. (2004). NtWBC1, an ABC transporter gene specifically expressed in tobacco reproductive organs. J. Exp. Bot. 55, 1643-1654.

Pagnussat, L., Burbach, C., Baluska, F., and de la Canal, L. (2012). An extracellular lipid transfer protein is relocalized intracellularly during seed germination. J. Exp. Bot. 63, 6555-6563.

Pan, X., Siloto, R.M., Wickramarathna, A.D., Mietkiewska, E., and Weselake, R.J. (2013). Identification of a pair of phospholipid:diacylglycerol acyltransferases from developing flax (*Linum usitatissimum* L.) seed catalyzing the selective production of trilinolenin. J. Biol. Chem. 288, 24173-24188.

Panikashvili, D., Shi, J.X., Schreiber, L., and Aharoni, A. (2009). The Arabidopsis DCR encoding a soluble BAHD acyltransferase is required for cutin polyester formation and seed hydration properties. Plant Physiol. 151, 1773-1789.

Panikashvili, D., Shi, J.X., Schreiber, L., and Aharoni, A. (2011). The Arabidopsis ABCG13 transporter is required for flower cuticle secretion and patterning of the petal epidermis. New Phytol. 190, 113-124.

Patton, J.S., and Burris, J.E. (1983). Lipid synthesis and extrusion by freshly isolated *Zooxanthellae* (symbiotic algae). Mar. Biol. 75, 131-136.

Petrie, J.R., Vanhercke, T., Sherestha, P., El Tachy, A., White, A., Zhou, X.-R., Liu, Q., Mansour, M.P., Nichols, P.D., and Singh, S.P. (2012). Recruiting a new substrate for triacylglycerol synthesis in plants: The monoacylglycerol acyltransferase pathway. In PLoS One.

Pighin, J.A., Zheng, H., Balakshin, L.J., Goodman, I.P., Western, T.L., Jetter, R., Kunst, L., and Samuels, A.L. (2004). Plant cuticular lipid export requires an ABC transporter. Science 306, 702-704.

Place, A.R., and Stiles, E.W. (1992). Living off the wax of the land - Bayberries and Yellow-Rumped Warblers. Auk 109, 334-345.

Pollard, M., Beisson, F., Li, Y., and Ohlrogge, J.B. (2008). Building lipid barriers: Biosynthesis of cutin and suberin. Trends Plant Sci 13, 236-246.

Ponnala, L., Wang, Y., Sun, Q., and van Wijk, K.J. (2014). Correlation of mRNA and protein abundance in the developing maize leaf. Plant J. 78, 424-440.

Pyee, J., and Kolattukudy, P.E. (1995). The gene for the major cuticular wax-associated protein and 3 homologous genes from Broccoli (*Brassica oleracea*) and their expression patterns. Plant J. 7, 49-59.

Pyee, J., Yu, H.S., and Kolattukudy, P.E. (1994). Identification of a lipid transfer protein as the major protein in the surface wax of broccoli (*Brassica olearcea*) leaves. Arch. Biochem. Biophys. 311, 460-468.

Quast, C., Pruesse, E., Yilmaz, P., Gerken, J., Schweer, T., Yarza, P., Peplies, J., and Glockner, F.O. (2013). The SILVA ribosomal RNA gene database project: improved data processing and web-based tools. Nucleic Acids Res. 41, D590-596.

Quilichini, T.D., Grienenberger, E., and Douglas, C.J. (2015). The biosynthesis, composition and assembly of the outer pollen wall: A tough case to crack. Phytochemistry 113, 170-182.

Raffaele, S., Vailleau, F., Leger, A., Joubes, J., Miersch, O., Huard, C., Blee, E., Mongrand, S., Domergue, F., and Roby, D. (2008). A MYB transcription factor regulates very-long-chain fatty acid biosynthesis for activation of the hypersensitive cell death response in Arabidopsis. Plant Cell 20, 752-767.

Rani, S.H., Krishna, T.H., Saha, S., Negi, A.S., and Rajasekharan, R. (2010). Defective in cuticular ridges (DCR) of Arabidopsis thaliana, a gene associated with surface cutin formation, encodes a soluble diacylglycerol acyltransferase. J. Biol. Chem. 285, 38337-38347.

Rensing, S.A., Lang, D., Zimmer, A.D., Terry, A., Salamov, A., Shapiro, H., Nishiyama, T., Perroud, P.F., Lindquist, E.A., Kamisugi, Y., Tanahashi, T., Sakakibara, K., Fujita, T., Oishi, K., Shin, I.T., Kuroki, Y., Toyoda, A., Suzuki, Y., Hashimoto, S., Yamaguchi, K., Sugano, S., Kohara, Y., Fujiyama, A., Anterola, A., Aoki, S., Ashton, N., Barbazuk, W.B., Barker, E., Bennetzen, J.L., Blankenship, R., Cho, S.H., Dutcher, S.K., Estelle, M., Fawcett, J.A., Gundlach, H., Hanada, K., Heyl, A., Hicks, K.A., Hughes, J., Lohr, M., Mayer, K., Melkozernov, A., Murata, T., Nelson, D.R., Pils, B., Prigge, M., Reiss, B., Renner, T., Rombauts, S., Rushton, P.J., Sanderfoot, A., Schween, G., Shiu, S.H., Stueber, K., Theodoulou, F.L., Tu, H., Van de Peer, Y., Verrier, P.J., Waters, E., Wood, A., Yang, L., Cove, D., Cuming, A.C., Hasebe, M., Lucas, S., Mishler, B.D., Reski, R., Grigoriev, I.V., Quatrano, R.S., and Boore, J.L. (2008). The *Physcomitrella* genome reveals evolutionary insights into the conquest of land by plants. Science 319, 64-69.

Roston, R.L., Hurlock, A.K., and Benning, C. (2014). Plastidic ABC proteins. In Plant ABC Transporters, M. Geisler, ed (New York: Springer.

Roughan, P.G., and Slack, C.R. (1982). Cellular organization of glycerolipid metabolism. Ann. Rev. Plant Phys. 33, 97-112.

Salas, J.J., and Ohlrogge, J. (2002). Characterization of substrate specificity of plant FatA and FatB acyl-ACP thioesterases. Arch. Biochem. Biophys. 403, 25-34.

Samuels, A.L., Kunst, L., and Jetter, R. (2008). Sealing plant surfaces: Cuticular wax formation by epidermal cells. Annu. Rev. Plant Biol. 59, 683-707.

Samuels, L., and McFarlane, H.E. (2012). Plant cell wall secretion and lipid traffic at membrane contact sites of the cell cortex. Protoplasma 249 Suppl 1, S19-23.

Schilmiller, A.L., Miner, D.P., Larson, M., McDowell, E., Gang, D.R., Wilkerson, C., and Last, R.L. (2010). Studies of a biochemical factory: tomato trichome deep expressed sequence tag sequencing and proteomics. Plant Physiol. 153, 1212-1223.

Schmid, R.D., and Verger, R. (1998). Lipases: Interfacial enzymes with attractive applications. Angew. Chem. Int. Ed. 37, 1608-1633.

Segel, I.H. (1968). Biochemical Calculations. (John Wiley and Sons).

Simpson, J.P., and Ohlrogge, J.B. (2015). A novel pathway for triacylglycerol biosynthesis is responsible for the accumulation of massive quantities of glycerolipids on the surface of Bayberry (*Myrica pensylvanica*) fruit. Plant Cell Submitted October, 2015.

Slack, C.R., Roughan, P.G., and Balasingham, N. (1977). Labelling studies in vivo on the metabolism of the acyl and glycerol moieties of the glycerolipids. Biochem. J. 162, 7.

Slack, C.R., Roughan, P.G., and Balasingham, N. (1978). Labelling of glycerolipids in the cotyledons of developing oilseeds by [1-14C] acetate and [2-3H] glycerol. Biochem. J. 170, 421-433.

Slack, C.R., Bertaud, W.S., Shaw, B.D., Holland, R., Browse, J., and Wright, H. (1980). Some studies on the composition and surface properties of oil bodies from the seed cotyledons of safflower. Biochem. J. 190, 10.

Stark, R.E., and Tian, S. (2006). The cutin biopolymer matrix. In Biology of the Plant Cuticle, M. Riederer and C. Muller, eds (Blackwell Publishers.

Stobart, A.K., and Stymne, S. (1985). The regulation of the fatty-acid composition of the triacylglycerols in microsomal preparations from avocado. Planta 163, 119-125.

Stobart, K., Mancha, M., Lenman, M., Dahlqvist, A., and Stymne, S. (1997). Triacylglycerols are synthesised and utilized by transacylation reactions in microsomal preparations of developing safflower (*Carthamus tinctorius* L) seeds. Planta 203, 58-66.

Suh, M.C., Samuels, A.L., Jetter, R., Kunst, L., Pollard, M., Ohlrogge, J., and Beisson, F. (2005). Cuticular lipid composition, surface structure, and gene expression in Arabidopsis stem epidermis. Plant Physiol. 139, 1649-1665.

Teutschbein, J., Gross, W., Nimtz, M., Milkowski, C., Hause, B., and Strack, D. (2010). Identification and localization of a lipase-like acyltransferase in phenylpropanoid metabolism of tomato (*Solanum lycopersicum*). J. Biol. Chem. 285, 38374-38381.

Thoma, S., Kaneko, Y., and Somerville, C. (1993). A non-specific lipid transfer protein from Arabidopsis is a cell wall protein Plant J. 3, 427-436.

Thoma, S., Hecht, U., Kippers, A., Botella, J., De Vries, S., and Somerville, C. (1994). Tissue-specific experssion of a gene encoding a cell wall-localized lipid transfer protein from Arabidopsis. Plant Physiol. 105, 35-45.

Thomas, A.E., Scharoun, J.E., and Ralston, H. (1965). Quantitative estimation of isomeric monoglycerides by thin-layer chromatography. J. Am. Oil Chem. Soc. 42, 789-792.

Tissier, A. (2012). Glandular trichomes: what comes after expressed sequence tags? Plant J. 70, 51-68.

Tjellstrom, H., Yang, Z., Allen, D.K., and Ohlrogge, J.B. (2012). Rapid kinetic labeling of Arabidopsis cell suspension cultures: implications for models of lipid export from plastids. Plant Physiol. 158, 601-611.

To, A., Joubes, J., Barthole, G., Lecureuil, A., Scagnelli, A., Jasinski, S., Lepiniec, L., and Baud, S. (2012). WRINKLED transcription factors orchestrate tissue-specific regulation of fatty acid biosynthesis in Arabidopsis. Plant Cell 24, 5007-5023.

Troncoso-Ponce, M.A., Kilaru, A., Cao, X., Durrett, T.P., Fan, J.L., Jensen, J.K., Thrower, N.A., Pauly, M., Wilkerson, C., and Ohlrogge, J.B. (2011). Comparative deep transcriptional profiling of four developing oilseeds. Plant J. 68, 1014-1027.

Tumaney, A.W., Shekar, S., and Rajasekharan, R. (2001). Identification, purification, and characterization of monoacylglycerol acyltransferase from developing peanut cotyledons. J. Biol. Chem. 276, 10847-10852.

Vailleau, F., Daniel, X., Tronchet, M., Montillet, J.L., Triantaphylides, C., and Roby, D. (2002). A R2R3-MYB gene, AtMYB30, acts as a positive regulator of the hypersensitive cell death program in plants in response to pathogen attack. Proc. Natl. Acad. Sci. USA 99, 10179-10184.

van de Loo, F.J., Broun, P., Turner, S., and Somerville, C. (1995). An oleate 12-hydroxylase from *Ricinus communis* L. is a fatty acid acyl desaturase homolog. Proc. Natl. Acad. Sci. USA 92, 6743-6747.

Vijayaraj, P., Jashal, C.B., Vijayakumar, A., Rani, S.H., Venkata Rao, D.K., and Rajasekharan, R. (2012). A bifunctional enzyme that has both monoacylglycerol acyltransferase and acyl hydrolase activities. Plant Physiol. 160, 667-683.

Voelker, T. (1996). Plant Acyl-ACP thioesterases: Chain-length determining enzymes in plant fatty acid biosynthesis. In Genetic Engineering, J. Setlow, ed (Springer US), pp. 111-133.

Volokita, M., Rosilio-Brami, T., Rivkin, N., and Zik, M. (2011). Combining comparative sequence and genomic data to ascertain phylogenetic relationships and explore the evolution of the large GDSL-lipase family in land plants. Mol. Biol. Evol. 28, 551-565.

Waite, M., and Sisson, P. (1973). Utilization of neutral glycerides and phosphatidylethanolamine by phospholipase A1 of the plasma membranes of rat liver. J. Biol. Chem. 248, 7985-7992.

Weber, A.P. (2015). Discovering new biology through RNA-Seq. Plant Physiol.

Wellesen, K., Durst, F., Pinot, F., Benveniste, I., Nettesheim, K., Wisman, E., Steiner-Lange, S., Saedler, H., and Yephremov, A. (2001). Functional analysis of the LACERATA gene of Arabidopsis provides evidence for different roles of fatty acid omega -hydroxylation in development. Proc. Natl. Acad. Sci. USA 98, 9694-9699.

Weng, J.K. (2014). The evolutionary paths towards complexity: a metabolic perspective. New Phytol. 201, 1141-1149.

Wilbur, R.L. (2002). The identity and history of *Myrica caroliniensis* (*Myricaceae*). Rhodora 104, 31-41.

Wilkerson, C.G., Mansfield, S.D., Lu, F., Withers, S., Park, T.-Y., Karlen, S.D., Gonzales-Vigil, E., Padmaksham, D., Unda, F., Rencoret, J., and Ralph, J. (2014). Monolignol ferulate transferase introduces chemically labile linkages into the lignin backbone. Science 344, 90-93.

Williams, L.O. (1958). Bayberry wax and bayberries. Econ Bot 12, 103-107.

Wolters-Arts, M., W.M., L., and Mariani, C. (1998). Lipids are required for directional pollen-tube growth. Nature 392, 818-821.

Xiao, F., Goodwin, S.M., Xiao, Y., Sun, Z., Baker, D., Tang, X., Jenks, M.A., and Zhou, J.-M. (2004). Arabidopsis CYP86A2 represses *Pseudomonas syringae* type III genes as is required for cuticle development. EMBO Journal 23, 2903-2913.

Xu, M., Wilderman, P.R., and Peters, R.J. (2007). Following evolution's lead to a single residue switch for diterpene synthase product outcome. Proc. Natl. Acad. Sci. USA 104, 7397-7401.

Yadav, V., Molina, I., Ranathunge, K., Castillo, I.Q., Rothstein, S.J., and Reed, J.W. (2014). ABCG transporters are required for suberin and pollen wall extracellular barriers in Arabidopsis. Plant Cell 26, 3569-3588.

Yamashita, A., Hayashi, Y., Nemoto-Sasaki, Y., Ito, M., Oka, S., Tanikawa, T., Waku, K., and Sugiura, T. (2014). Acyltransferases and transacylases that determine the fatty acid composition of glycerolipids and the metabolism of bioactive lipid mediators in mammalian cells and model organisms. Prog. Lipid. Res. 53, 18-81.

Yang, W., Simpson, J.P., Li-Beisson, Y., Beisson, F., Pollard, M., and Ohlrogge, J.B. (2012). A land-plant-specific glycerol-3-phosphate acyltransferase family in Arabidopsis: substrate specificity, *sn*-2 preference, and evolution. Plant Physiol. 160, 638-652.

Yang, W.L., Pollard, M., Li-Beisson, Y., Beisson, F., Feig, M., and Ohlrogge, J. (2010). A distinct type of glycerol-3-phosphate acyltransferase with *sn*-2 preference and phosphatase activity producing 2-monoacylglycerol. Proc. Natl. Acad. Sci. USA 107, 12040-12045.

Yang, Z., and Ohlrogge, J.B. (2009). Turnover of fatty acids during natural senescence of Arabidopsis, Brachypodium, and switchgrass and in Arabidopsis beta-oxidation mutants. Plant Physiol. 150, 1981-1989.

Yeats, T.H., Howe, K.J., Matas, A.J., Buda, G.J., Thannhauser, T.W., and Rose, J.K. (2010). Mining the surface proteome of tomato (*Solanum lycopersicum*) fruit for proteins associated with cuticle biogenesis. J. Exp. Bot. 61, 3759-3771.

Yeats, T.H., Huang, W., Chatterjee, S., Viart, H.M., Clausen, M.H., Stark, R.E., and Rose, J.K. (2014). Tomato Cutin Deficient 1 (CD1) and putative orthologs comprise an ancient family of cutin synthase-like (CUS) proteins that are conserved among land plants. Plant J. 77, 667-675.

Yeats, T.H., Martin, L.B., Viart, H.M., Isaacson, T., He, Y., Zhao, L., Matas, A.J., Buda, G.J., Domozych, D.S., Clausen, M.H., and Rose, J.K. (2012). The identification of cutin synthase: Formation of the plant polyester cutin. Nat. Chem. Biol. 8, 609-611.

Yen, C.L., Stone, S.J., Cases, S., Zhou, P., and Farese, R.V. (2002). Identification of a gene encoding MGAT1, a monoacylglycerol acyltransferase. Proc. Natl. Acad. Sci. USA 99, 8512-8517.

Youngken, H.W. (1915). The comparative morphology, taxonomy and distribution of the *Myricaceae* of the eastern United States PhD, 69.

Zhang, D., Liang, W., Yin, C., Zong, J., and Gu, F. (2010). OsC6, encoding a lipid transfer protein, is required for postmeiotic anther development in rice. Plant Physiol. 154, 149-162.

Zheng, Z.F., Xia, Q., Dauk, M., Shen, W.Y., Selvaraj, G., and Zou, J.T. (2003). Arabidopsis AtGPAT1, a member of the membrane-bound glycerol-3-phosphate acyltransferase gene

family, is essential for tapetum differentiation and male fertility. Plant Cell 15, 1872-1887.